Bachelor Thesis

Effect of Light and Hydrostatic Pressure on Properties of Optical Oxygen Sensors

Bachelor thesis

at the

Graz University of Technology

submitted by

Laura Martínez Vidal

Faculty of Technical Chemistry, Chemical and Process Engineering and Biotechnology

Institute of Analytical Chemistry and Food Chemistry

June 2015

Supervisor: Ass.Prof. kand. Sergey Borisov

Assessor: Dipl.-Ing. BSc Peter Wilhelm Zach

STATUTORY DECLARATION

I declare that I have authored this thesis independently, that I have not used other than the declared sources / resources, and that I have explicitly marked all material which has been quoted either literally or by content from the used sources.

…… ……..

date (signature)

Abstract

The aim of this project was the testing of the stability of different sensor materials under harsh conditions. To attain this objective, two main courses of study have been followed. The first part of the thesis focuses on the characterization of optical sensors at high hydrostatic pressure for oceanographic applications. In the second part, the photostability of different sensing materials has been studied in order to verify their adequate functioning in various applications where high light intensities are used or long measurements are performed.

Index

1 Introduction

Oxygen is one of the basic chemical elements. In its most common form, it is a colorless gas found in air and one of the life-sustaining elements on Earth. The quantification of oxygen concentration is very important in many fields such as industry, environmental monitoring, medicine, water quality monitoring and biotechnology. Due to its importance, during the last years there has been a lot of research focused on developing new sensor devices and procedures to continuously monitor oxygen.

1.1 Context

There are several methods for oxygen detection. In general one could classify them on the basis of the principle used in electrochemical (amperometric, potentiometric, or conductometric), optical (absorption changes or photoluminescence), and chemical (Winkler titration). However, in the last three decades, optical sensor technology has received increasing attention due to the fact that optical oxygen sensors are rather inexpensive, easy to miniaturize, can be used remotely, are virtually noninvasive or minimally invasive and, most of all, do not suffer from electrical interference nor consume oxygen (1).
The basic components of an optical oxygen sensor are a luminescent indicator and a sensor matrix. Several dyes have been synthesized in the last years for this purpose (1). Important factors to take into account are the solubility of the dye, its sensitivity, its photophysical and chemical stability and the availability of the starting materials. For each purpose one should consider which of these factors are more important and try to find the most suitable dye to use.

1.2 Objectives

Two factors that may influence the performance of optical oxygen sensors are the light (due to photobleaching of the indicator dye) and hydrostatic pressure (may have influence the sensitivity of the sensor).
Oxygen monitoring has high importance for oceanography and marine biology. For this reason it is necessary to know the reliability of the sensors under these conditions, when they are under high hydrostatic pressures at high depth.
The second factor is probably the most important one. Since light is required for the measurement with optical oxygen sensors (excitation of the dye) it is necessary to know how this factor varies the behavior of a dye. Therefore photostability tests with different dyes were performed.

1.3 Scope

No synthesis has been performed during this project. All dyes tested were already synthesized in the laboratory. The samples, cocktails and foils were prepared and tested in the different set-ups available for every experiment and the data has been processed,

analyzed and discussed. Furthermore some improvements in the methods and the different set-ups have been suggested for further investigation in this field.

2 Theoretical fundamentals of optical sensing

2.1 Luminescence

Most optical oxygen sensors are based on the principle of luminescence quenching by oxygen. Luminescence consists of the emission of ultraviolet, visible or infrared photons from an electronically excited species during de-excitation, and it is one of the possible effects resulting from the interaction between light and matter.

2.1.1 Basic principles of light absorption by molecules

An electronic transition is the promotion of an electron from an orbital of a molecule in the ground state to an unoccupied orbital by absorption of a photon. The molecule is then said to be in an excited state.

2.1.1.1 Types of orbitals and electronic transitions

A molecular orbital (or MO) is a mathematical function describing the wave-like behavior of an electron in a molecule. This function can be used to calculate chemical and physical properties such as the probability of finding an electron in any specific region.

A σ orbital can be formed either from two s atomic orbitals, or from one s and one p atomic orbital, or from two p atomic orbitals having a collinear axis of symmetry. The bond formed in this way is called a σ bond. The σ electrons are associated with single covalent bonds, so they are tightly bound. In order to excite them, radiation of high energy is required. The excitation takes place from a bonding MO (σ-MO) to an antibonding (σ*-MO) and the resulting transition is known as σ→σ* transition.

A π orbital is formed from two p atomic orbitals overlapping laterally. The resulting bond is called a π bond. The π electrons are rather easily excited to the higher level. In this case, the transition is from a bonding pi MO (π-MO) to anti-bonding pi MO (π*-MO) and it is known as π→π* transition.

If a molecule contains a hetero atom, it has unshared electron pairs which are non-bonding in nature. They can be excited to either σ* MO or π* MO resulting n→σ* or n→π* transitions. (2)

The energy required for the mentioned transitions obey the following order:

$$\sigma \rightarrow \sigma^* > n \rightarrow \sigma^* > \pi \rightarrow \pi^* > n \rightarrow \pi^*$$

In absorption and fluorescence spectroscopy, two important types of orbitals are considered: the Highest Occupied Molecular Orbitals (HOMO) and the Lowest Unoccupied Molecular Orbitals (LUMO). Both of these refer to the ground state of the molecule.

When one of the two electrons of opposite spins (belonging to a molecular orbital of a molecule in the ground state) is promoted to a molecular orbital of higher energy, its spin is in principle unchanged so that the total spin quantum number remains equal to zero. Because the multiplicities of both the ground and excited states, is equal to 1, both are called singlet state. The corresponding transition is called a singlet–singlet transition. A molecule in a singlet excited state may undergo conversion into a state where the promoted electron has

changed its spin; because there are then two electrons with parallel spins, the total spin quantum number is 1 and the multiplicity is 3. Such a state is called a triplet. According to Hund's rule, the triplet state has a lower energy than that of the singlet state of the same configuration.

2.1.2 Transitions between electronic states

The Jablonski diagram represents the energy of photoluminescent molecule in its different energy states. The lowest and darkest horizontal line represents the ground-state electronic energy of the molecule which is the singlet state labeled as S_0.
The upper lines represent the energy state of the three excited electronic states: S_1 and S_2 represent the electronically excited singlet states (left) and T_1 represents the first electronic triplet state (right). The upper darkest line represents the ground vibrational state of the three excited electronic state. The energy of the triplet state is lower than the energy of the corresponding singlet state.

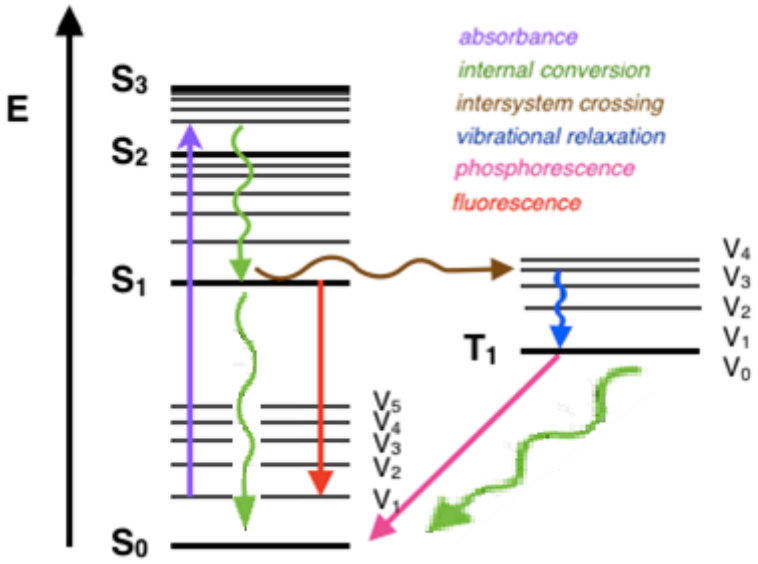

Figure 1: Jablonski diagram

The colored lines in Figure 1 show the main subsequent possible de-excitation processes when a photon is absorbed by a luminescent molecule and is excited from its ground state (S_0) to some higher vibrational level of either the first or second electronic state (S_1 or S_2) (3).

The first way that energy may be dissipated once an electron is excited is through vibrational relaxation, a non-radiative process. This is indicated on the Jablonski diagram as a curved blue arrow between vibrational levels.
Vibrational relaxation is where the energy deposited by the photon into the electron is given away to other vibrational modes as kinetic energy. This kinetic energy may stay within the same molecule, or it may be transferred to other molecules around the excited molecule, largely depending on the environment of the probed sample. This process is also very fast, between 10^{-14} and 10^{-11} seconds. Since this is a very fast transition, it is extremely likely to occur immediately following absorbance.

However, the excited electron can also move from a vibration level in one electronic state to another vibration level in a lower electronic state. This process is called internal conversion and is mechanistically identical to the vibrational relaxation. It is indicated as a curved green line in the Jablonski diagram, between two vibrational levels in different electronic states. Internal Conversion occurs because of the overlap of vibrational and electronic energy states. It takes also between 10^{-14} and 10^{-11} seconds, therefore, is a very likely way for molecules to dissipate energy from light perturbation.

Another pathway for molecules to deal with the received energy from photons is fluorescence, and it consists of emission of a photon. It is indicated on a Jablonski diagram as a straight red line going down on the energy axis between electronic states.
Fluorescence is a slower process on the order of 10^{-9} to 10^{-7} seconds; therefore, it is not a very likely path for an electron to dissipate energy especially at electronic energy states higher than the first excited state.
Fluorescence is most often observed between the first excited electronic state and the ground state for any particular molecule because at higher energies it is more likely that energy will be dissipated through internal conversion and vibrational relaxation.

Another path a molecule may take in the dissipation of energy is called intersystem crossing. In this case, the molecules spin multiplicity changes from an excited singlet state to an excited triplet state. It is indicated by a horizontal brown curved arrow from one column to another. This is the slowest process in the Jablonski diagram, on the order of 10^{-8} to 10^{-3} s, several orders of magnitude slower than fluorescence.
Intersystem crossing leads to several routes back to the ground electronic state. One direct transition is phosphorescence: a radiative transition from an excited triplet state to a ground state. Another possibility is delayed fluorescence, the transition back to the first excited singlet level, leading to the emission and radioactive transition to the ground electronic state.
Other non-emitting transitions from excited state to ground state exist and account for the majority of molecules not exhibiting fluorescence or phosphorescent behavior. One process is the energy transfer between molecules through molecular collisions. Another path is through quenching, energy transfer between molecules through overlap in absorption and fluorescence spectrums. These are non-emitting processes that will compete with fluorescence as the molecule relaxes back down to the ground electronic state.

2.2 Oxygen quenching

Luminescence can be decreased by a wide variety of processes. Such decreases in intensity and lifetime are called quenching.
Quenching can occur by different mechanisms. Collisional quenching happens when the excited-state is deactivated upon contact with some other molecule, which is called quencher. The molecules are not chemically altered in the process. This phenomenon is shown in Figure 2.

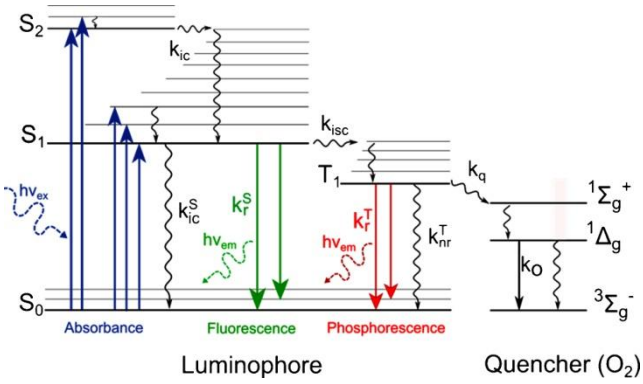

Figure 2: Jablonski diagram of the luminophore and the quencher (1)

A wide number of molecules can act as collisional quenchers. The majority of the optical sensors developed for oxygen detection rely on quenching of the luminescence of an indicator dye by molecular oxygen (4).

For collisional quenching the decrease in intensity and lifetime is described by the well-known Stern-Volmer equation:

$$\frac{I_0}{I} = \frac{\tau_0}{\tau} = 1 + k_q \tau_0 pO_2 = 1 + K_{sv} pO_2$$

In this expression K is the Stern-Volmer quenching constant, k_q is the bimolecular quenching constant, I and I_0 are the luminescence intensities in the presence and absence of the quencher, τ and τ_0 are the lifetimes of the luminophore in the presence and absence of the quencher and Ksv is the Stern–Volmer quenching constant (5).

2.3 Sensing methodologies

Optical oxygen sensors rely on collisional quenching of the luminescence of the indicator by molecular oxygen. This results in a decrease of the luminescence intensity and the decay time.

The ability of oxygen to quench the luminescence emitted by the probe depends mainly upon the natural lifetime of the excited luminescent state in the absence of oxygen, the rate of diffusion and solubility of oxygen in the encapsulating medium and the efficiency of quenching (6).

Luminescent transition metals complexes, especially metalloporphyrins, are frequently used as indicators dyes. Polymers are mainly employed as matrix materials. Usually, the indicator dye is entrapped in the matrix and the resulting sensor is deposited onto an optical fiber or a support (7).

2.3.1 Dyes used for the experiments

Numerous classes of oxygen indicators based on the quenching of luminescence of appropriate indicators by molecular oxygen exist and feature significantly different photophysical and sensing properties (1).

When deciding the most suitable dye, there are many criteria that must be considered, such as the absorption and emission spectra, the luminescence brightness of the probe, the luminescence decay times, the chemical stability and photostability, the cross-sensitivity to other parameters, the solubility in polymeric matrices, but of course also the toxicity and the commercial and the availability of the starting materials. (1)

This thesis focuses on the analysis of one of these criteria: the photostability of the dye. Although the chemical stability of the majority of the indicators used for oxygen sensing is acceptably good, their photostability in harsh conditions (high pressure and continuous high light exposition) can be poor.

Among all the existing indicators for optical oxygen sensors, Pt(II) and (Pd) porphyrins are the most popular luminophores. A large number of platinum and palladium porphyrin complexes have been synthetized and modified to improve their photophysical and solubility properties. In this work, these properties are compared in order to determine which dyes are more resistant and robust.

Table 1 shows the structures and absorption wavelengths of all dyes used in the measurements.

Dye	Structure	λ_{max}^{abs} [nm]
Pt-TPTBP	$C_{60}H_{36}N_4Pt$ 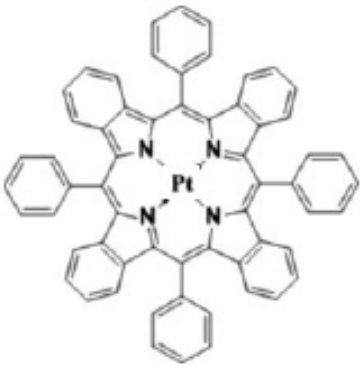	430 614
Pt-TPTBPF	$C_{60}H_{32}F_4N_4Pt$ 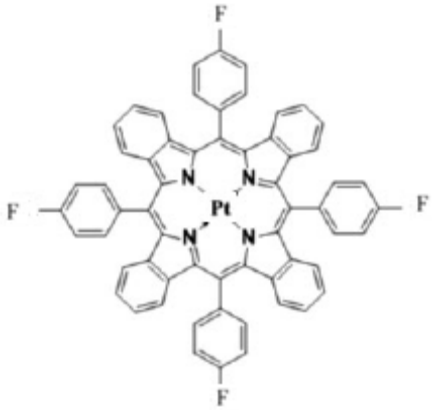	430 615

Pt-TertButyl I	$C_{84}H_{92}N_4Pt$ 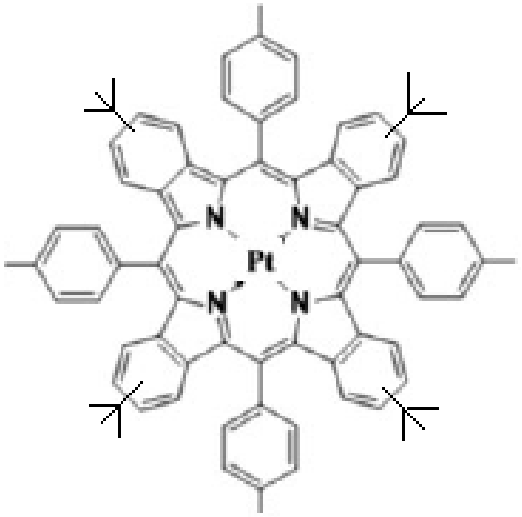	437 619
Pt-TertButyl II	$C_{60}H_{84}N_4Pt$ 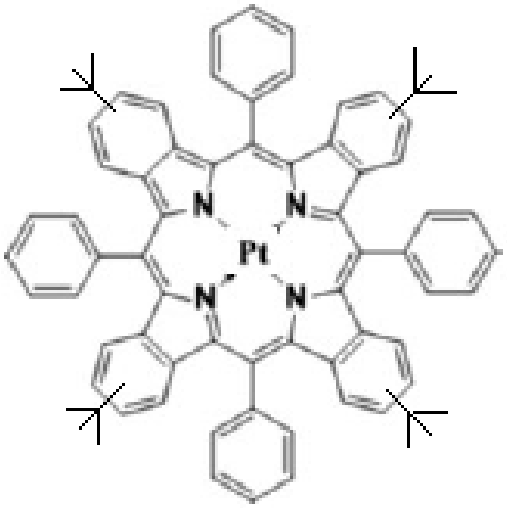	430 618
Pt-Cl-Benzo	*The structure of this dye can't be shown because of its use in some companies projects*	435 618

Pt-TetraSulfon	$C_{92}H_{96}F_4N_4O_8PtS_4$ 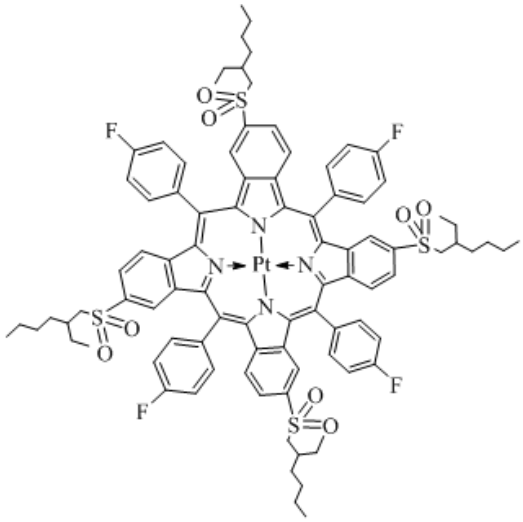	442 618
Pt-OctaSulfon	$C_{124}H_{160}F_4N_4O_{16}PtS_8$ 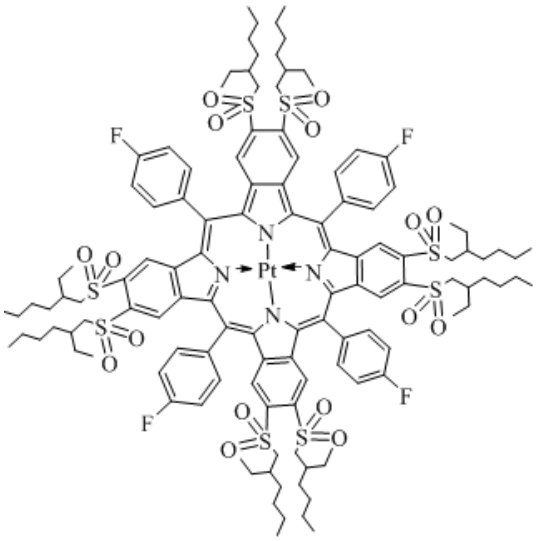	455 621

Table 1: Porphyrin dyes used for photostability studies

The first dye is used as a reference to compare to all the others which have been modified adding different groups of substituents.

Due to the fact that photosensitized singlet oxygen is often responsible for the photodegradation of indicator dyes through oxidation, the introduction of electron-withdrawing substituents in the indicator molecule improves their photostability. For this reason, complexes of platinum with highly electronegative groups (F, Cl) have been tested. However, this kind of groups tend to make the complex less soluble.

In order to achieve a highly soluble molecule, one can add t-butyl groups to the basic porphyrin. These groups increase the solubility of the dye but due to their electron-donating character, they give electrons to the molecule, making it more prone to oxidation.

The last molecules shown were prepared in attempt to improve both properties at the same time. The sulfon group withdraws electrons potentially making the dye more photostable whereas the hydrocarbon group facilitates its solubility.

3 Pressure measurements

The first part of this thesis is focused on the characterization of optical sensors at high hydrostatic pressure for oceanographic applications. With the aim of accomplishing this purpose a pressure chamber was used for several tests. Oxygen in several samples was measured with optical sensors inside this chamber at different pressures, and the results were plotted and analyzed with two main targets: detect possible malfunctions of the set up or the procedure for its following improvement and characterize the behavior of the sensors in hard conditions (high hydrostatic pressures).
Before starting with all the experiments, some tests had to be performed, since all the set-up used was new. In order to set the appropriate conditions and the most suitable mode of action, measurements were started by checking first the operation of the chamber and then adding more conditions which led to the results one wanted to examine.
Some failures and required improvements were detected in the course of the analysis and even though one couldn't draw precise conclusions about the behavior of the dyes in different pressures, improved practices and new guidelines were developed for further work in this field.

3.1 Experimental set-up

The basic requirement of this part of the project was a reactor able to change the pressure of a certain medium without exchanging fluids to the exterior. This reactor had to make it possible to measure continuously the concentration of oxygen in the medium.
With this purpose a pressure chamber built in the laboratory was used, connected to the devices and technology acquired from PyroScience.

3.1.1 Pressure chamber

The pressure chamber was designed and constructed due to the need to perform these experiments.

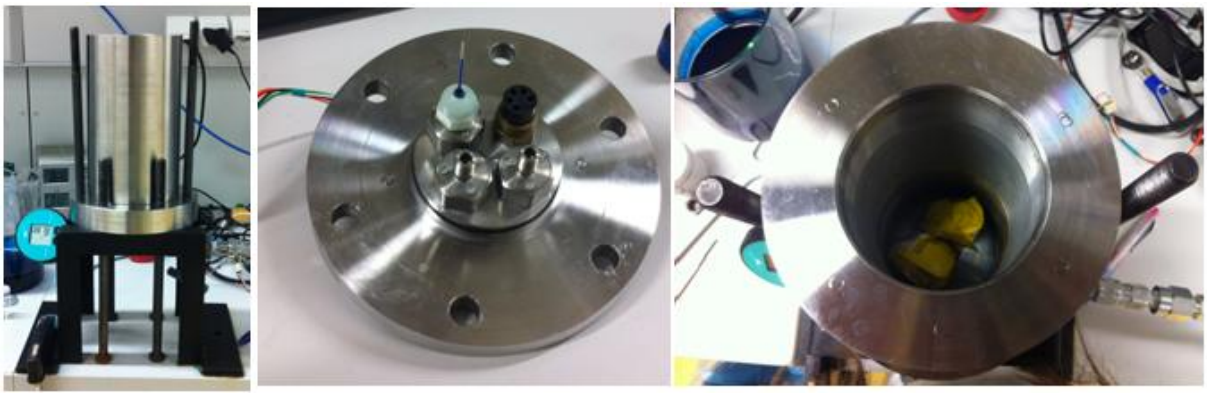

Figure 3: Pressure chamber pictures

As it can be seen in Figure 3, it consists of a cylindrical chamber of steel fixed to the table with a metallic support. The top, also made of steel, has three holes in order to fix the devices there, allowing connect the glass fibers with the dye in the part that is placed inside the chamber and the electronic devices to get the signal in the other side. It has also one connection for the stirrer, which is placed inside the chamber. The top is fixed to the cylinder with 6 screws.
In the left side of the reactor there is a manometer to measure all the time the pressure inside the chamber. On the right, there is a valve connected to the pump tube.

3.1.1.1 Assembly instructions

- In a beaker, distilled water was stirred and bubbled with pressure air for 15 min
- Fill half of the chamber with the water
- Introduce the stirrer
- Fill the chamber with the rest of the water to the top
- Connect the stirrer. Verify it is working.
- Put the top on the chamber ensuring that the coatings don't get damaged, open the two valves of the pump and fix it manually being careful that no oxygen comes inside.
- Scroll the screws and connect the devices
- Open the software system and start logging the data

3.1.1.2 Operating instructions

Once the reactor is properly closed, the pump can be used to change the pressure inside the chamber.

3.1.1.2.1 Increase the pressure

- Open the chamber valve
- Pump until the manometer indicates the desired pressure
- Close the chamber valve

3.1.1.2.2 Decrease the pressure

- Open the pump valve carefully until the manometer of the pump indicates a lower pressure than the desired one
- Close the pump valve
- Open the chamber valve
- Check the pressure in the manometer chamber. Repeat the process until the pressure is correct

3.1.2 Optical oxygen meter

The optical oxygen meters used were the "FireStingO2 Mini", Figure 4, which are a high precision, PC-controlled (USB) fiber-optic oxygen meters available with 1 channel for optical oxygen sensors from Pyro Science.

Figure 4: FireStingO2 Mini by PyroScience

3.1.3 Software

This device was used with the versatile Windows logger software "Pyro Oxygen Logger". This software allowed saving and showing the data measured with the sensors for its future plotting and interpretation. The main interface of the program is shown in Figure 5.

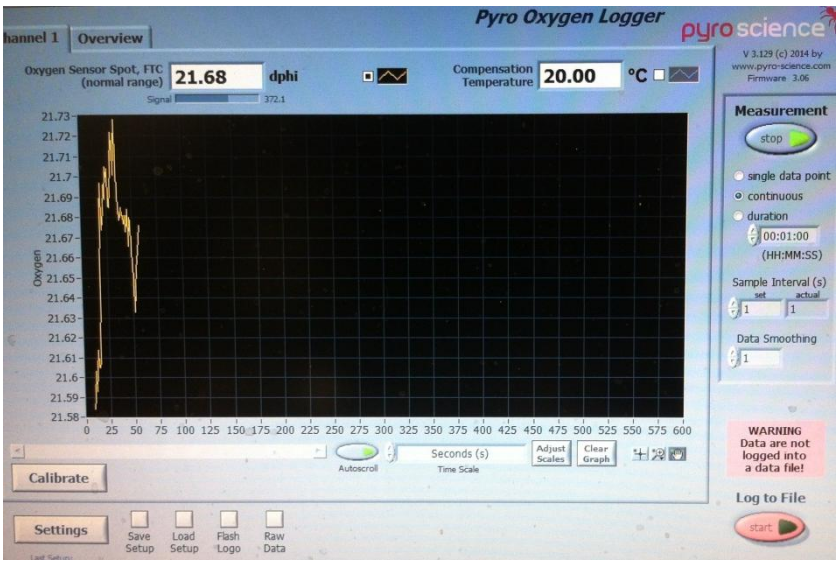

Figure 5: Screenshot of the sofware used

3.2 Preparation of the sensor

The dye used in this part of the thesis was Pt-Cl-Benzo. The “cocktail” had been already prepared. The sensing material was tip-coated onto a distal end of optical fiber to be placed in the top of the pressure chamber, as it is shown in Figure 6

Figure 6: Tip-coated optical glass fiber

3.3 Measurements

First measurements with the assembly were performed to test its correct operation and to set the most appropriate working conditions.
Before beginning with the experiments some problems had to be examined more closely. The pump wasn't working and it had to be fixed changing the water inside. It was spoiled because of the air that accidentally had come inside, so it was filled again and the water was pumped until no bubbles were coming outside to make sure there was no air.
After doing these arrangements one realized that it was still not working because there was a hole in the sack. New sacks were bought and one of them was placed in the reactor. The measurements performed are listed in Table 2.

Exp.	Dye used	Description
150310	Pt-Cl-Benzo	Air-saturated water inside the reactor
150311	Pt-Cl-Benzo	Air-saturated water inside the reactor and vial with normal water
150312	Pt-Cl-Benzo	Air-saturated water inside the reactor and vial with sodium sulfite solution
150313	Pt-Cl-Benzo	Air-saturated water inside the reactor. Sample interval: 5 seconds
150316	Pt-Cl-Benzo	Air-saturated water inside the reactor. 4 stabilizing short cycles
150317	Pt-Cl-Benzo	Air-saturated water inside the reactor. 4 stabilizing short cycles + 2 long cycles
150323	Pt-Cl-Benzo	Air-saturated water inside the reactor. 4 stabilizing short cycles + 1 cycle overnight
150324	Pt-Cl-Benzo	Air-saturated water inside the reactor. 4 stabilizing short cycles + 1 cycle overnight

Table 2: Summary of the initial high pressure measurements performed

3.3.1 Saturated water inside the reactor

The experiment ***150310*** was started after changing the sack and the water inside the pump and using three new coatings. Air-saturated water (1250 ml stirred during 15 min) was placed inside the reactor.
The measurement was started with good signal (approximately 500 mV) and oxygen was measured changing the pressure: 0-100-150-200-250-200-150-100-0 bar (waiting in each level ten minutes to be sure it was stabilized).

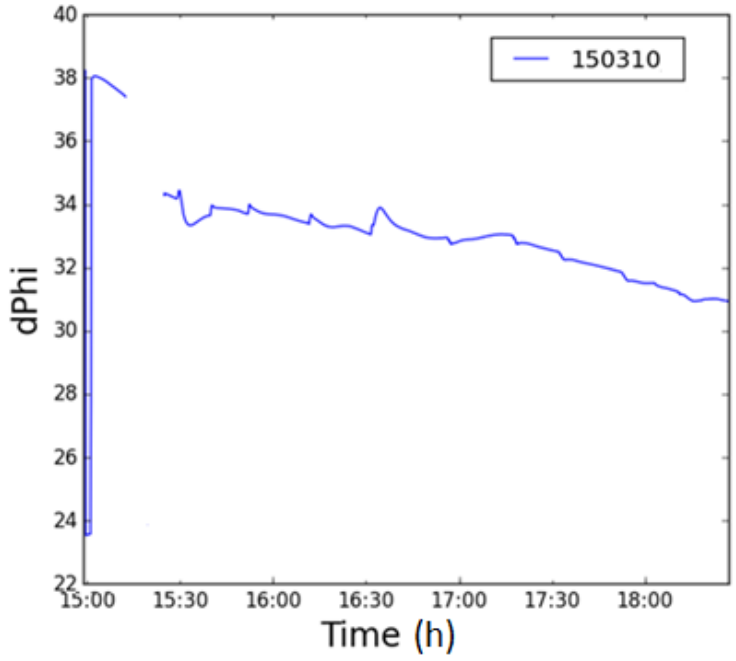

Figure 7: Experiment 150310. Phase angle dependency on hydrostatic pressure

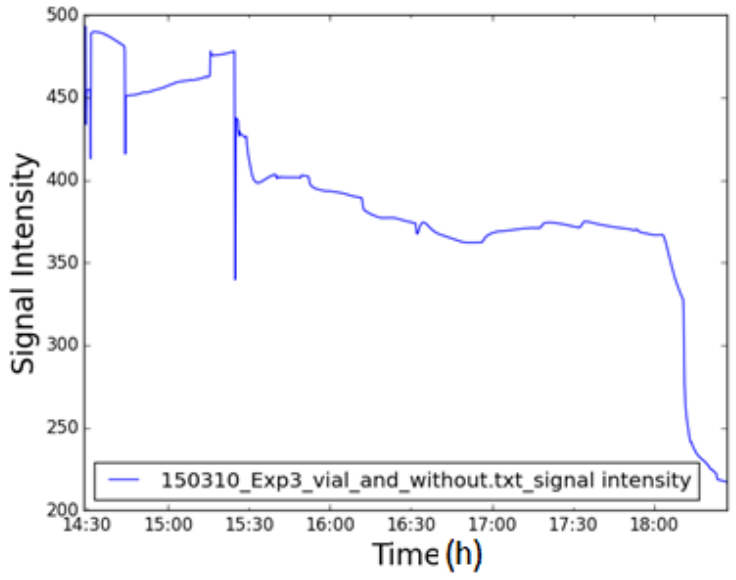

Figure 8: Experiment 150310. Signal intensity dependency on hydrostatic pressure

3.3.2 Measurements with vials

Experiment ***150311*** was performed under the same conditions as experiment 150310 but two kinds of samples were measured: air-saturated water (1250 ml stirred during 15 min) was placed inside the reactor and a vial was filled with no saturated water.

As it can be seen in the graph, the experiment showed a clear trend. It seems that some time is needed to stabilize the phase angle when one starts the measurement but then it reaches a more or less constant value. Every change on the pressure is easily detected in the curves because of a sudden variation of the phase angle (it always increases and then decreases

again when one is going to a higher pressure and acts the opposite way when one is going to a lower pressure). One can see that the signal is quite constant in each stage. The phase angle increases with the pressure but when the pressure decreases it does the same, achieving almost the same value that the one it had first in that pressure. This effect may be due to the more tight connections between the fibers and the devices at higher pressures, which improve the signal intensity and thus the phase angle (considering that certain background fluorescence is present in the system).

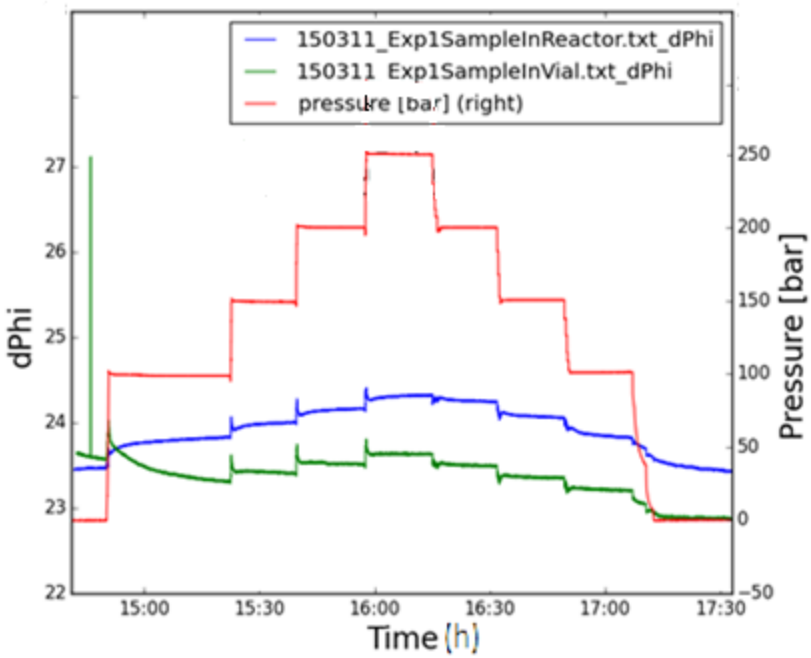

Figure 9: Experiment 150311. Phase angle dependency on hydrostatic pressure

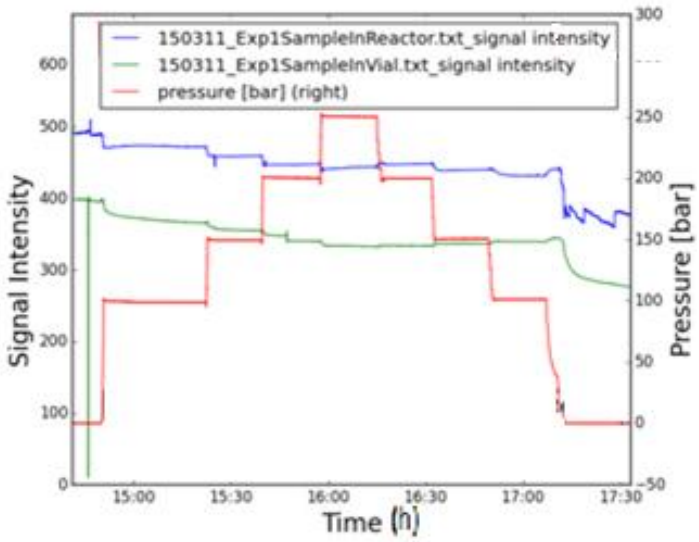

Figure 10: Measurement 150311. Signal intensity dependency on hydrostatic pressure

At this point, the performance of the system in air-saturated solution was investigated. In order to measure in deoxygenated conditions, a solution of 5.5 g of sodium sulfite in 25 ml of water was prepared.

The homogeneous solution was placed inside a vial with an optical fiber previously coated and inserted through the tap. Making sure that no bubbles were inside, the vial was closed and fixed in one of the connections in the tap of the reactor. A new bigger stirrer (egg one) was used.

In experiment ***150312***, two signals were evaluated. One measured the water (coming from 1250 ml stirred and bubbled for 15 min) inside the chamber and the other one the solution inside the vial. The signal was quite good for both devices (169 mV for the one inside the reactor and 700 mV for the one inside the vial).

After opening the reactor, one could notice that the stirrer wasn't working so for the next experiments it would be replaced for the small one again.

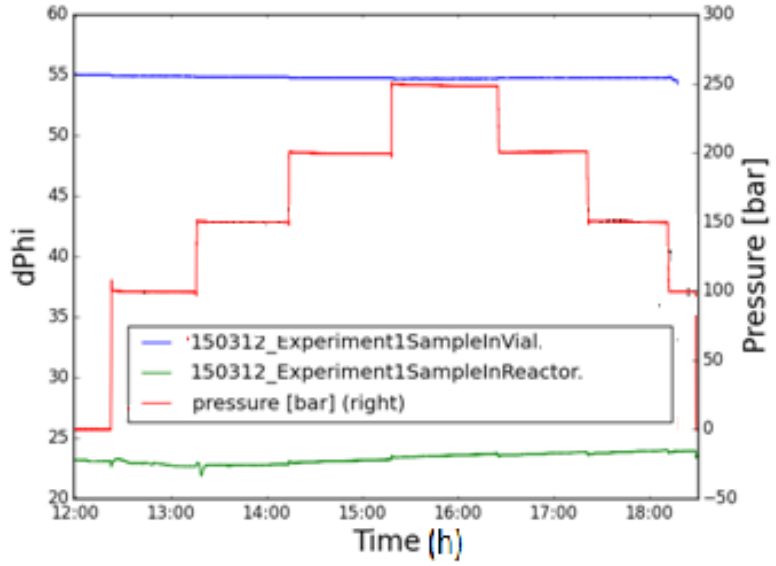

Figure 11: Experiment 150312. Phase angle dependency on hydrostatic pressure

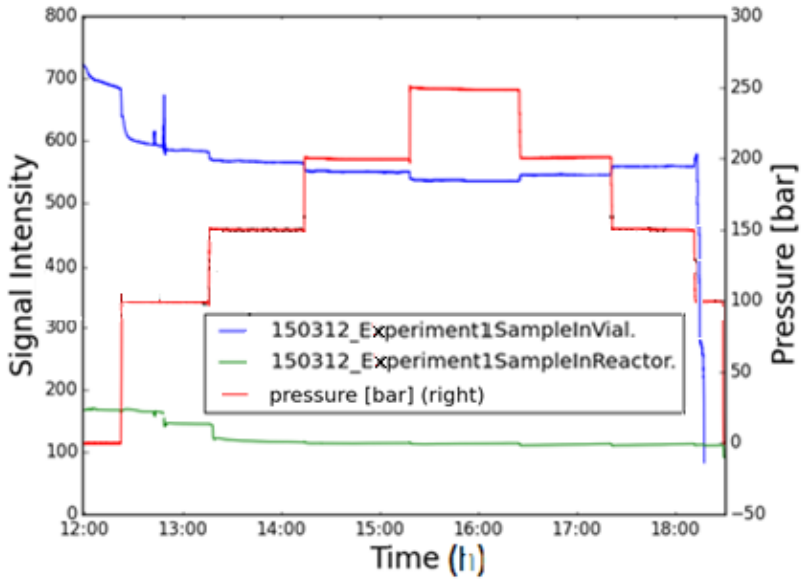

Figure 12: Measurement 150312. Signal intensity dependency on hydrostatic pressure

The graph shows quite constant values in the vial, although they decrease with the time. For the data in the reactor one can see the opposite behavior, the last values of the phase angle

were higher than the ones measured initially in the same pressure. For this reason, one considered necessary to check if the measuring conditions were affecting the results stored.

3.3.3 Change of the sample interval

First thing done was cleaning the chamber to ensure there was no solution inside. As every time, 1250 ml of water were bubbled and stirred for 15 min. The coatings were changed for two new ones.

The settings were changed. Only one device was used and its integration time was changed to 5 ms and the sample interval was 5 seconds (to check if the light causes photobleaching and therefore affects the measured values of the dye). Measurement ***150313*** consisted of one long cycle without stirring.

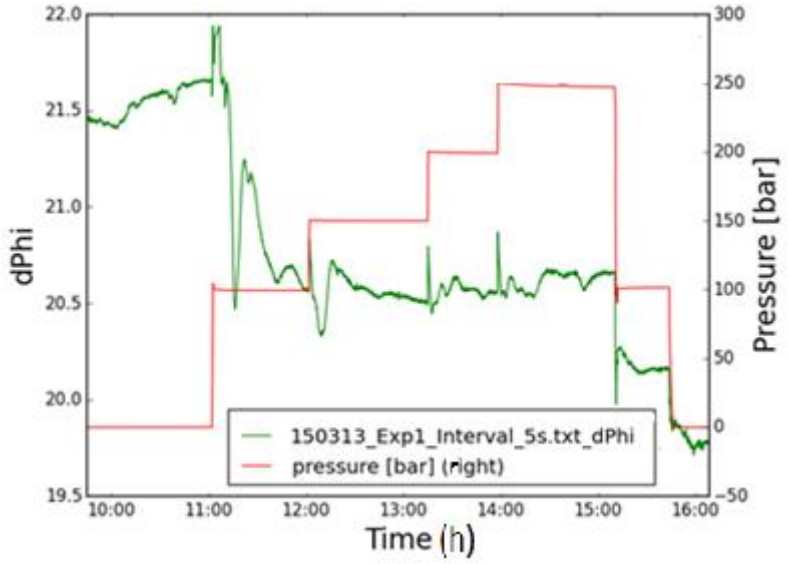

Figure 13: Experiment 150313. Phase angle dependency on hydrostatic pressure

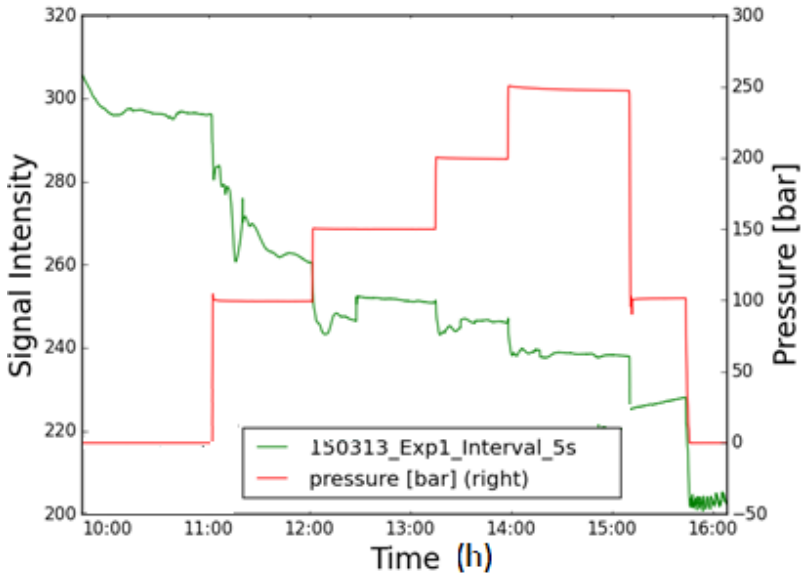

Figure 14: Measurement 150313. Signal intensity dependency on hydrostatic pressure

The graph shows the values were not really constant and although after longer waiting time in each pressure to stabilize the phase angle was changing all the time.
Finally, one new device was acquired, so following experiments were performed with 3 devices (measuring with 3 new coatings).

3.3.4 Short stabilizing cycles

After a close examination of all results so far, an unexplainable first stretch and then, after stabilization, more constant stretches, were detected. In order to check if there was hysteresis or any other effect, 4 cycles from 0 to 150 bar were performed in measurement ***150316***. One of the coatings (the one connected to the new device) failed after 10 minutes of measuring so the results only show the data from the old devices.

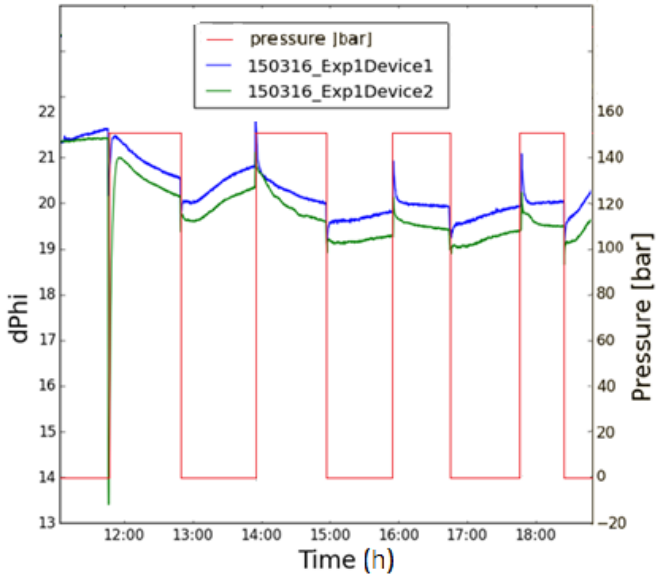

Figure 15: Experiment 150316. Phase angle dependency on hydrostatic pressure

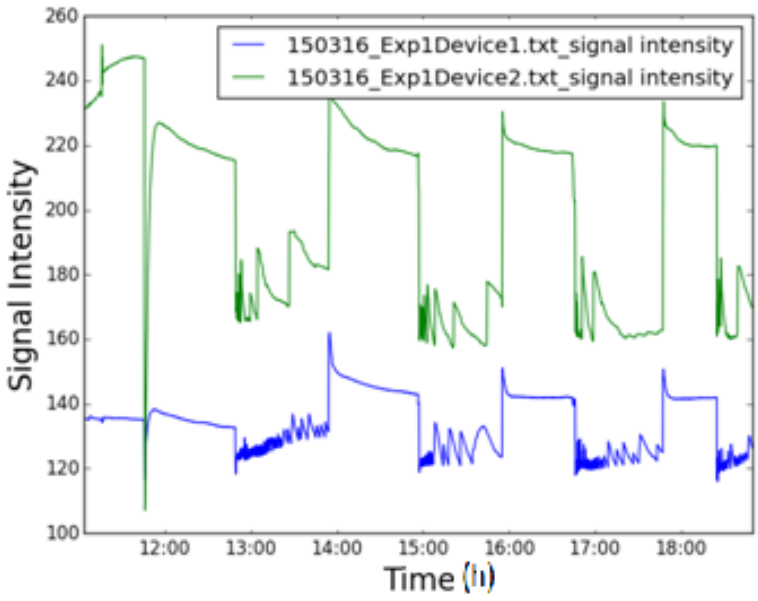

Figure 16: Measurement 150516. Signal intensity dependency on hydrostatic pressure

This graph shows the same trend for all the cycles, and with the time it seems they are getting more constant. For this reasons it would be interesting to repeat the same cycles until they are constant and then measure a curve.

Measurement ***150317*** continued with the previous cycles to stabilize the readings. In this case, the pressure curve consisted of 4 first short cycles from 0 to 150 bar (waiting 15 min in each stage) and 2 long cycles from 0 to 150 bar (waiting 30 min in 0 bar and 1 hour in 150 bar).

Three different attachments were used: the new device was fixed to a newly-coated fiber, and the two old ones were attached to different fibers: one newly-coated and one used the day before. The sample interval was 10 seconds and the stirrer was working.

One expected to see more stable values after the 4 first cycles but the phase angle didn't achieve a constant value afterwards.

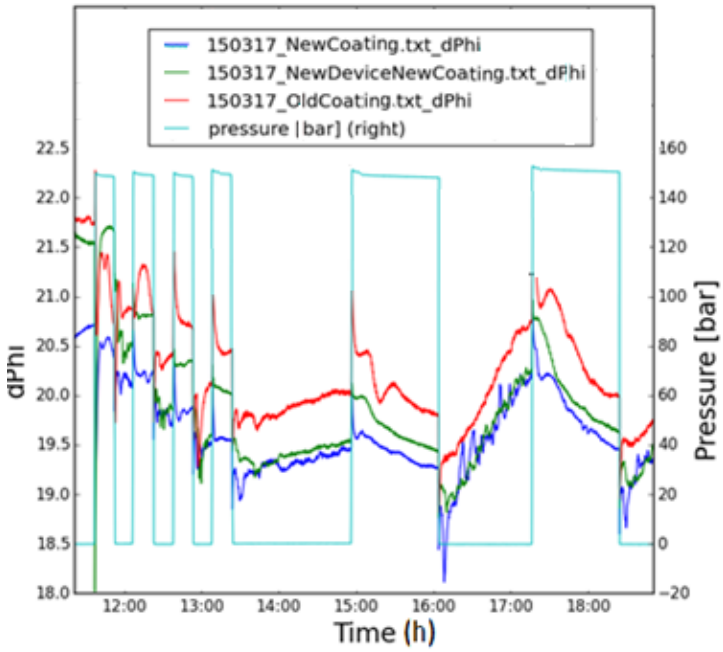

Figure 17: Experiment 150317. Phase angle dependency on hydrostatic pressure

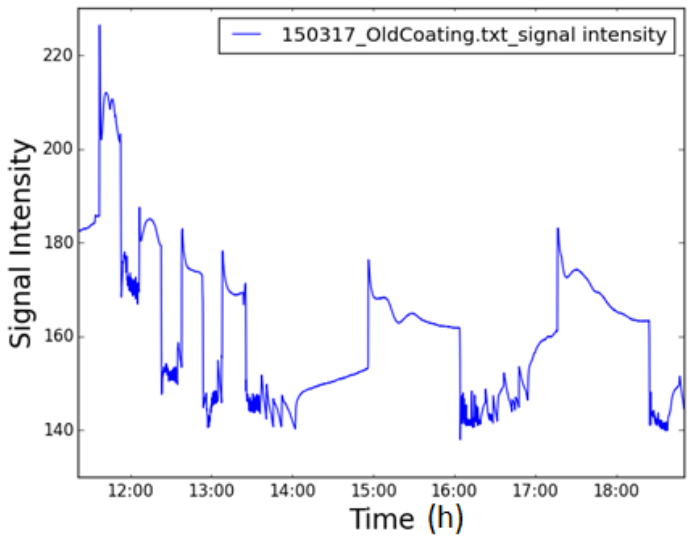

Figure 18: Experiment 150317. Signal intensity dependency on hydrostatic pressure

3.3.5 Long measurements overnight

Again, 4 previous cycles were performed in the measurement ***150323***. After the first part, the pressure was changed measuring every 100 bar until 300 bar and going down again, waiting one hour in each stage. Once the cycle was done, the devices were left measuring during the whole night to see if there were changes in the oxygen concentration or if it was possible to reach a stable value after several hours without pressure changes. The sample interval was 10 seconds and the stirrer was working. All the coatings were new.

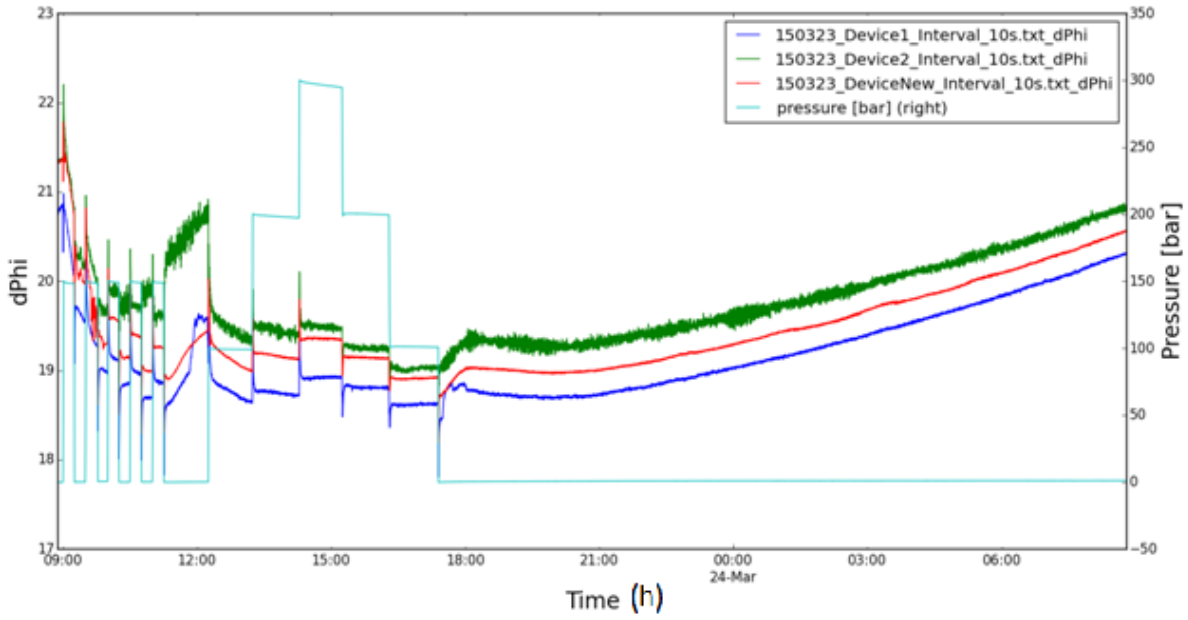

Figure 19: Experiment 150323. Phase angle dependency on hydrostatic pressure

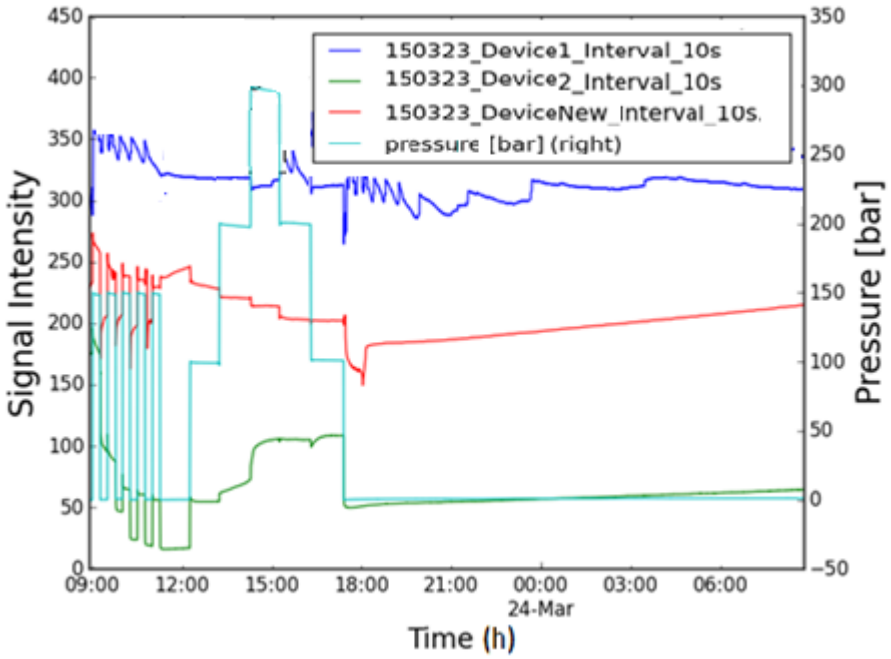

Figure 20: Experiment 150523. Signal intensity dependency on hydrostatic pressure

This time it seems that the 4 cycles helped to stabilize the next values and the cycle from 0 to 300 shows really constant values in each pressure stage, achieving almost the same value for the same pressures, and for the first two hours at 0 bar after the cycle, it seems that the value of the phase angle is constant. However, during the night (from 8:30pm) the phase angle starts to increase (increasing more with the time).

For the experiment ***150324***, as the last two times, 4 fast stabilizing cycles were performed in the beginning. The pressure was raised from 0 bar to 150 bar again and then to 300 bar before going down. The conditions were the same as the experiment 150323.

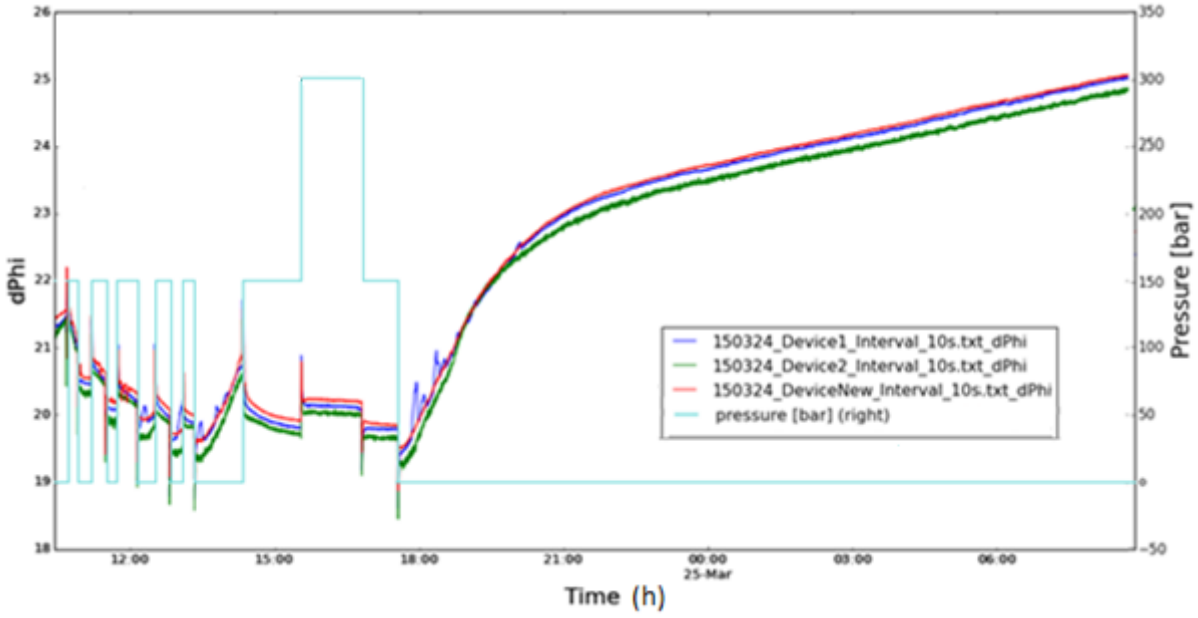

Figure 21: Experiment 150324. Phase angle dependency on hydrostatic pressure

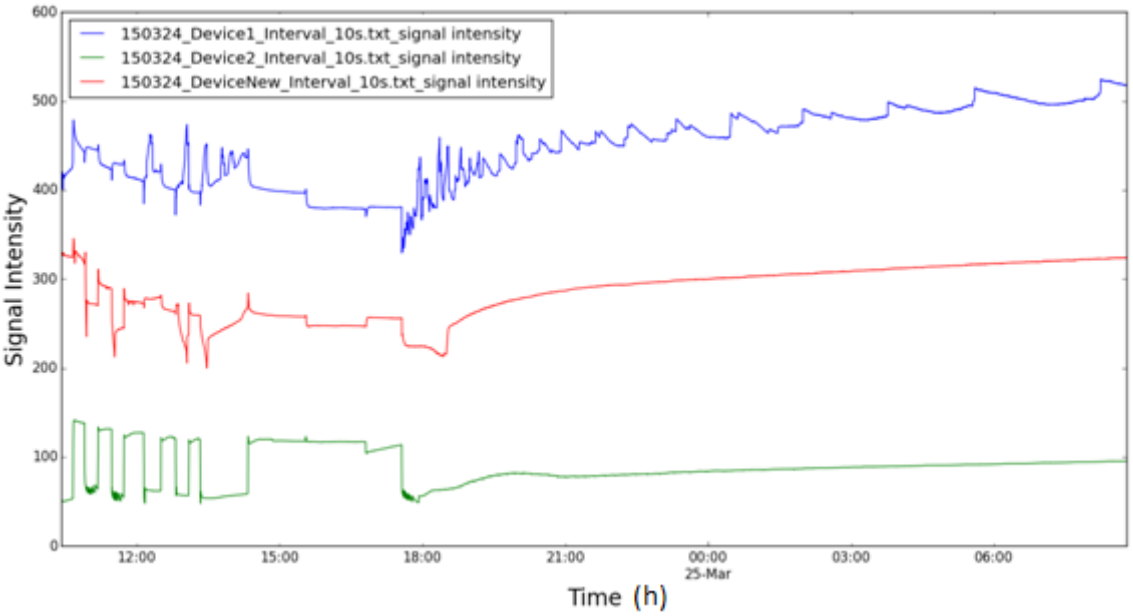

Figure 22: Experiment 150524. Signal intensity dependency on hydrostatic pressure

The graph shows again constant values for the long cycle but this time the phase angle in 0 bar after the cycle don't stabilize at any time. It increases really fast the first hours and then keeps increasing but at a slower pace.

3.4 Tests and corrections

The results recorded during all the experiments performed with the reactor didn't show a constant trend so one considered necessary to assess whether that unexplained behavior was caused by a failure in the set-up or the procedure.
A new sensor "cocktail" had to be prepared for the tests since the first one was empty. The amounts showed in Table 1Table 3 were used. To begin, the previously calculated quantity of the desired dye was dissolved in a specific mass of chloroform. Then, the Polystyrene 250,000 was added and mixed until it was a homogeneous solution, and the cocktail was covered with aluminum paper and stirred for 30 minutes.

Dye	**Mass Dye** [mg]	**wt% Dye** [%]	**PS** [g]	**wt%PS** [%]	**$CHCl_3$** [g]
Pt-Cl-Benzo	0,75	1,50	0,050	8,33	0,6000

Table 3: Composition of the cocktail used in the tests of the pressure chamber

3.4.1 Checking if the pump is functioning

The functioning of the pump was one of the aspects checked. In order to verify its regular operation, some of its conditions, such as the number of pumps and the volume of remaining water in the big test tube used to pump inside the sack, also were recorded.

Time	Pressure [bar]	Pumps	Volume [ml]
	150506		
11:56	0	-	560
12:16	98,6	10	490
12:36	198,2	5	480
12:58	297,8	4	480
12:18	404,0	4	470
	150507		
11:33	0	-	540
11:48	56,8	8	470
12:04	167,0	6	470
12:20	217,6	2	470

	150512		
12:51	0	-	500
13:11	52,6	8	450
13:33	149,8	7	450
13:53	200,6	4	450
08:46	148,4	-	470
09:06	51,0	-	480
09:26	0	-	500
	150513		
16:12	0	-	600
16:32	51,2	7	590
16:52	153,0	12	570
17.12	204,6	5	590
09:00	150,8	-	590
09:20	51,4	-	600
09:47	0	-	600

Table 4: Conditions of the pump during the tests

The results for the values noted were expected to be constant for every measurement (same pumps needed and same volume of water used). As it is shown in Table 4, the volume of water used to every change of pressure is quite similar, even though there are some differences in the amount of pumps.

The numbers obtained in ***150513*** seem to be the most different ones, but one could attribute this shift to the fact that the sack and the water were changed before the measurement since there was a hole in it. The most easily comparable experiments are ***150507*** and ***150512*** due to its similar pressure curve. In both cases, similar number of pumps to reach every pressure stage and similar volumes of water are noted.

After these tests, one can conclude that probably it should be necessary to improve the pumping system since there are many things that can fail –and have failed- and may affect the results obtained. Some of the problems faced during the measurements were due to the presence of air in the pump tubes or the possibility of a hole in the sack.

3.4.2 Coloring of the pump water

One of the possible failures considered was the release of water from the pump to the chamber. This malfunction was checked by coloring the water inside the pump with a food color and by taking samples after the pressure measurements to look if it contained traces of the colorant.

Two coloring materials were considered for this purpose: blue and red water-soluble dyes. In intend to compare both and determinate the one that could be used, a concentrated solution of each one was prepared.

The absorption spectrums of both solutions were used as a reference to compare with the absorption spectra of different test-samples of water and 10 µl of the concentrated solution. This experiment was performed due to the necessity to ensure that the presence of the colored solution was possible to detect in the water of the chamber even if there was only a really small amount of it inside. The blue colorant was easier to detect in the absorption spectrum at low concentrations so it was chosen for the tests.

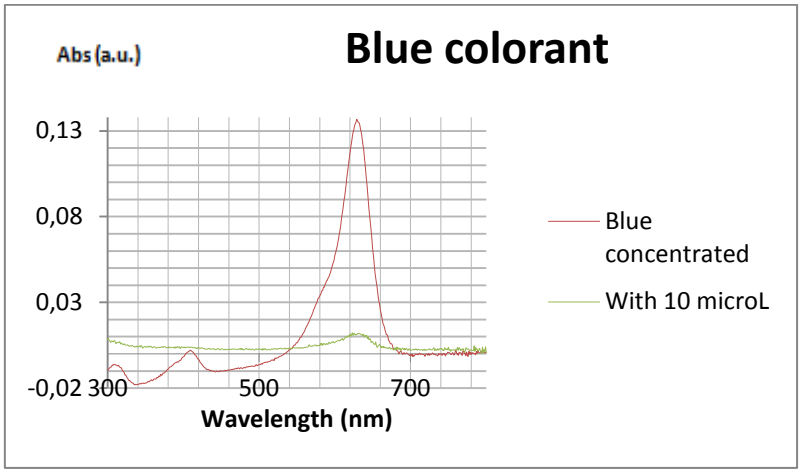

Figure 23: Absorption spectrum of the blue dye in solution

Figure 23 shows the absorption spectrum of the blue concentrated sample that was going to be used in the pump and the spectrum of a sample of water equivalent to the volume of water in the reactor plus 10 µL of blue concentrated water. This way one ensured that quantities of 10 µL or more of water coming from the pump could be detected with the absorption spectrum of the sample.

The first experiment, ***150505***, consisted of a long cycle from 0 to 300 bar measuring in between at 50 and 150 bar and then going from 300 to 0 bar following the same middle steps. The sample interval was 10 seconds and the stirrer was working.

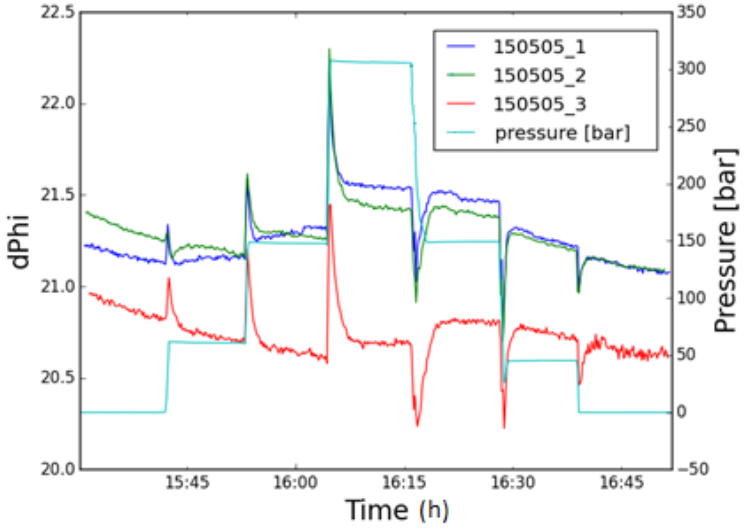

Figure 24: Experiment 150505. Phase angle dependency on hydrostatic pressure

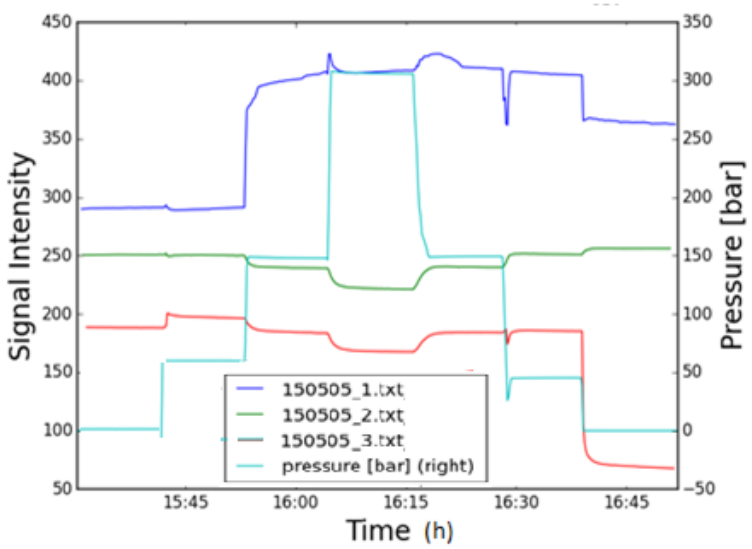

Figure 25: Experiment 150505. Signal intensity dependency on hydrostatic pressure

Once the cycle was finished, the water was analyzed. A sample of the initial stirred water was used to measure the baseline and then two samples were plotted: the water inside the reactor before starting the cycle and the water inside the reactor after it.

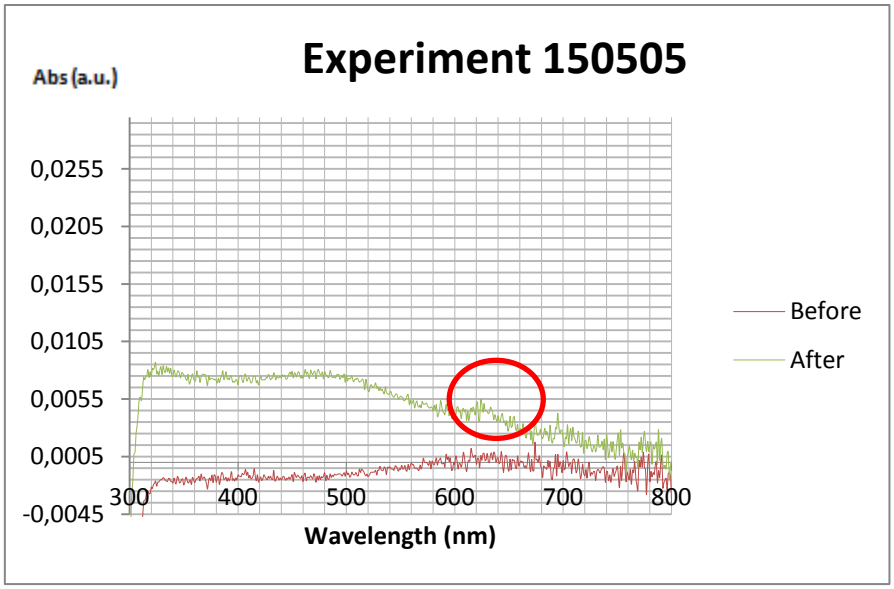

Figure 26: Experiment 150505. Detection of color in the sample

The results obtained are shown in Figure 26. A little curve is observed. This means that more than 10 µl came into the reactor.

In order to check if no water was coming from the pumb at higher pressures, the experiment **150506** was repeated at increased pressure of 400 bar, overnight. The extraction and measurement of the water samples was performed as described above.

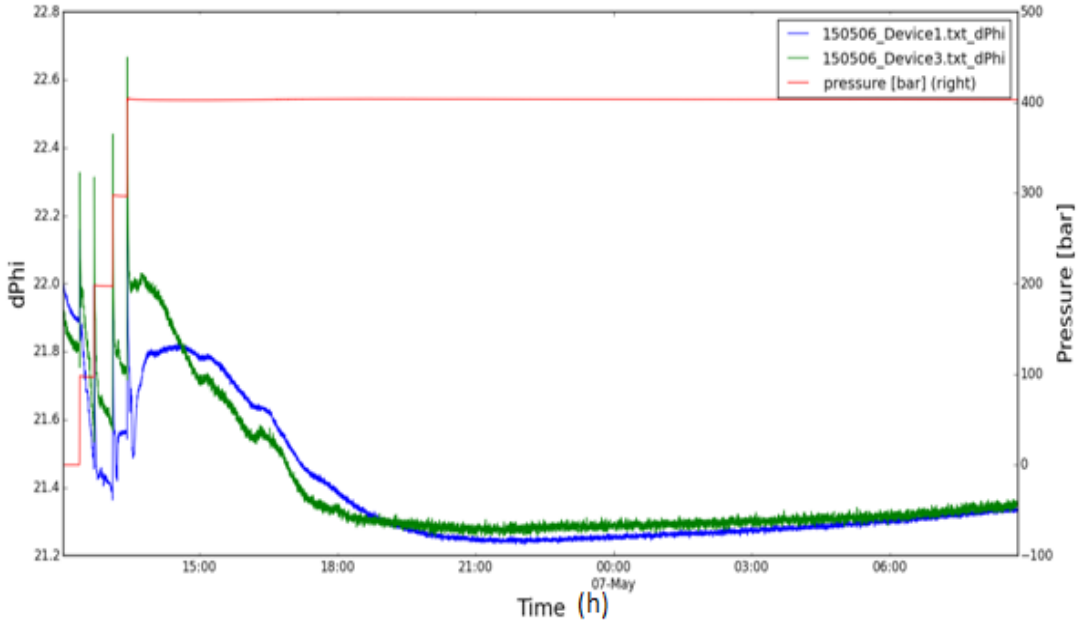

Figure 27: Experiment 150506. Phase angle dependency on hydrostatic pressure

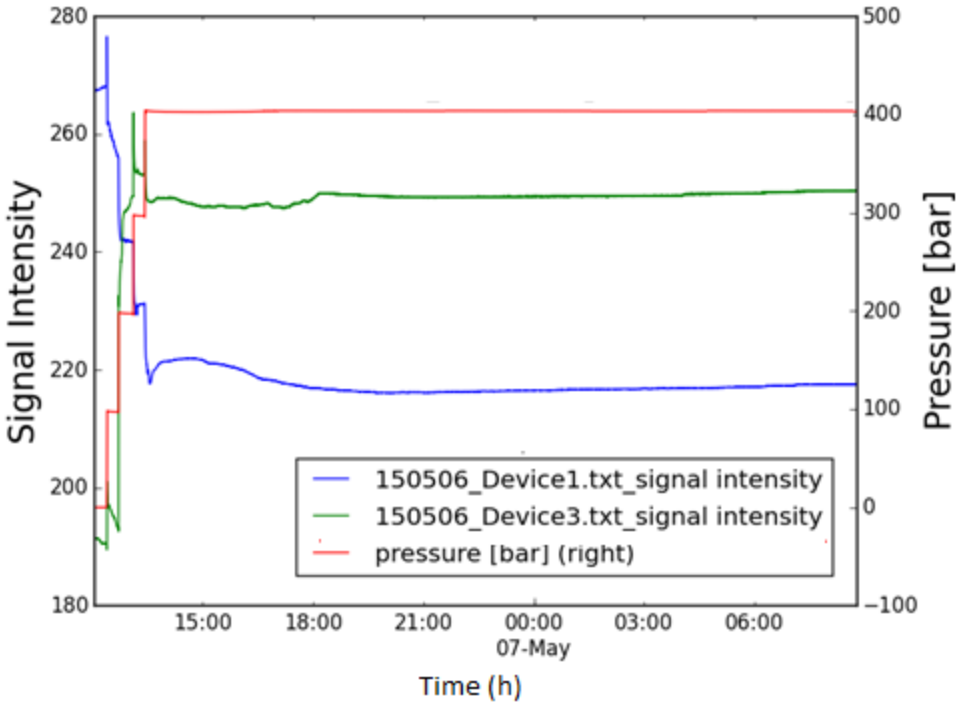

Figure 28: Experiment 150506. Signal intensity dependency on hydrostatic pressure

Figure 29 shows the absorption spectrum of the samples. A curve at the wavelength of 629 nm can be easily detected, which means some blue water from the pump came inside the reactor.

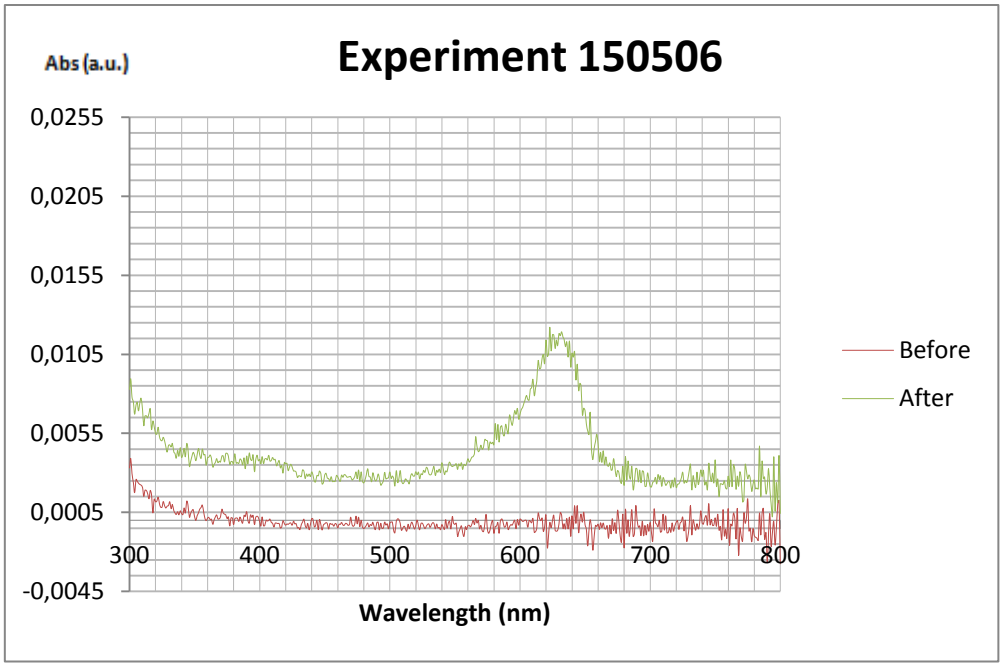

Figure 29: Experiment 150506. Detection of color in the sample

To verify the results, and because pressure of 400 bar was considered really high, a new test was performed. The pressure chamber was left at 200 bar for 4 days. Experiment **150507** should ensure that there was no exchange of water between the chamber and the pump at lower pressures even if the period of time was longer.

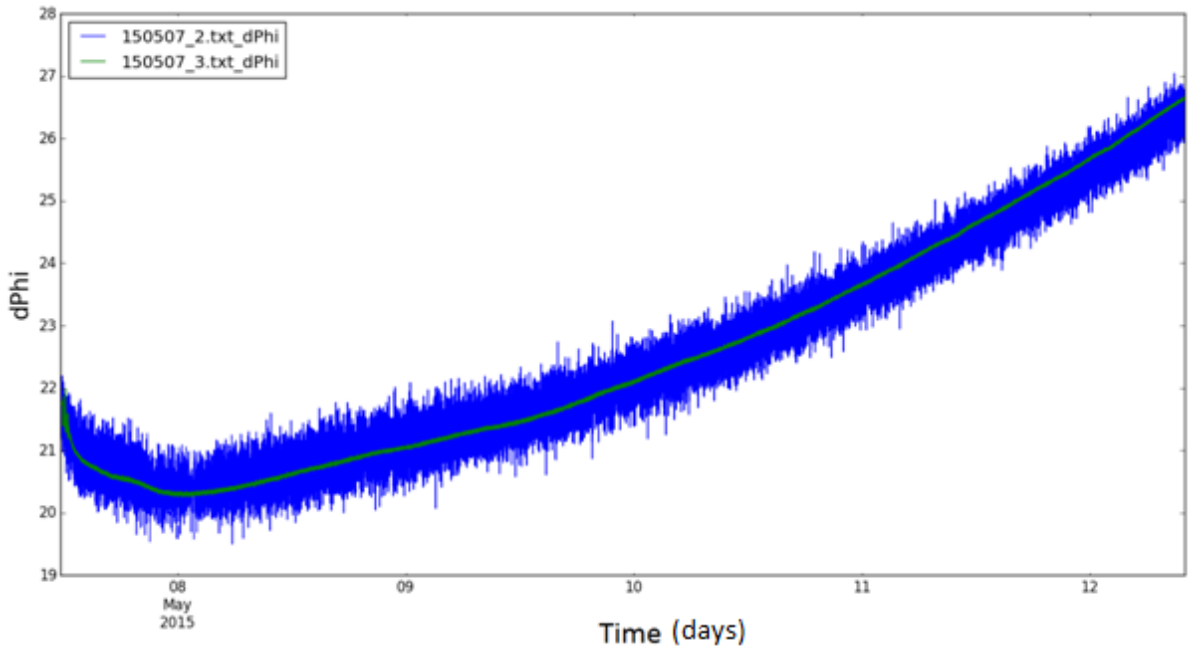

Figure 30: Experiment 150507. Phase angle dependency on hydrostatic pressure

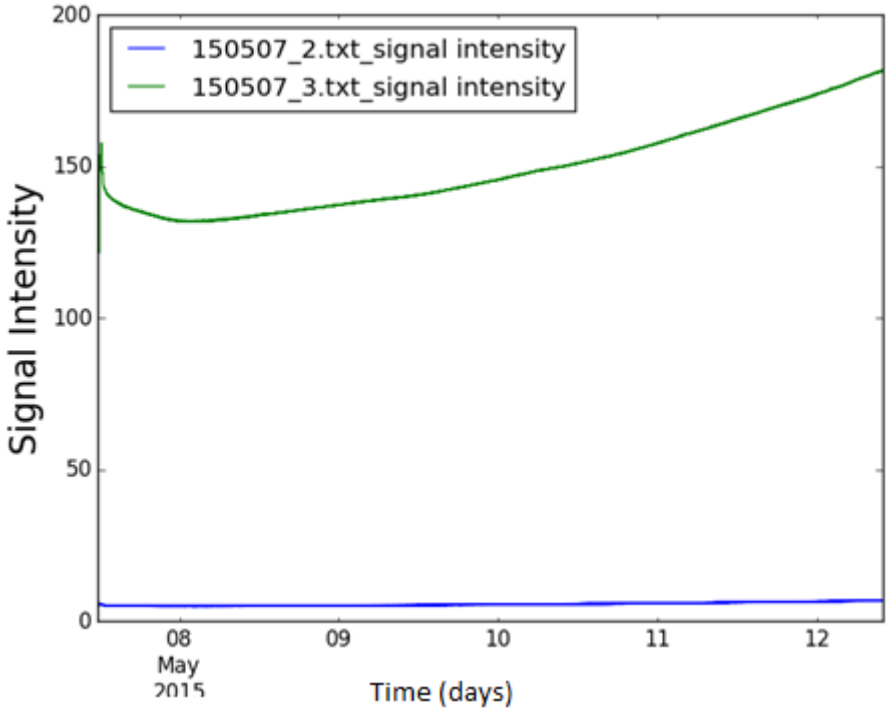

Figure 31: Experiment 150507. Signal intensity dependency on hydrostatic pressure

Figure 32 shows the presence of blue water in the reactor after the experiment. Despite the fact that the pressure was lower there was water coming inside the reactor again.

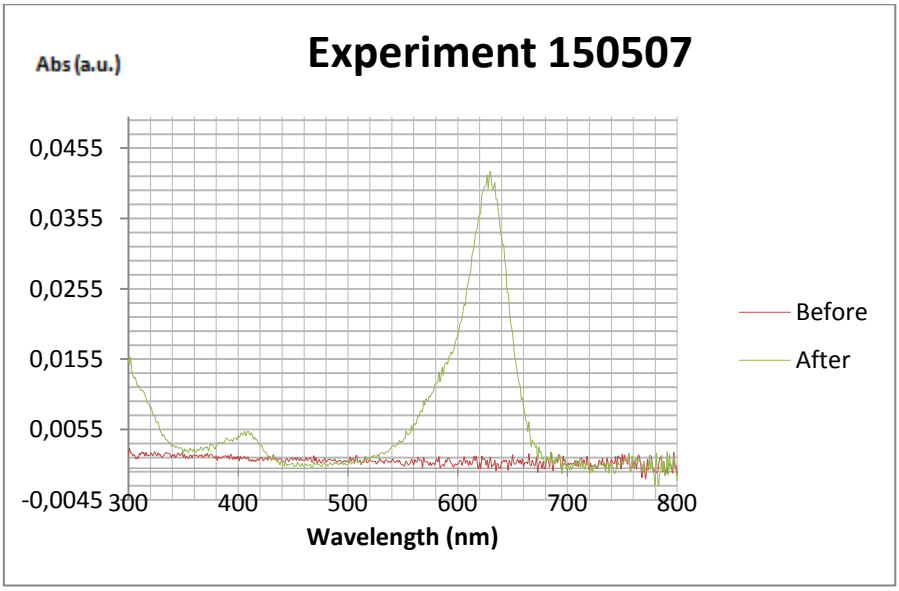

Figure 32: Experiment 150507. Detection of color in the sample

These experiments showed that some arrangements had to be made to avoid more water from the pump coming inside the reactor since this undesired event affects significantly the phase angle measured during every test and could be one reason for the unexplainable curves obtained in the previous measurements.

3.4.3 Coloring of the chamber water

Because some measurements had been performed with vials inside the reactor which didn't contain the same substance as the reactor, it was necessary to check if there was water from the reactor coming inside the vials during the measurements. This could then mean that the results obtained with that assembly were not valid since the sample inside the vial might be also contaminated.

With this purpose, blue water was prepared in the same way that the one inside the pump to fill the chamber and one vial with non colored water was placed inside the reactor.

First of all, one sample of the water inside the vial was taken, in order to compare its absorption spectrum with the absorption spectrum of the water inside the vial after the experiment. The reactor was left during one night at 200 bar. Device 1 measured the water inside the vial and device 2 measured the water inside the chamber.

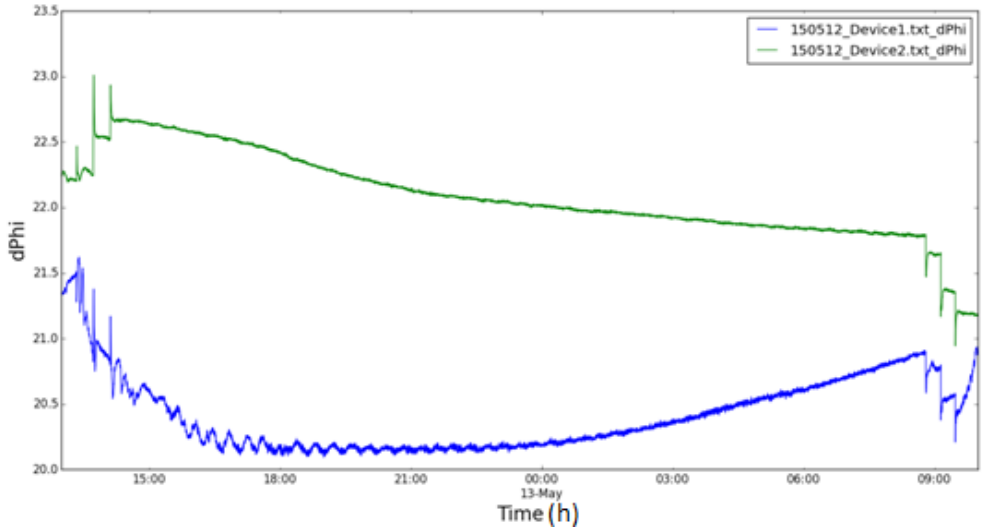

Figure 33: Experiment 150512. Phase angle dependency on hydrostatic pressure

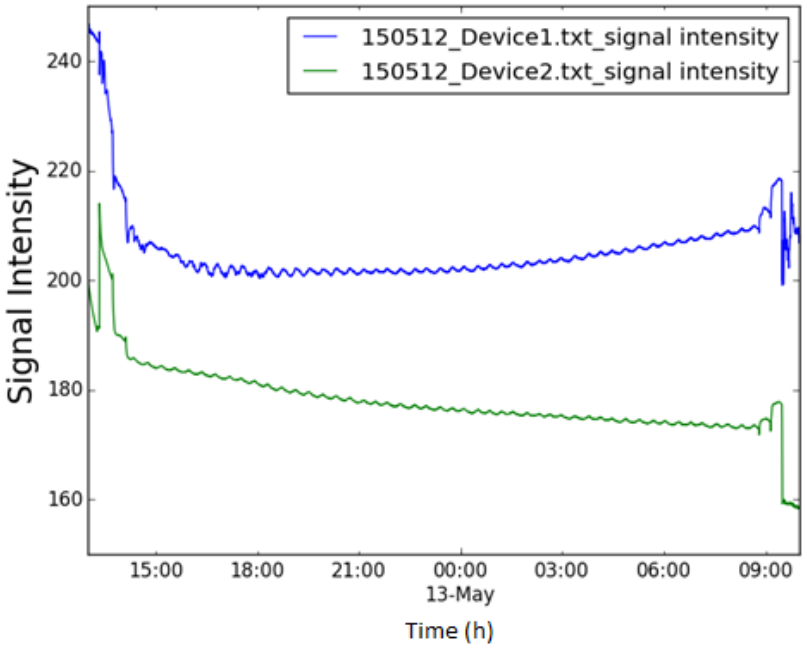

Figure 34: Measurement 150512. Signal intensity dependency on hydrostatic pressure

With this experiment, one also wanted to know if the substance inside the vial could be contaminated after opening it. For this reason the absorption spectrum of the water before the trial was compared to the sample from the vial obtained without opening it. This sample was taken with the help of a syringe.
Observing Figure 35 one can conclude that some of the blue water had came inside the vial (blue path) and that after opening the vial some drops of the solution inside the reactor can easily come inside the vial. This means that if one needs to analyze a sample from a vial it has to be obtained via syringe.

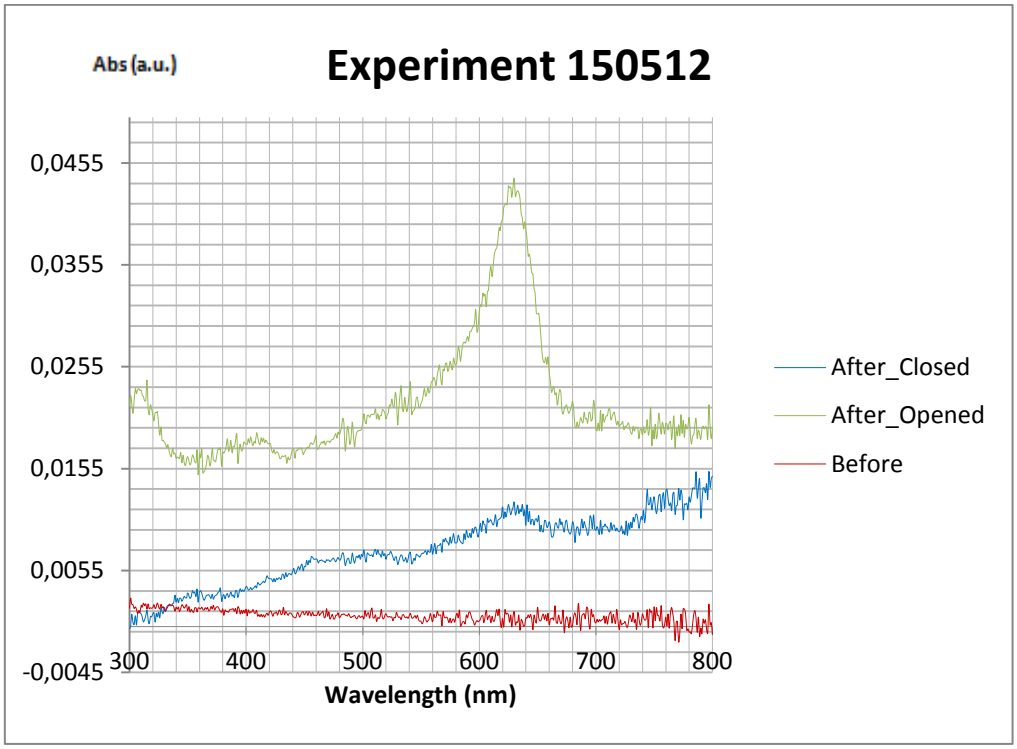

Figure 35: Experiment 150512. Detection of color in the sample

Due to the need to find one way to perform the experiments with vials, a thicker membrane was tried to tap the vial. Experiment ***150513*** consisted of a long cycle, starting at 0 bar, raising the pressure to 50 bar, 150 bar and finally 200 bar.
The reactor was left measuring for one day at that pressure and then the pressure was decreased with the same steps. Two vials were used: the thin membrane used in all the other trials and a new thicker one.
The water inside the vials was replaced by a solution of 5 % Na_2SO_3. The solution was prepared weighting the desired mass of sodium sulfite with the analytical balance and adding water. A crystal of $CoCl_2$ was added to catalyze the reaction.
Finally, the solution was stirred until it was completely dissolved and then filled inside the vials.
The coating of the thick vial felt and its phase angle and intensity of signal was not recorded.

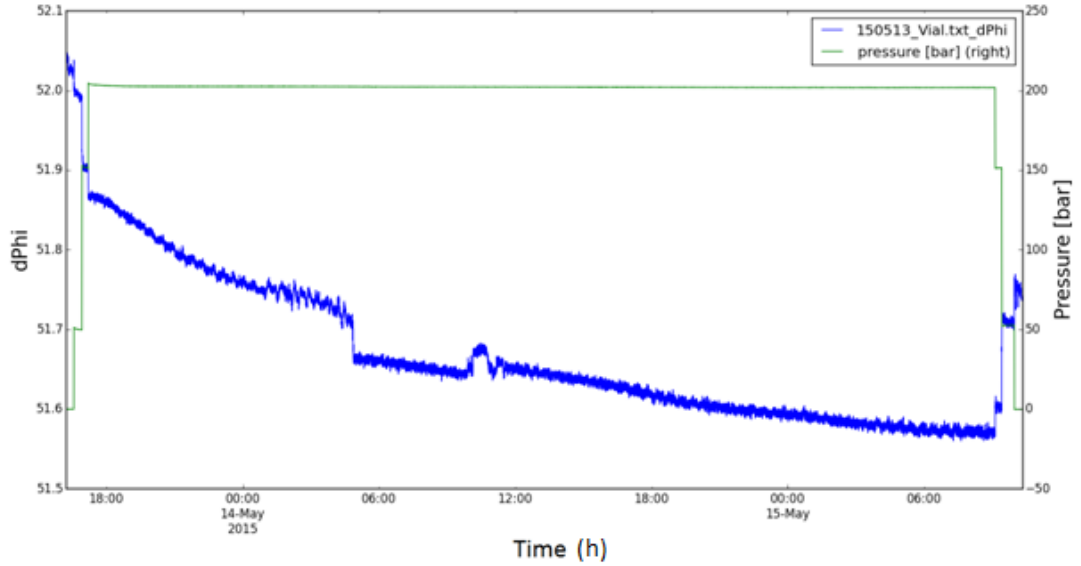

Figure 36: Experiment 150513. Phase angle dependency on hydrostatic pressure

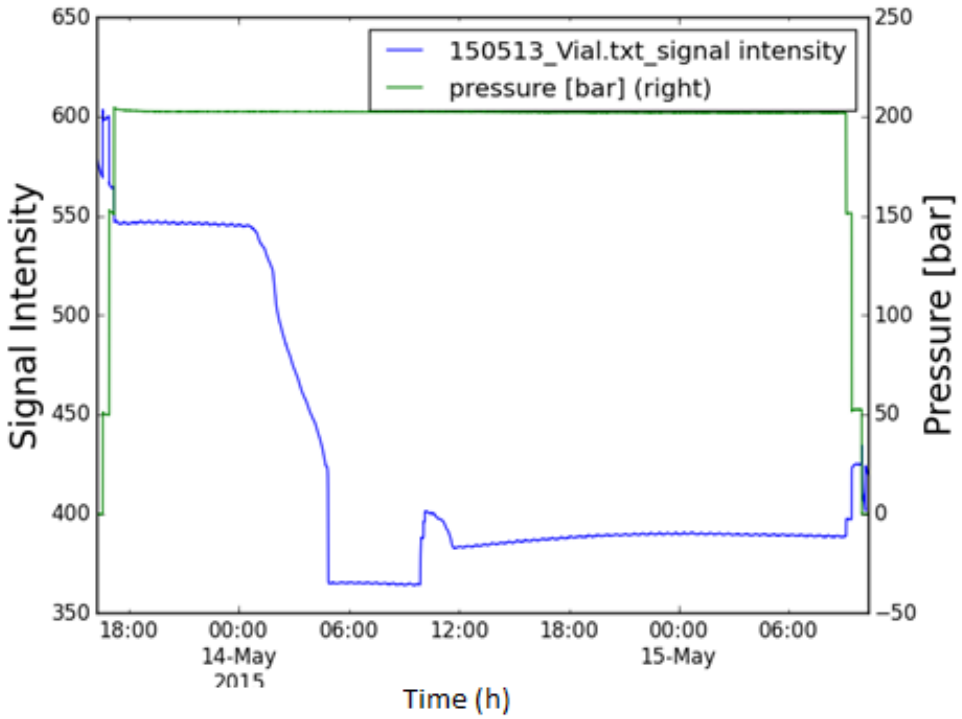

Figure 37: Experiment 150513. Signal intensity dependency on hydrostatic pressure

The samples from both vials were obtained with syringes to avoid their pollution. The results of the experiment, shown in Figure 38 verify the fact that the thin septum is not appropriate for the measurements since it allows the water in the reactor to get into the vial. On the other hand, the thicker septum shows really good results with no presence of the blue dye in the sample.

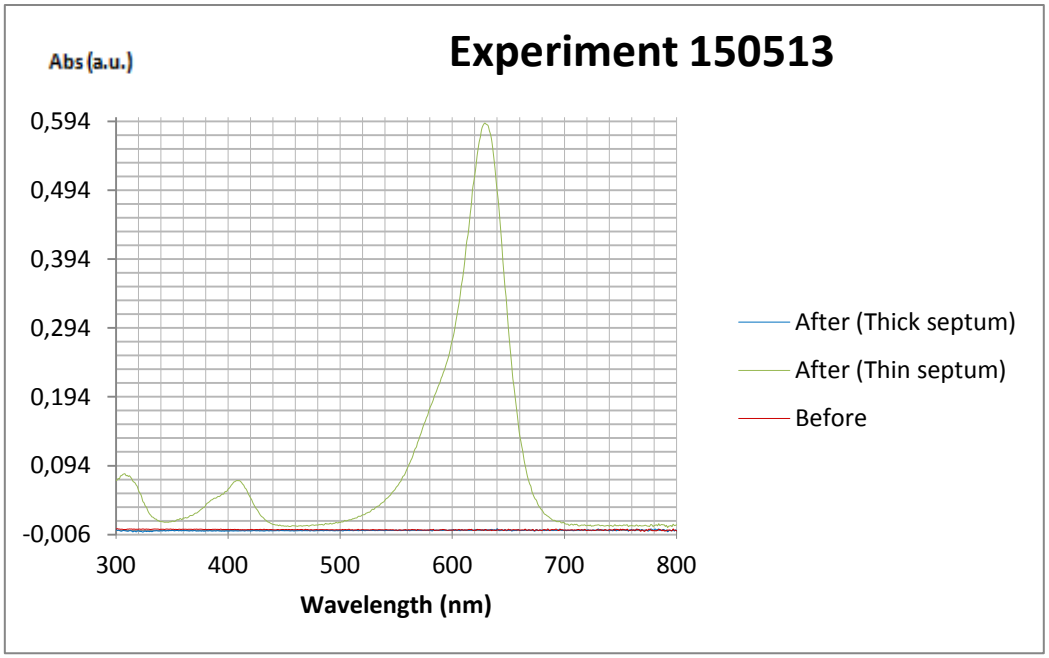

Figure 38: Experiment 150513. Detection of color in the samples

3.5 Conclusions and future suggestions

The results of all the experiments have a really strong dependence on the correct operation of the designed set-up. That makes it very important to detect, localize and eliminate errors or, even better, to avoid them. With all the tests performed, some ideas for improving and conclusions can be listed:

- Fix the tube filled with water of the pump with the probe tube which contains the water used by the pump to avoid air coming inside the tube.
- Improve the connection between the pump and the reactor to avoid exchange of water between both devices.
- Try to find new and more resistant sacks.
- Obtain the samples from the vials without opening them.
- Use a thicker tap for the vials to avoid water from the reactor coming inside.

Furthermore, observing the functioning of the reactor and the nature of the tests that one wants to perform with it, there are many proposals and suggestions that could be tried in the future to improve the measurements and ensure the correct functioning of the set-up:

- Proofing of the effect the silicone from the stirrer has on the sensor (in case it goes accidentally to the reactor).
- Improving of the stirrer function
- Checking the oxygen impermeability of the sack

4 Photostability measurements

In this second part of the thesis, the stability of the dyes is measured by calculating the decrease in the absorption bands for all the indicators after continuous irradiation with a high intensity light at 617 nm. Additionally, the stability of the dyes in a sensor foil (polystyrene) is also accessed via measuring the change in the phase angle under air-saturated and deoxygenated conditions.
One has to mention that the measurements were performed at really hard conditions, to see the results and changes easily, and for this reason a LED was used. Photobleaching in typical sensing applications is not that critical since they are usually illuminated by short light pulses.

4.1 Experimental set-up

The key element of these measurements was the exposition to light, so one had to develop a system capable of fixing the cuvettes that were used (the 1 mm path one and the 10 mm path one) and irradiating them with the high intensity LED at 617 nm.

4.1.1 Spectrometer

The spectrometer was used to measure the absorption spectrum of the samples and to calculate how much dye was remaining after the light exposition, comparing the absorption spectrum before and after the measurement.

4.1.2 Light exposure assembly

Continuous irradiation was performed with a high power 617 nm LED (28 V, 550 mA, photon flux: 18999 µmol s^{-1} m^{-2} µA). Two different types of cuvettes were used: one used for samples in solution (10 mm path) and the other for samples in foil (1 mm path).
A plaster plate with a hole which fitted perfectly with the 10 mm path cuvette was used to hold the samples, and one plastic adaptor was used to fix perfectly into the 1 mm cuvette to the hole. The lamp was placed in front of the plate focusing the light directly to the samples. The whole set-up is shown in Figure 39.

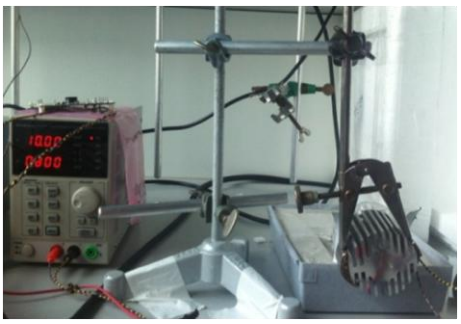

Figure 39: Light exposure assembly

4.2 Preparation of the samples

For optical oxygen sensors the matrix has to be permeable to oxygen, while being impermeable to other potential quenchers. Additional requirements for the matrix materials include availability, chemical stability and solubility.
First samples were prepared in solution which has the advantage of providing a homogeneous environment. Beside toluene, trimethylbenzene was chosen as second solvent, in order to reduce the evaporation in comparison to other solvents.
For the next measurements polystyrene (PS) was chosen as matrix because it has adequate oxygen and it is often used in literature.

4.2.1 Solution of an indicator dyes in toluene

For the measurements in solution, the dyes were directly mixed with the solvent. The absorption of the solution was determined with the absorption spectra and corrected until getting an absorption of approximately 0,5 at the wavelength of the Q-band.

4.2.2 Solution of an indicator dye in trimethylbenzene

The dyes were dissolved in the organic solvent and measured with the spectrometer until the appropriate absorption was achieved.

4.2.3 Sensors based on dyes dissolved in polystyrene

Cocktails were prepared by first dissolving a previously calculated amount of the desired dye in a specific mass of chloroform. Then, the polystyrene MW 250,000 was added and mixed until it was a homogeneous solution, and the vial was covered with aluminum paper and stirred for 30 minutes. The exact amounts used for every dye are showed in Table 5.

Dye	**PM** [g/mol]	**Mol Dye** [mol]	**Mass Dye** [mg]	**Wt% Dye** [%]	**PS** [g]	**wt%PS** [%]	**$CHCl_3$** [g]
Pt-TPTBP	1008,06	3,968E-7	0,4	0,80	0,050	8,33	0,600
Pt-TPTBPF	1080,02	1,389E-6	1,5	0,75	0,200	8,00	2,500
Pt-OctaSulfon	2490,21	4,016E-7	1	2,00	0,050	8,33	0,600
Pt-TetraSulfon	1785,12	4,033E-7	0,72	1,44	0,050	8,33	0,600
Pt-Cl-Benzo	-	-	1,5	0,75	0,200	8,00	2,500
Pt-TertButyl II	1295,63	1,158E-6	1,5	0,75	0,200	8,00	2,500

Table 5: Composition of the cocktails used for the knife coating in PS

When the cocktails were ready, sensor foils were prepared by knife coating on a dust-free mylar foil support using a 1mm Gardner coating knife. The sensor foils were left in the oven at 60ºC drying for 24 hours to ensure all the solvent was removed.
The foil was cut into appropriate-sized shapes and placed inside a 1 mm path glass cuvette.

Figure 40: Preparation of the samples in foil

4.3 Measurements

The cuvettes with the sensor material were placed in the assembly during chosen intervals depending on the nature of the dye and the medium used and were measured every time with the spectrometer.

4.3.1 Oxygenated conditions

Two different procedures had to be developed in order to perform the measurements in air-statured conditions, one for the samples in foil and another one for the solutions.
For the first ones mentioned, one only had to place the cuvette with the foil and measure directly.
The ones in solution needed few additional steps in order to ensure the oxygen saturation. Before every measurement the cuvette was shaken, opened and blown with air. Then, it was closed again for the measurement and for the following light exposure.

4.3.2 Deoxygenated conditions

For the experiments without oxygen, the same approach was taken: samples in foil and solution were treated in a different way.
On one hand, samples coated in foils were first deoxygenated by bubbling Argon into the closed cuvette for 10 minutes for the first measure. Following this, they were exposed to the light and simultaneously deoxygenated with Argon. The injection of Argon was only stopped during the use of the spectrometer.

4.3.3 Results

The results obtained with the spectrometer were plotted and for each dye/matrix/conditions, as it is shown in Figure 41. All the other graphs are included in Appendix 1 and Appendix 2.

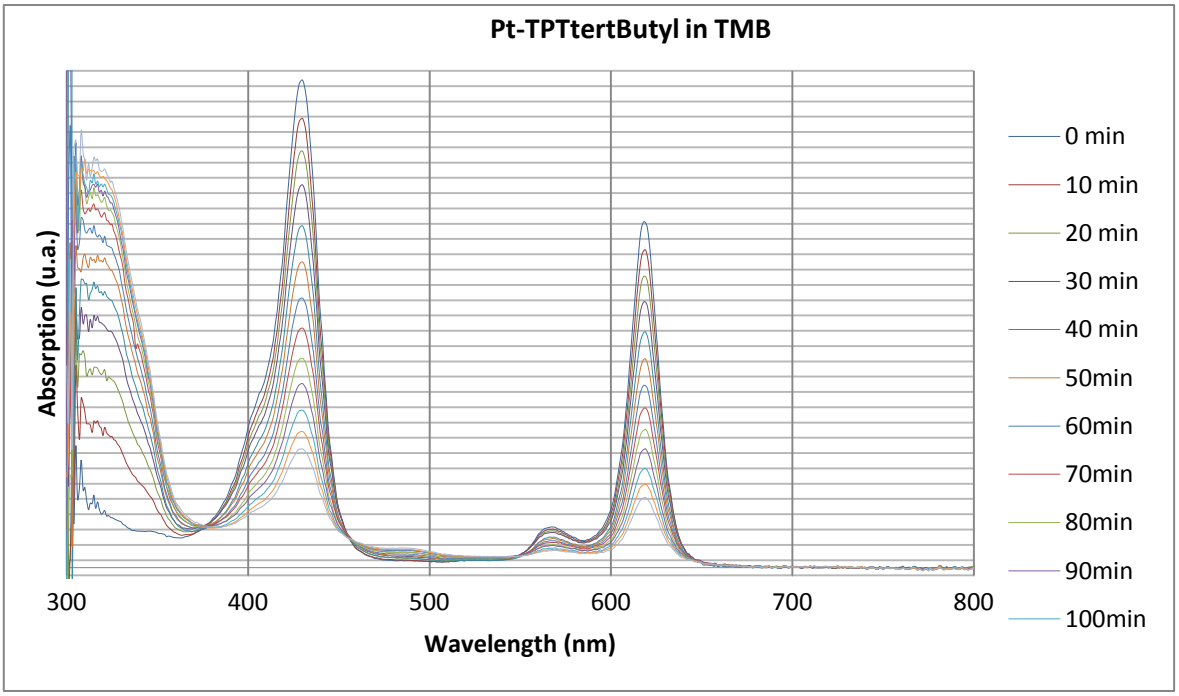

Figure 41: Absorption spectra of Pt-TertButyl I in TMB (air-saturated conditions)

The values of all the measurements are shown in Table 6.They show the absorption values for the Q-band and Soret-band for every dye and experiment and the percentage of reduction in the absorption spectrum. Detailed information about all the measured values is shown in Appendix 3.

Dye	Conditions	Time of the experiment [min]	A(Soret) before/after	A(Q) before/after	Bleaching (Soret/Q) [%]	Bleaching average [%]
PtTPTBP	PS - Anoxic	147	0,796/0,743	0,510/0,470	6,7/7,9	7,3
	TMB - Anoxic	14	0,791/0,286	0,279/0,178	63,9/36,2	50,1
	Toluene- Air saturated	540	0,712/0,707	0,471/0,468	0,7/0,5	0,6
Pt-TertButyl I	PS - Anoxic	147	0,352/0,341	0,227/0,222	3,0/2,1	2,6
	PS - Air saturated	130	0,371/0,314	0,247/0,203	15,4/18,1	16,8
Pt-TertButyl II	TMB - Anoxic	14	0,772/0,185	0,534/0,095	76,1/82,2	79,2
	TMB - Air saturated	120	0,638/0,156	0,451/0,092	75,6/79,6	77,6
	Toluene- Air saturated	450	0,695/0,629	0,469/0,421	9,6/10,2	9,9

Pt-Cl-Benzo	PS - Anoxic	147	0,422/0,409	0,276/0,268	3,2/2,9	3,1
	PS - Air saturated	150	0,444/0,275	0,293/0,163	38,1/44,5	41,3
	TMB - Anoxic	14	0,685/0,174	0,479/0,102	74,6/78,7	76,7
	TMB - Air saturated	120	0,685/0,392	0,473/0,258	42,7/45,4	44,1
Pt-Tetrasulfon	PS - Anoxic	147	0,311/0,303	0,178/0,171	2,3/3,7	3
	PS - Air saturated	150	0,282/0,236	0,160/0,129	16,4/19,0	17,7
	TMB - Anoxic	10	0,843/0,425	0,493/0,233	49,6/52,7	51,2
	TMB - Air saturated	120	0,819/0,547	0,481/0,313	33,2/34,9	68,2
	Toluene- Air saturated	420	0,907/0,905	0,509/0,506	0,2/0,5	0,4
Pt-OctaSulfon	PS - Anoxic	150	0,556/0,482	0,332/0,281	13,3/15,2	14,3
	PS - Air saturated	147	0,511/0,430	0,311/0,258	15,8/17,2	16,5
	TMB - Anoxic	14	0,765/0,227	0,503/0,127	70,3/75,8	73,1
	TMB - Air saturated	100	0,689/0,545	0,451/0,352	20,9/22,1	21,5
	TMB - Anoxic filter 50%	30	0,686/0,225	0,448/0,128	67,2/71,4	69,3
	TMB - Anoxic filter 25%	30	0,778/0,419	0,510/0,257	46,1/49,6	47,9
	Toluene- Anoxic	149	0,833/0,836	0,515/0,515	0/0	0
	Toluene- Air saturated	360	0,733/0,743	0,450/0,458	0/0	0

Table 6: Sumerized results for all the dyes

When all the measurements were performed and all the data plotted, the curves were examinated in order to compare all the used sensing materials. Figure 42 shows the results for the dyes in Toluene. As it can be seen in the graph, all the dyes were really photosatable. The samples were exposed to light of 617 nm over a long period of time and their destruction was almost insignificant. The only dye which presented some quenching was Pt-TertButyl I, confirming the expected behavior due to oxidation.

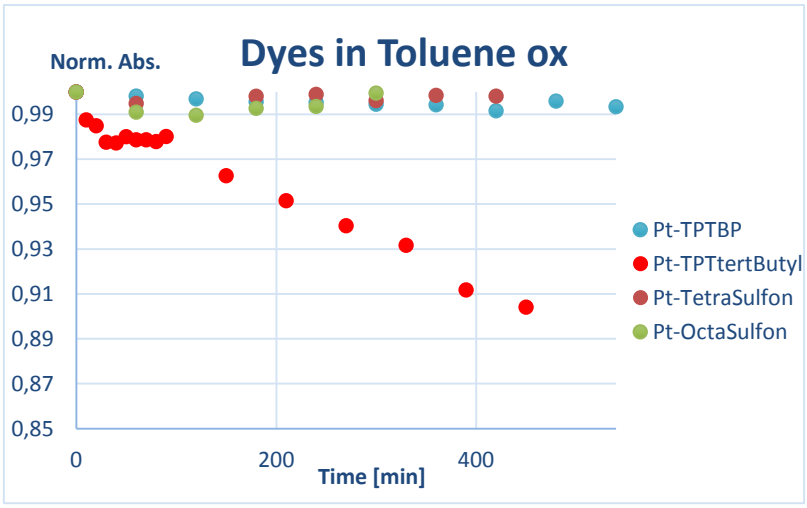

Figure 42: Dyes in Toluene (Air-saturated conditions)

Figure 43 shows the absortion spectrum of Pt-OctaSulfon in Toluene in deoxinated conditions. One can see that even the exposure to light for a long period of time, resulted in no photobleaching in the dye. This confirms in both conditions, air-saturated and anoxic ones, the dyes are really photostable.

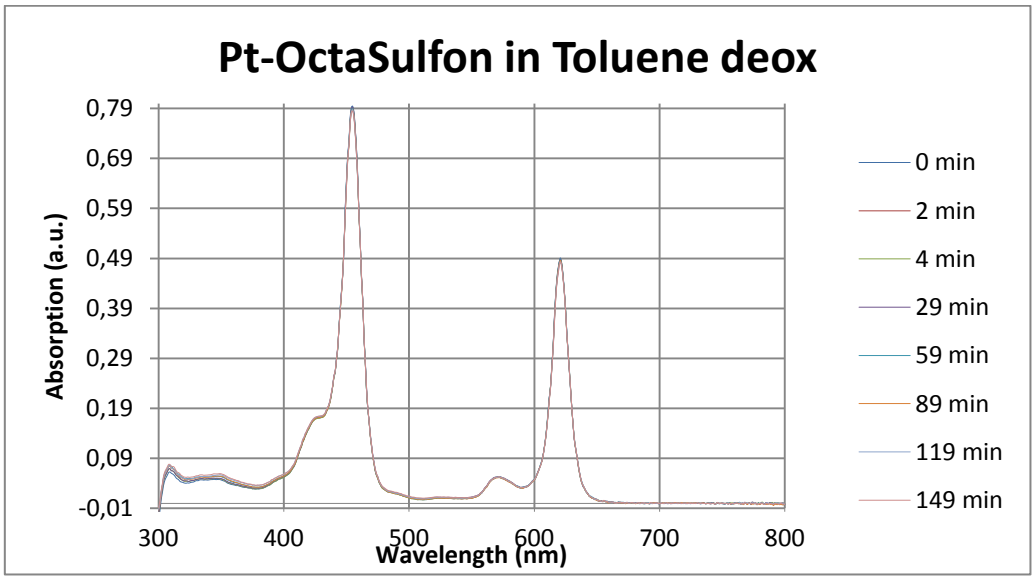

Figure 43: Absorption spectra of Pt-OctaSulfon in Toluene (Anoxic conditions)

The next solvent used was trimethylbenzene in order to avoid the evaporation. The results of the absorption values of dyes in TMB, in Figure 44, show a clear increase of photobleaching of the dyes in this solvent. In air conditions one can see the expected trend for the photobleaching rate. The Pt-TertButyl I dye is much less photostable in comparison with Pt-MonoSulfon and Pt-OctaSulfon, which is the most photostable one.

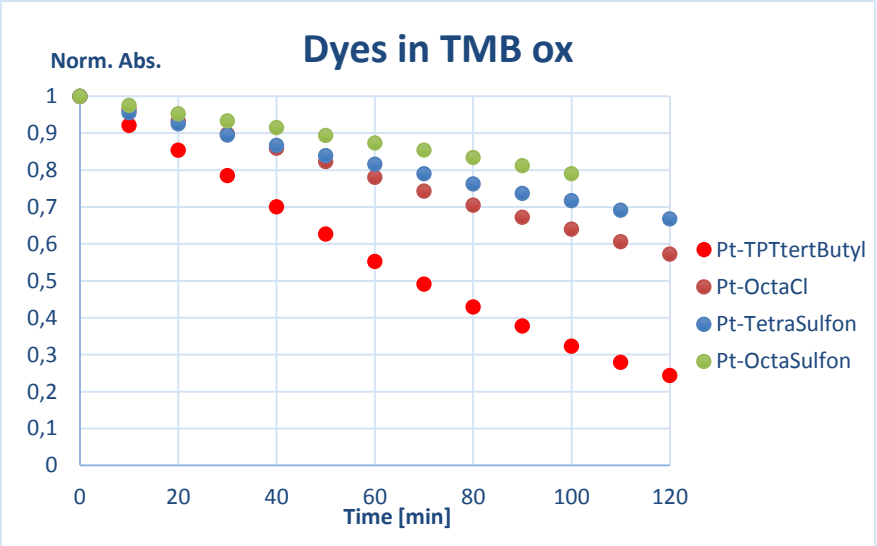

Figure 44: Dyes in TMB (Air-saturated conditions)

In Figure 45 one can see a dramatic increase of photobleaching in deoxygenated conditions, since in only 14 minutes all the dyes were almost destroyed. The dramatic increase in photobleaching compared to toluene may be due to red-ox processes occurring with participation of the solvent and the dye in excited state. This means one has to be careful with the solvent used because there may be other de-excitation processes besides oxidation with singlet oxygen. This is shown by much faster photobleaching in anoxic conditions compared to air-saturated conditions.

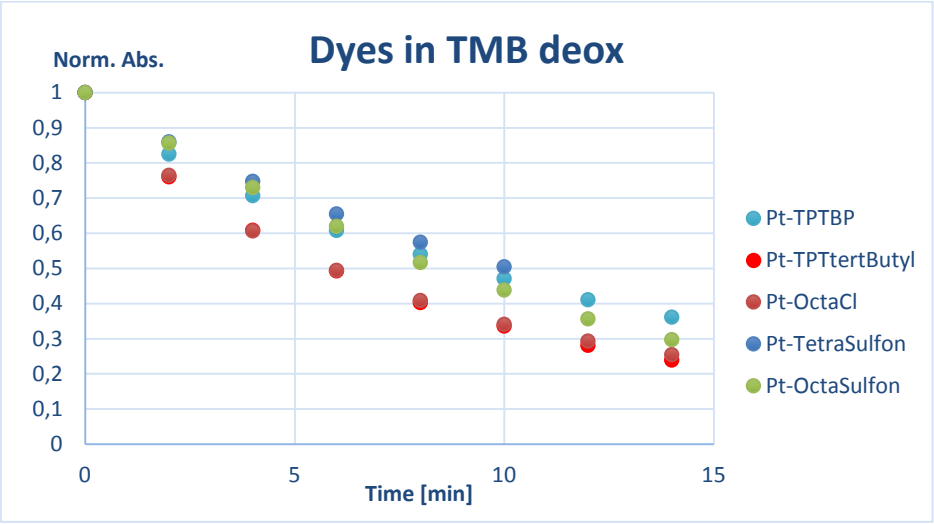

Figure 45: Dyes in TMB (Anoxic conditions)

Some experiments with filters were performed using the Pt-OctaSulfon dye to test if photobleaching had something to do with collision of molecules of the dye in excited state since the intensity of the light was very high. Less light should mean less amount of excited state molecules inside the solution and therefore fewer collisions between them. The results

obtained are shown in this table and demonstrate that the photobleaching is due to interaction between excited molecules with the solvent, but not the excited dye molecules with each other; since if not, the photobleaching would have decreased in factor of 4.

Filter	Bleaching [%]	Norm. Bleaching
100%	70	1,00
50%	40	0,50
25%	25	0,25

Table 7: Photobleaching of the dyes in filter measurements

The behavior of the dyes in foil is quite similar and the quenching under oxygenated conditions does not vary greatly, as it can be seen in Figure 46. Despite the fact that one could expect Pt-Cl-Benzo to be one of the most photostable ones due to the electronegativity of its substituents, it seems that is the less photostable dye measured in this conditions.

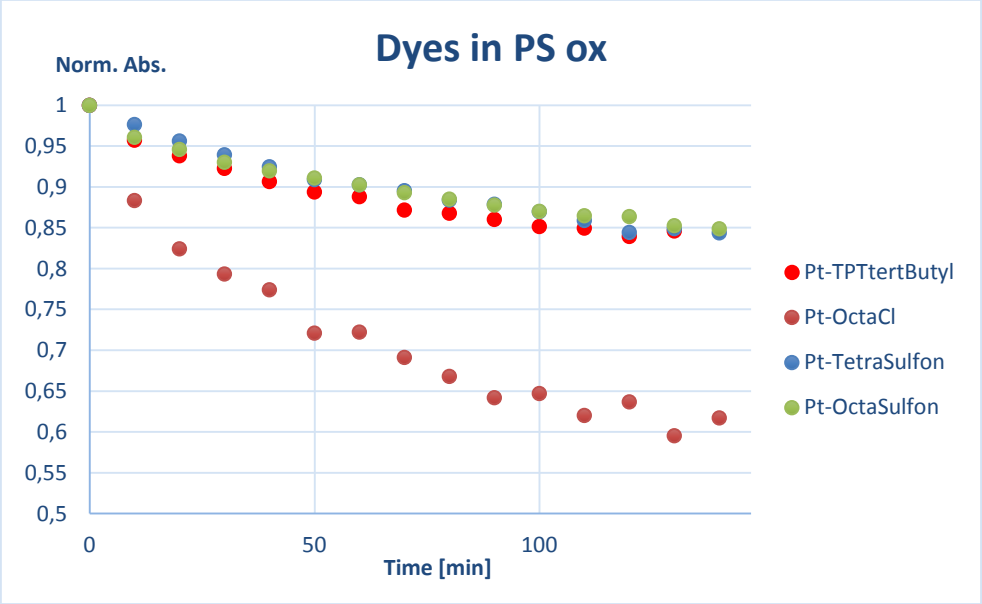

Figure 46: Dyes in PS (Air-saturated conditions)

In deoxygenated conditions, the values for the quenching are much lower (Figure 47). This can be explained by the lack of oxygen and therefore less affection of the reactive singlet oxygen. One unexplainable fact is the high destruction of the Pt-OctaSulfon dye comparing to the other dyes, since it was expected to be more photostable.

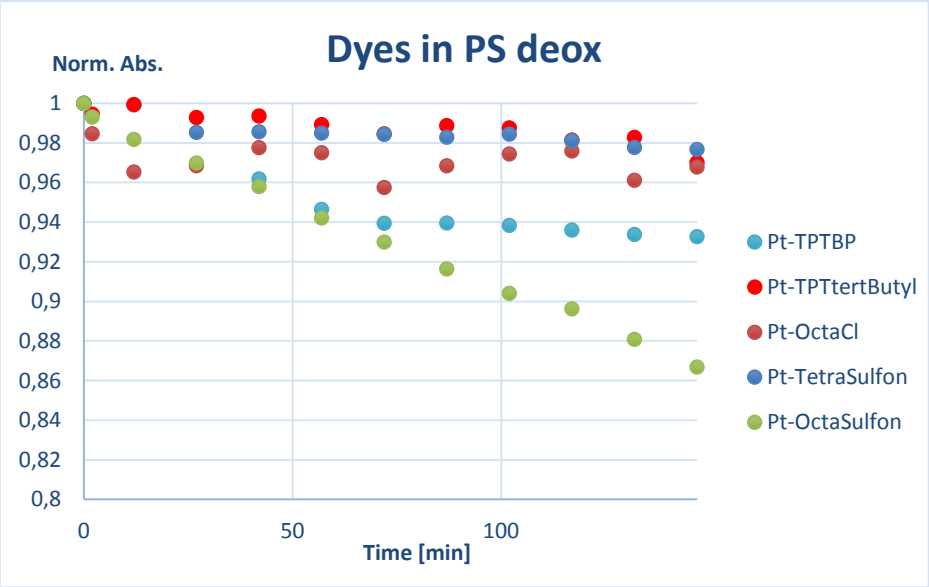

Figure 47: Dyes in PS (Anoxic conditions)

4.4 Characterization of the decay times

After measurement of all the dyes under different conditions to compare their photostability a complementary experiment was performed. All dyes in PS were exposed to the light for the same time and the phase angle was measured before and after the light exposition.

For these new measurements, two new cocktails were prepared using the following dyes: Pt-TPTBPF and Pt-OctaSulfon. One proceeded as the same way as the other cocktails embedded in PS.
One had already a Pt-OctaSulfon dye, but since certain values related to this dye were different as expected; there was a need to ensure the results were valid and not affected by the presence of impurities. For this reason a new Pt-OctaSulfon cocktail was prepared and knife-coated on foil.
Exact amounts of all dyes tested in this part can be seen in Table 8 the new ones marked with one asterisk.

Dye	PM [g/mol]	MolDye [mol]	Mass Dye [mg]	wt% Dye [%]	PS [g]	wt%PS [%]	$CHCl_3$ [g]
Pt-TPTBP	1008,06	3,968E-7	0,4	0,80	0,050	8,33	0,600
Pt-TPTBPF*	1080,02	1,389E-6	1,5	0,75	0,200	8,00	2,500
Pt-OctaSulfon	2490,21	4,016E-7	1	2,00	0,050	8,33	0,600
Pt-TetraSulfon	1785,12	4,033E-7	0,72	1,44	0,050	8,33	0,600
Pt-Cl-Benzo		-	1,5	0,75	0,200	8,00	2,500
Pt-TertButyl I	1295,63	1,158E-6	1,5	0,75	0,200	8,00	2,500
Pt-OctaSulfon*	2490,21	4,016E-7	1	2,00	0,050	8,33	0,600

Table 8: Composition of the cocktails used in the phase angle measurements

4.4.1 Procedure

The measurements were done before and after a light exposition of 120 minutes for all the dyes.
First, the absorption spectrum was measured with the spectrometer and a FireStingO2-Mini (SPOT) from PyroScience was used to measure the decay time. This test was performed under oxygenated conditions (approaching the device to the cuvette with the foil directly) and under deoxygenated conditions (the same procedure but injecting argon directly to the cuvette while the device was measuring).
After the light exposition one repeated the tests in order to see the differences between both values.

4.4.2 Results

The values from the absorption spectrum and the photobleaching the dyes suffered after the light exposition are shown in Table 9.

Dye	Wavelength [nm]	Absorption Time= 0 min	Absorption Time= 120 min	% photobleaching
Pt-TPTBP	616,03	0,4973	0,4134	16,84
Pt-TPTBPF*	616,03	0,1521	0,1158	23,84
Pt-OctaSulfon	622,06	0,3012	0,2695	10,51
Pt-TetraSulfon	618,97	0,1733	0,1494	13,74
Pt-Cl-Benzo	621,03	0,2582	0,1706	33,91
Pt-TertButyl I	620,00	0,2215	0,2023	8,64
Pt-Octasulfon*	621,03	0,5141	0,4725	8,09

Table 9: Results of the absorption spectrum of the days before and after light exposition

The measured phase angles for each dye are drawn up in Table 10. Observing the values listed, one can notice a decrease in τ_0 for all the dyes. This is likely to be due to change in the environment of the dye (very close to the molecule). The modified polymer particles act as a quencher for the dye. The quenching values are different, so the process is different for every dye.

Examining the last two columns one can also declare that balk polymer is not affected, since Kg before and after the light exposition are identical.

Dye	Air, ϕ in °		N2, ϕ in °		Air, τ in µs		N2, τ in µs		% decr.	$\tau_0/\tau_{\alpha i \rho}$	$\tau_0/\tau_{\alpha i \rho}$	Ksv in kPa^{-1}		Kq in $Pa^{-1}s^{-1}$	
	0 min	120 min	0 min	120 min	0 min	120 min	0 min	120 min	of τ_0	0 min	120 min	0 min	120 min	0 min	120 min
Pt-TPTBP	17,52	16,11	51,27	44,38	12,56	11,49	49,61	38,94	21,52	3,95	3,39	0,15	0,12	2,97	3,07
Pt-TPTBPF	17,25	17,16	53,86	50,53	12,35	12,29	54,48	48,32	11,32	4,41	3,93	0,17	0,15	3,13	3,03
Pt-OctaSulfon	22,19	21,3	49,29	46,46	16,23	15,51	46,24	41,87	9,46	2,85	2,70	0,09	0,08	2,00	2,03
Pt-TetraSulfon	21,67	21,23	52,29	50,44	15,81	15,46	51,46	48,16	6,41	3,26	3,12	0,11	0,11	2,19	2,20
Pt-Cl-Benzo	22,9	21,22	52,03	45,59	16,81	15,45	50,98	40,62	20,33	3,03	2,63	0,10	0,08	1,99	2,01
Pt-TertButyl I	22,27	21,67	53,75	52,34	16,29	15,81	54,26	51,55	4,99	3,33	3,26	0,12	0,11	2,15	2,19
Pt-Octasulfon*	19,25	18,44	50,01	45,75	13,89	13,27	47,44	40,84	13,89	3,41	3,08	0,12	0,10	2,54	2,54

Table 10: Phase angle and decay times of the dyes before and after light exposition

5 Summary and comments

To conclude, this investigation provides a general overview of the effects of the different environmental conditions on optical oxygen sensors.

Although the measurements under high hydrostatic pressures haven't provided the desired results, some progress has been made in this field of study, setting appropriate conditions for the measurements, making arrangements to the initial techniques performed and proposing new ideas and improvements in regard to the available set-up.

This kind of experiments could give really interesting information for oceanographic applications, so one can affirm that all the set-up and procedure should be reviewed in order to widen the investigation already done in this first part of the thesis and thereby achieving a reliable set-up capable to provide reproducible and better interpretable results.

The research reported in the second part of this thesis gives a perspective of the response of the different sensor materials available for optical sensing applications to the effect of light.

Different matrixes have been used and new partly unexpected results have been obtained, such as the fact that other degradation processes can occur besides the singlet oxygen oxidation process due to the interaction of the solvent with the dye. This makes the election of the matrix an important fact to take in account when measuring properties of a dye.

Finally, one could say that there is no dye that is appropriate for all conditions (solvent and matrix). However, the results have shown that the new dyes, Pt-TetraSulfon and Pt-OctaSulfon, have a really good photostability, thus becoming a promising option for sensing activities and further future investigation.

Bibliography

1. *Indicators for optical oxygen sensors .* **Quaranta, Michela, Borisov, Sergey M. y Klimant, Ingo.** 2012, Bioanalytical reviews, págs. 115-157.
2. **Charan Dash, Dhruba.** *Analytical Chemistry.* Nova Dehli : PHI Learning Private Limited, 2011.
3. **McEwen, Jordan.** Jablonski Energy Diagram. *ChemWiki.* [En línea] [Citado el: 1 de June de 2015.] http://chemwiki.ucdavis.edu/Physical_Chemistry/Spectroscopy/Electronic_Spectroscopy/Jablonski_diagram#Fluorescence.
4. *Optical chemical sensors.* **McDonagh, Colette, Burke, Connor S. y MacCraith, Brian D.** 2008, Chemical reviews, págs. 400-422.
5. **Lakowicz, Joseph R.** *Principles of Fluorescence Spectroscopy.* s.l. : Springer Science & Business Media, 2007.
6. *Optical Oxygen Sensors.* **Mills, Andrew.** 1997, Platinum metals review, págs. 115-127.
7. *Materials for fluorescence-based optical chemical sensors.* **Wolfbeis, Otto S.** 2005, Journal of Materials Chemistry, págs. 2657-2669.
8. **Valeur, Bernard y Berberan-Santos, Mario Nuno.** *Molecular Fluorescence: Principles and Applications.* Verlag : Wiley-VCH, 2012.
9. *Oxygen Sensors Based on Luminescence Quenching.* **Demas, James N., DeGraff, B. A. y Coleman, Patricia B.** 1999, Analytical Chemistry News & Features, págs. 793A-800A.

List of Figures

List of tables

Abbreviations

PS	Polystyrene
wt%	Mass percentage
TMB	Tetramethylbenzene
MO	Molecular Orbitals
LUMO	Lowest Unoccupied Molecular Orbitals
HOMO	Highest Unoccupied Molecular Orbitals
A	Absorbance

Appendix

Appendix 1: Oxygenated photostability measurements

Pt-TPTBP in Toluene

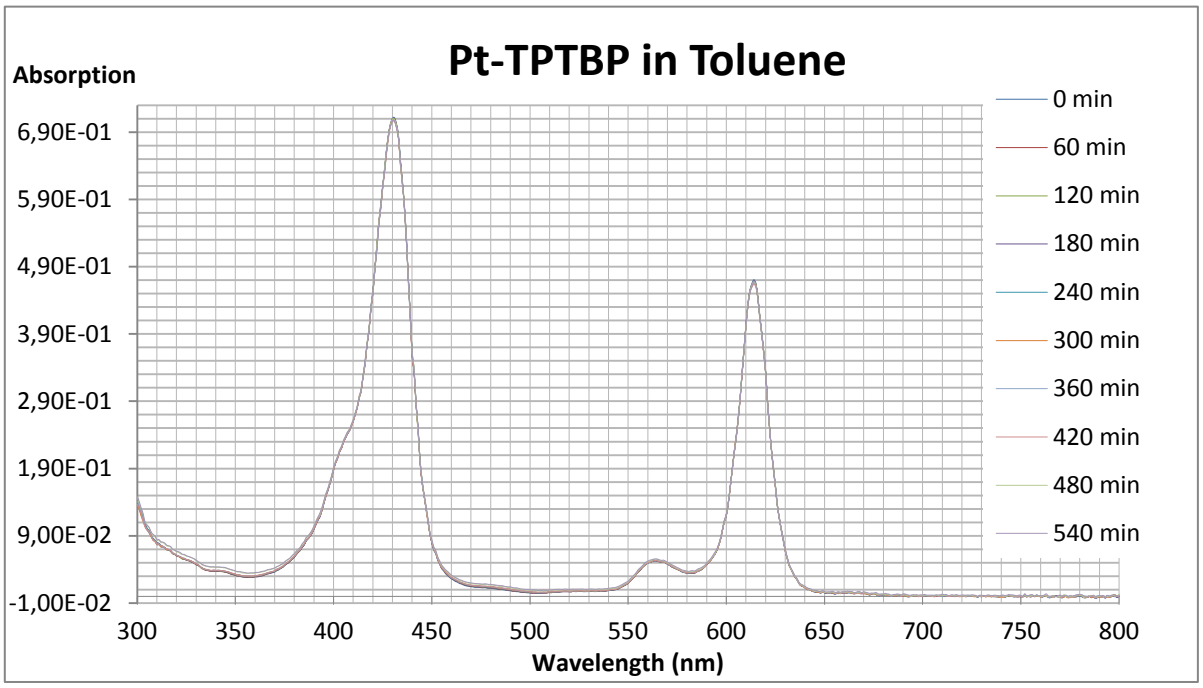

Absorption values		
Wavelength=430,9234619nm		
Time [min]	Abs	Norm Abs
0	0,71185279	1
60	0,71055698	0,99817967
120	0,70966913	0,99693243
180	0,70875638	0,99565021
240	0,70856215	0,99537737
300	0,70797111	0,99454708
360	0,70779608	0,9943012
420	0,70589178	0,99162607
480	0,70896529	0,99594369
540	0,70717578	0,99342982

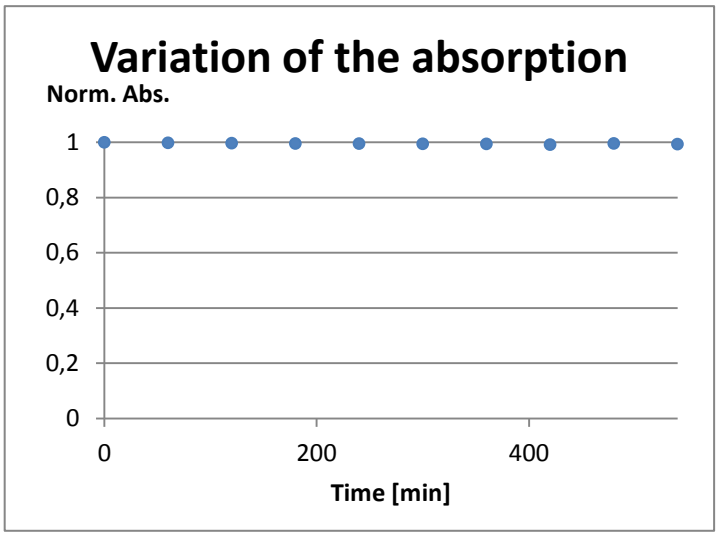

Pt-TertButyl II in PS

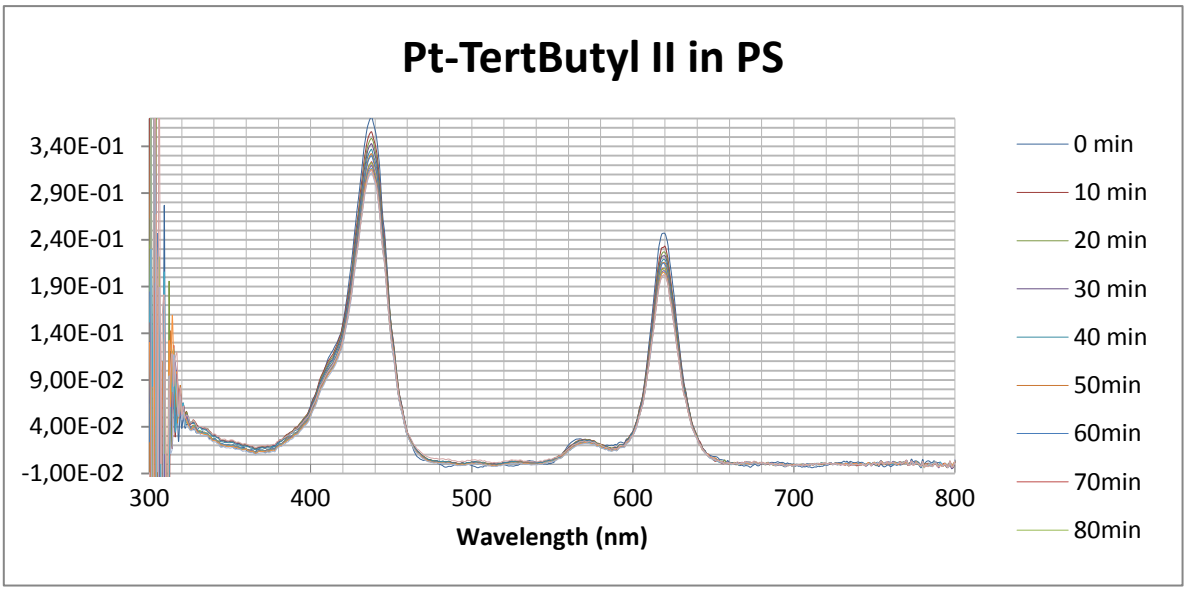

Absorption values		
Wavelength=437,9728699nm		
Time [min]	Abs	Norm Abs
0	0,37125457	1
10	0,35541727	0,95734114
20	0,34834476	0,93829082
30	0,34262029	0,92287158
40	0,33663067	0,90673813
50	0,33188553	0,89395675
60	0,32975434	0,88821624
70	0,32366237	0,87180711
80	0,32223823	0,86797109
90	0,31941009	0,86035329
100	0,31618806	0,85167453
110	0,31545338	0,84969562
120	0,31167559	0,83951988
130	0,31416459	0,84622418

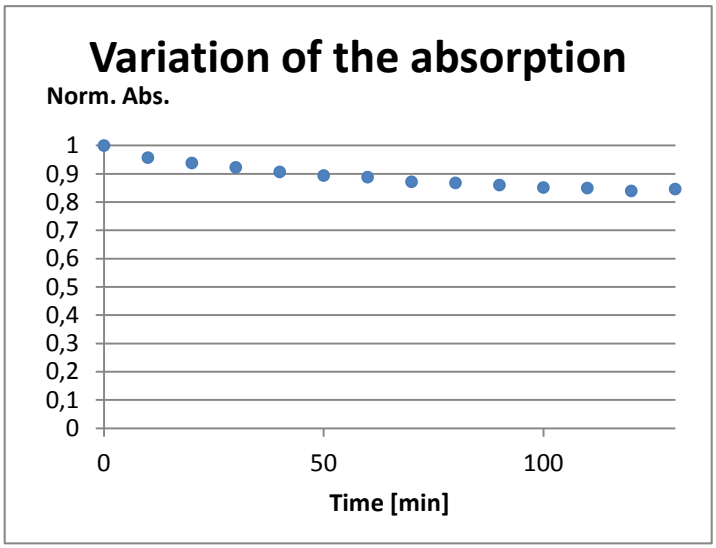

Pt-TertButyl I in TMB

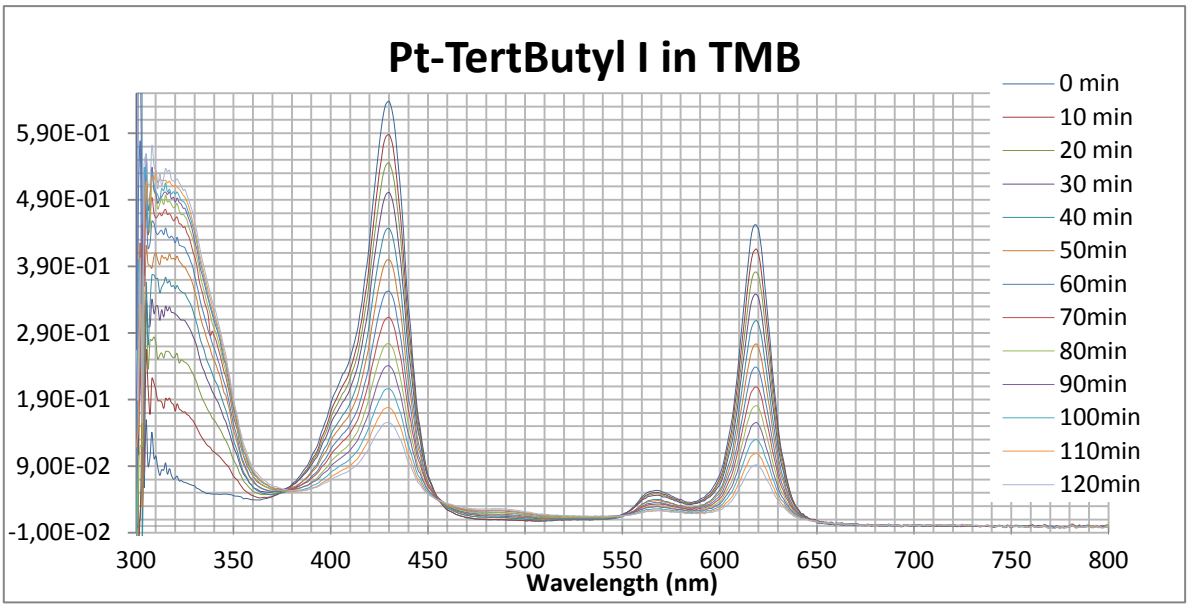

Absorption values		
Wavelength=430,0033264nm		
Time [min]	Abs	Norm Abs
0	0,63773845	1
10	0,58767966	0,92150576
20	0,54479396	0,85425923
30	0,50089741	0,78542765
40	0,44701658	0,70094029
50	0,39998588	0,62719423
60	0,35257267	0,55284838
70	0,31347235	0,49153748
80	0,27406016	0,42973754
90	0,24111346	0,37807577
100	0,20625392	0,32341459
110	0,17832609	0,27962261
120	0,15563482	0,24404177

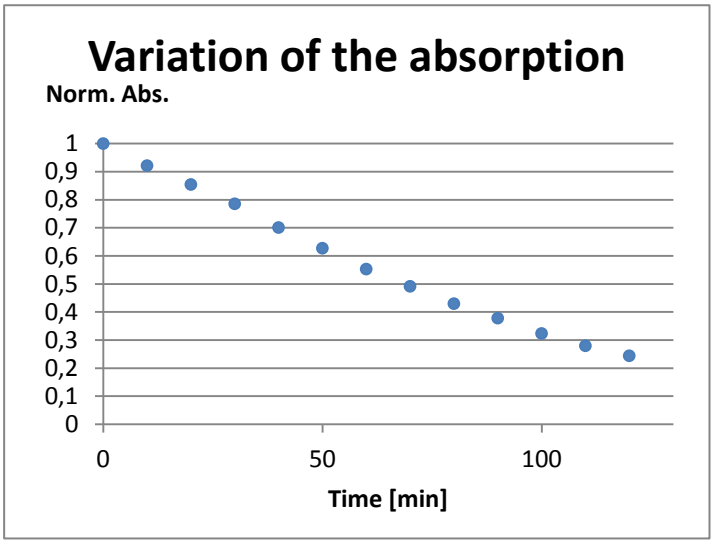

Pt-TertButyl I in Toluene

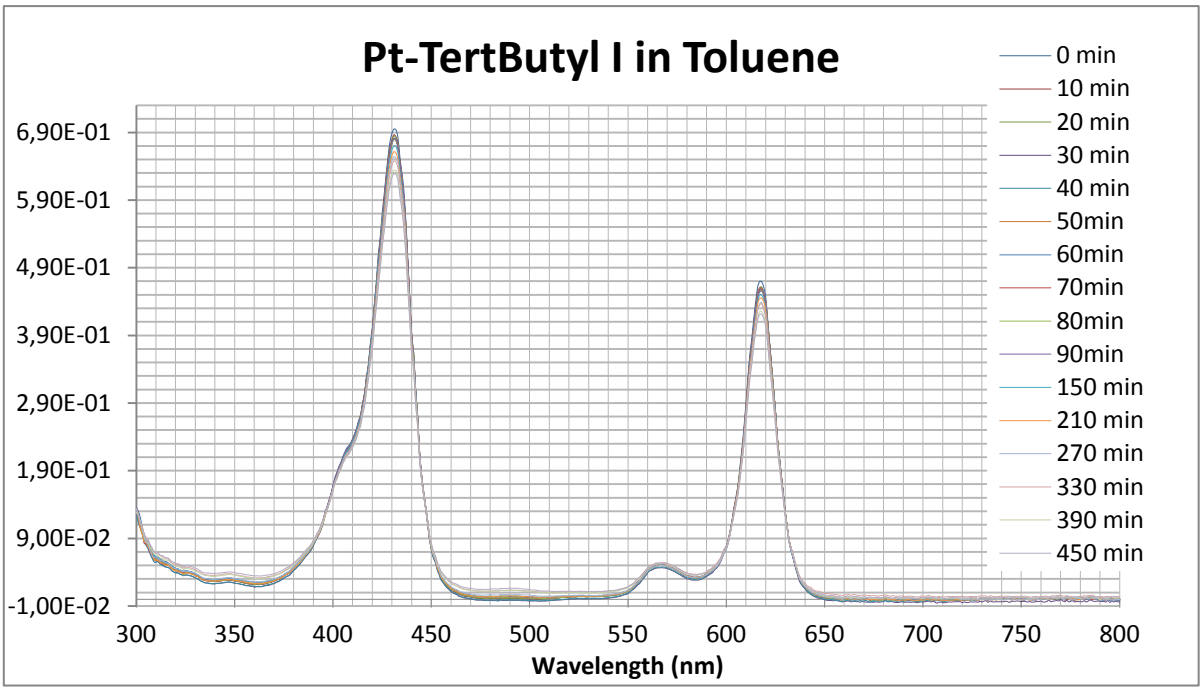

Absorption values		
Wavelength=430,9234619nm		
Time [min]	Abs	Norm Abs
0	0,69514377	1
10	0,6865013	0,98756736
20	0,68467947	0,98494656
30	0,67959714	0,97763537
40	0,67936066	0,97729518
50	0,68130293	0,98008923
60	0,68033399	0,97869536
70	0,68033399	0,97869536
80	0,67979309	0,97791725
90	0,68136139	0,98017333
150	0,66922176	0,96270985
210	0,66148131	0,95157481
270	0,65373149	0,94042631
330	0,6476729	0,9317107
390	0,63384239	0,91181482
450	0,62851706	0,90415405

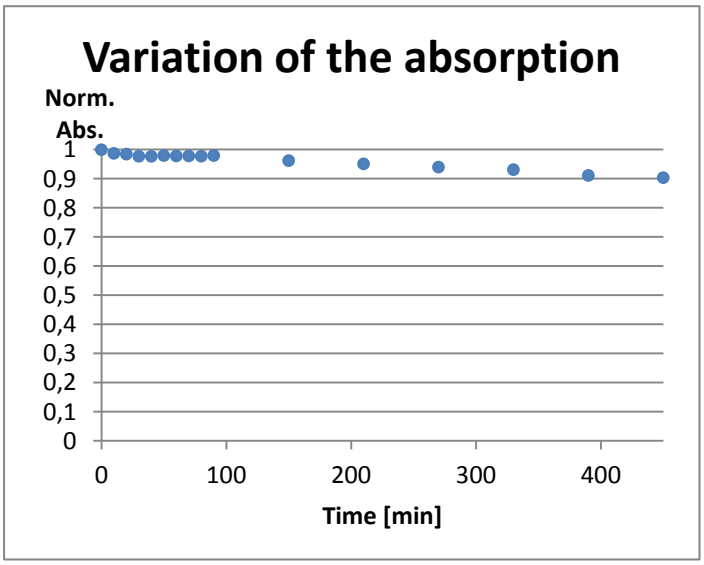

Pt-Cl-Benzo in PS

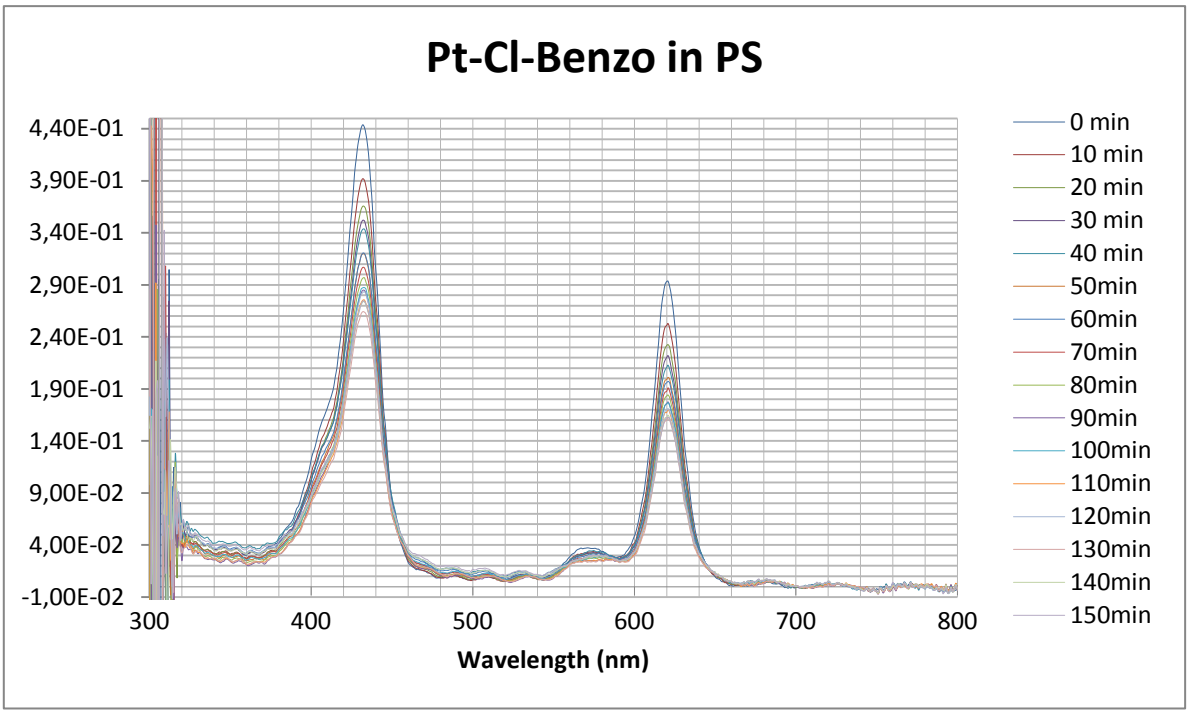

Absorption values		
Wavelength=431,9967651nm		
Time [min]	Abs	Norm Abs
0	0,44371255	1
10	0,39200895	0,88347502
20	0,36576763	0,82433467
30	0,3520948	0,79352005
40	0,34352453	0,77420513
50	0,3199791	0,72114052
60	0,32054035	0,72240541
70	0,30678867	0,69141312
80	0,29647782	0,66817542
90	0,28490063	0,64208378
100	0,28717596	0,64721171
110	0,27526557	0,62036913
120	0,28263058	0,63696773
130	0,26423234	0,59550342
140	0,27390779	0,6173091
150	0,27461226	0,61889675

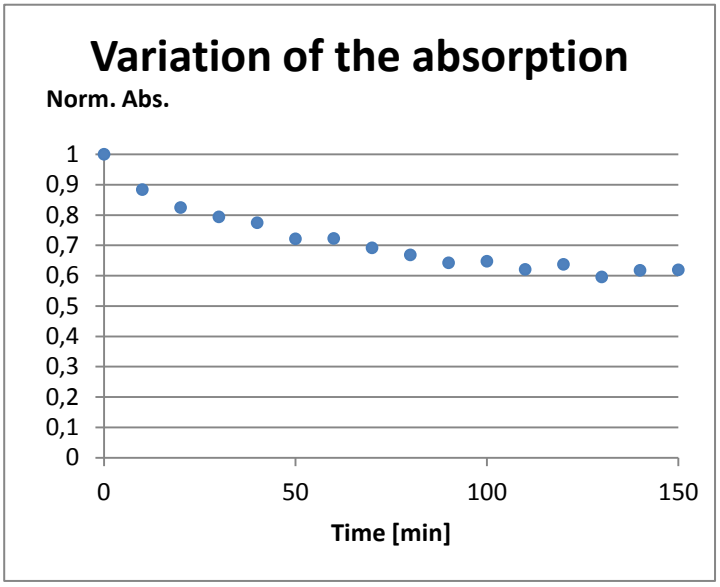

Pt-Cl-Benzo in TMB

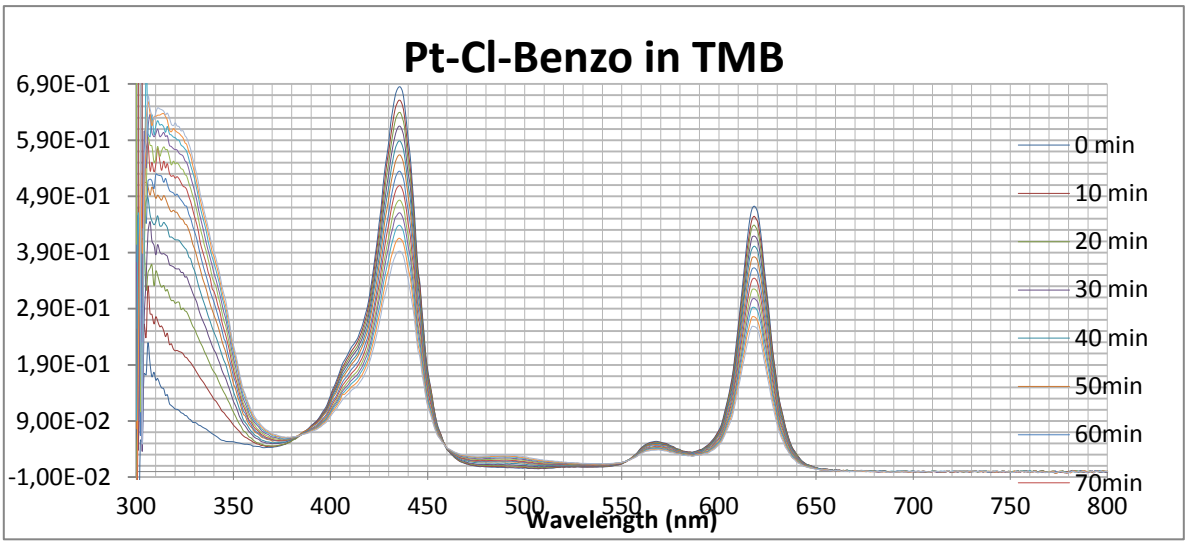

Absorption values		
Wavelength=435,0622253nm		
Time [min]	Abs	Norm Abs
0	0,68445668	1
10	0,66104936	0,96580162
20	0,6385974	0,932999
30	0,61460142	0,89794058
40	0,58830577	0,85952228
50	0,56353986	0,82333898
60	0,53439292	0,78075493
70	0,50881537	0,74338579
80	0,48273866	0,70528739
90	0,46035887	0,67259022
100	0,43834291	0,64042463
110	0,41505093	0,60639474
120	0,39203651	0,57277038

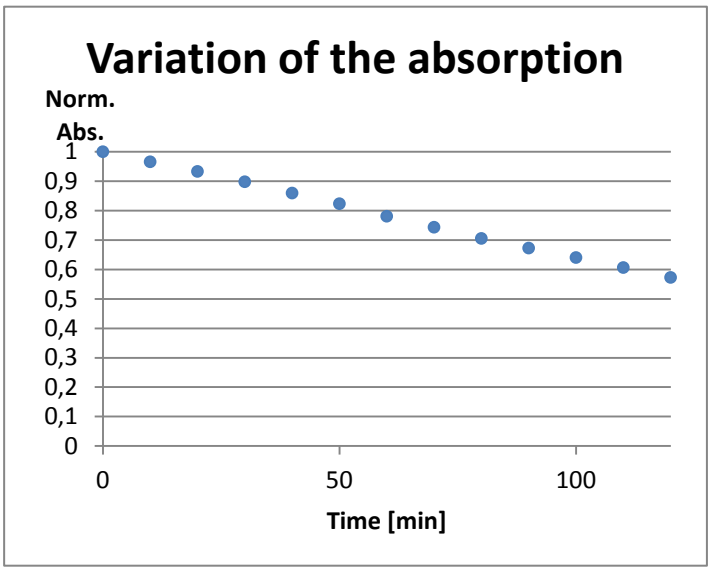

Pt-TetraSulfon in PS

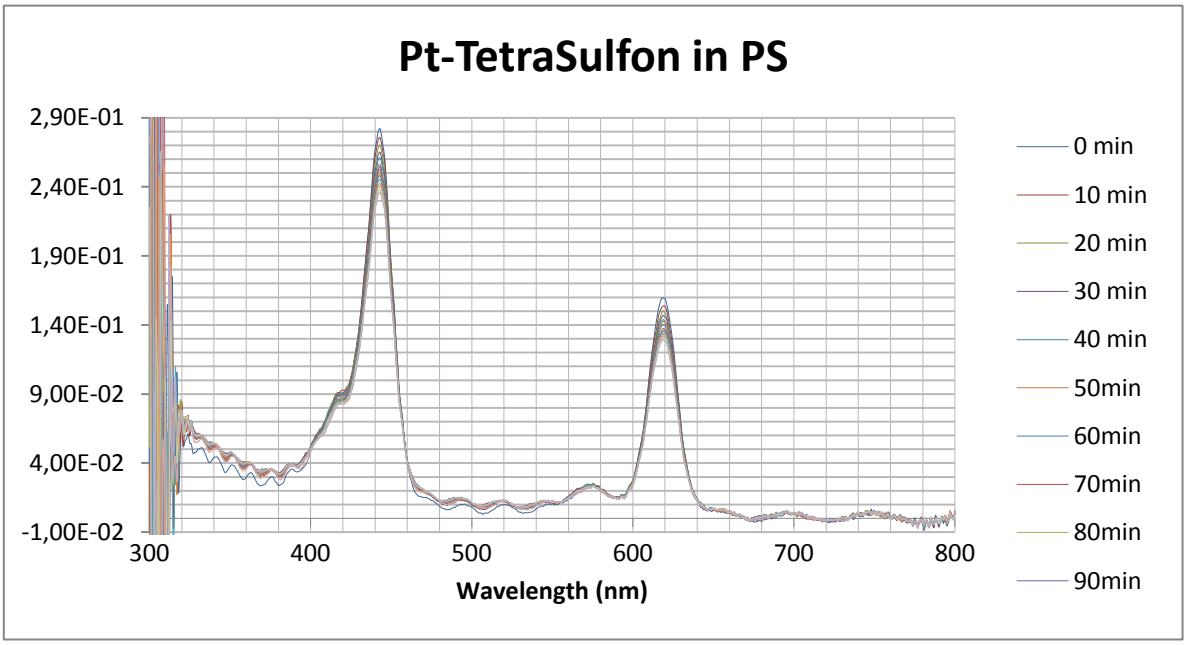

Absorption values		
Wavelength=443,0245361nm		
Min	Abs	Norm Abs
0	0,28221151	1
10	0,27559757	0,97656389
20	0,26989953	0,95637322
30	0,26513401	0,93948688
40	0,26099937	0,92483603
50	0,25656227	0,90911342
60	0,25478801	0,90282643
70	0,2527383	0,8955634
80	0,24949202	0,88406042
90	0,24804261	0,8789245
100	0,24547923	0,8698413
110	0,24244119	0,85907621
120	0,23832014	0,84447351
130	0,23962091	0,84908269
140	0,23815807	0,84389923
150	0,23600432	0,83626751

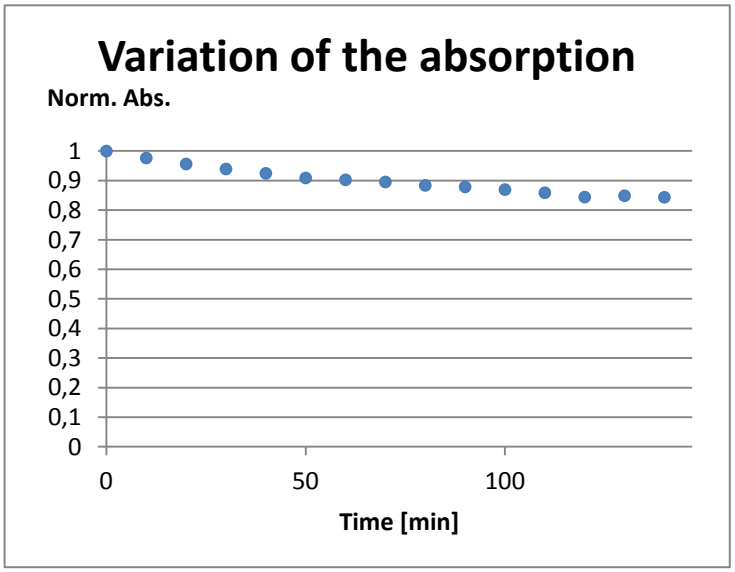

Pt-TetraSulfon in TMB

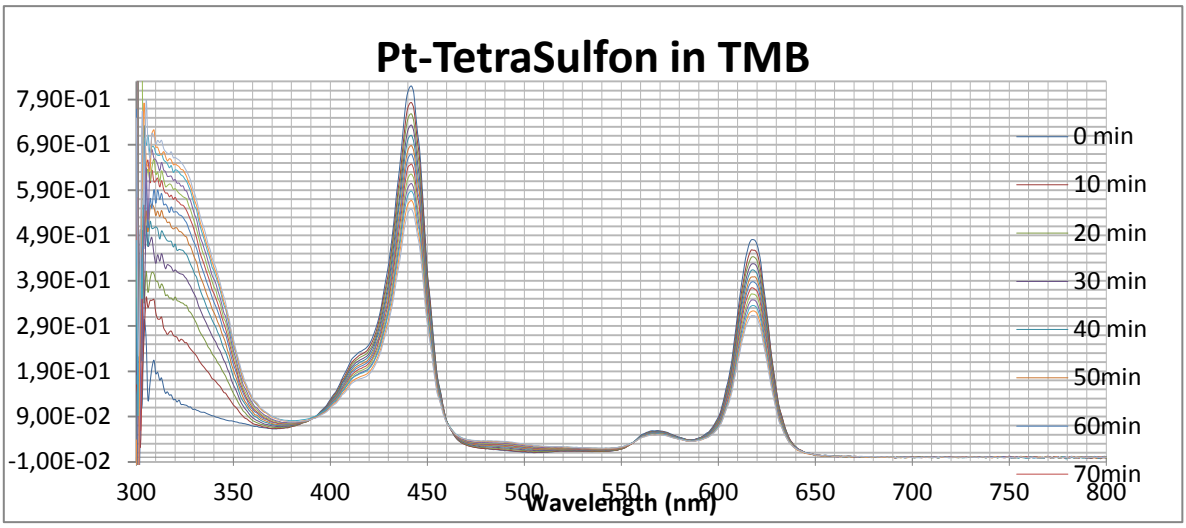

Absorption values		
Wavelength=441,9533691nm		
Time [min]	Abs	Norm Abs
0	0,81908557	1
10	0,78301949	0,95596787
20	0,75814741	0,9256022
30	0,73317961	0,89511967
40	0,71027874	0,8671606
50	0,68765021	0,83953402
60	0,66863461	0,81631838
70	0,64749195	0,79050586
80	0,62481075	0,76281498
90	0,60390415	0,73729067
100	0,58780966	0,71764133
110	0,56659751	0,69174397
120	0,54729406	0,6681769

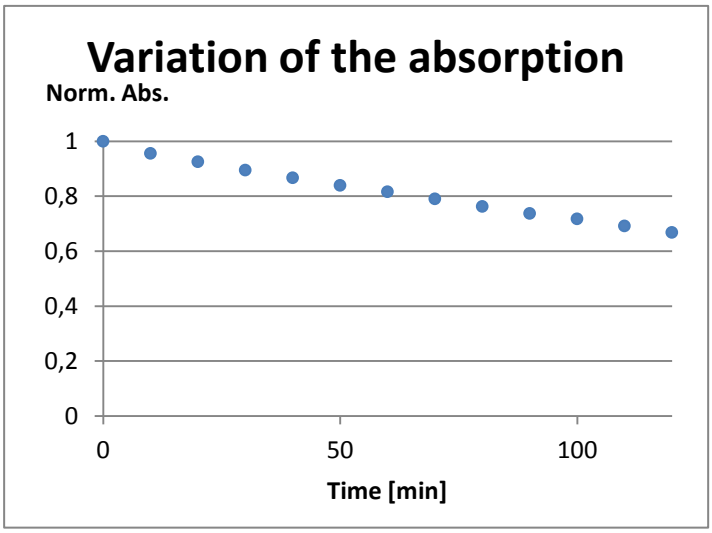

Pt-TetraSulfon in Toluene

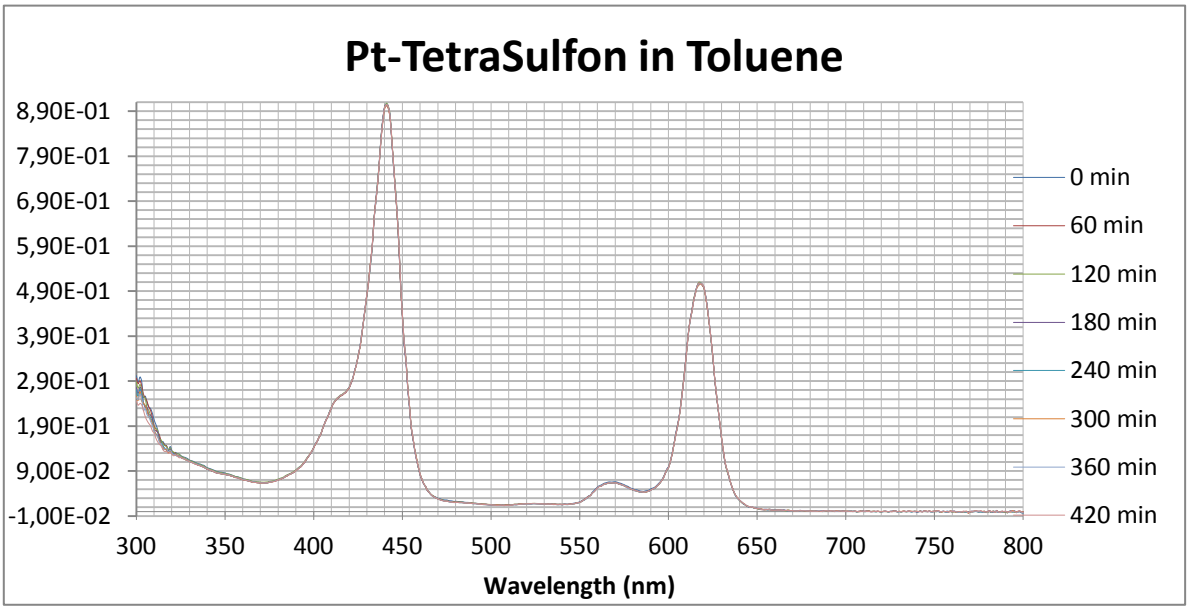

Absorption values		
Wavelength=441,0350342nm		
Time	Abs	Norm Abs
0	0,90655326	1
60	0,90193173	0,99490208
120	0,90745907	1,00099917
180	0,90483358	0,99810306
240	0,90559218	0,99893985
300	0,90306919	0,9961568
360	0,905188	0,998494
420	0,90488229	0,99815679

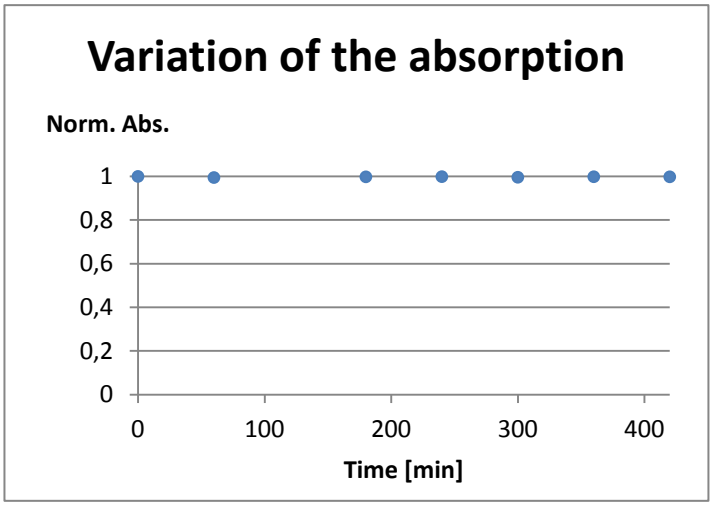

Pt-OctaSulfon in PS

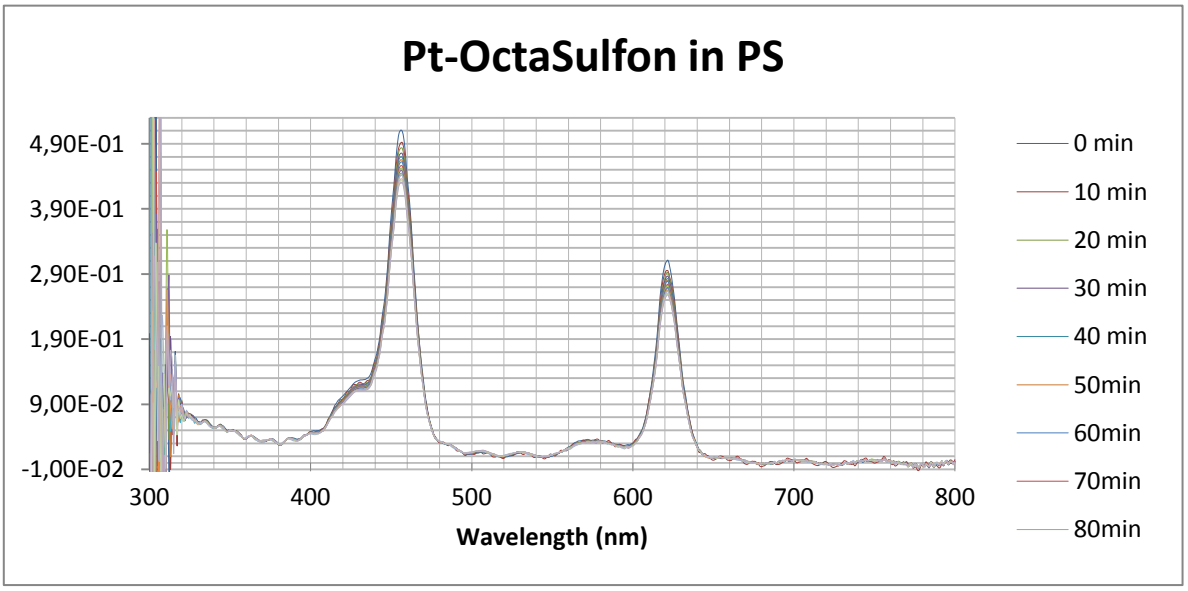

Absorption values		
Wavelength=454,9463196nm		
Time [min]	Abs	Norm Abs
0	0,73240905	1
10	0,72569497	0,99083288
20	0,72712152	0,99278063
30	0,72594101	0,99116881
40	0,72760505	0,99344083
50	0,7304604	0,9973394
60	0,73132105	0,99851448
70	0,7335762	1,00159357
80	0,73239027	0,99997436
90	0,73530809	1,00395822
100	0,73802421	1,0076667
110	0,74680104	1,01965021
120	0,74342531	1,01504112
130	0,74893552	1,02256453
140	0,74370606	1,01542445
150	0,74259569	1,0139084

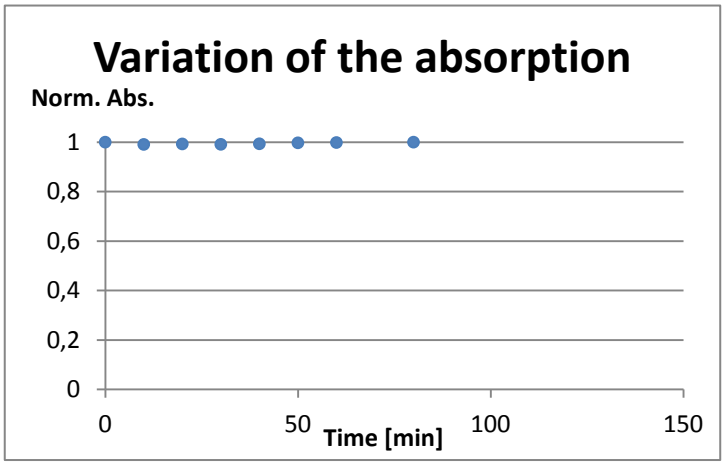

Pt-OctaSulfon in TMB

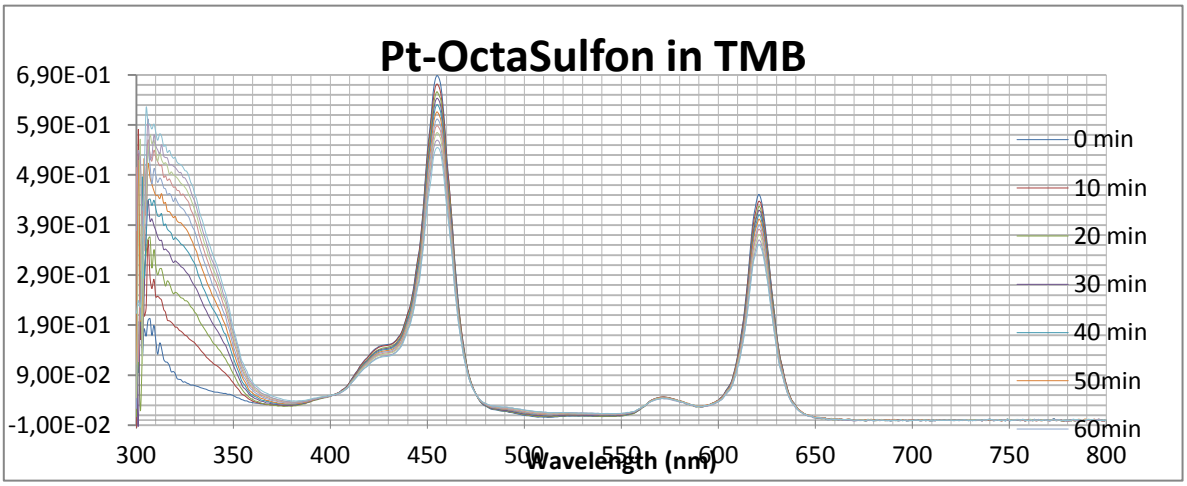

Absorption values		
Wavelength=454,9463196nm		
Time [min]	Abs	Norm Abs
0	0,68874519	1
10	0,67197927	0,9756573
20	0,65630666	0,95290199
30	0,64300415	0,93358788
40	0,63049188	0,9154211
50	0,61582625	0,89412784
60	0,60173624	0,87367033
70	0,58858809	0,85458033
80	0,57473956	0,83447343
90	0,55944114	0,81226141
100	0,54449874	0,7905663

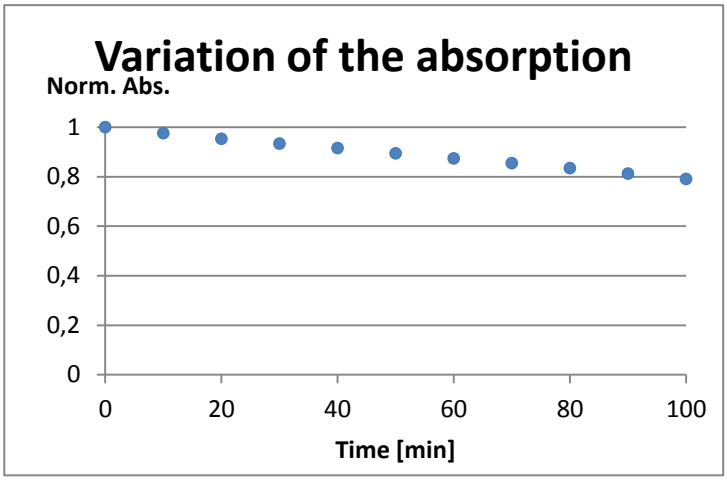

Pt-OctaSulfon in Toluene

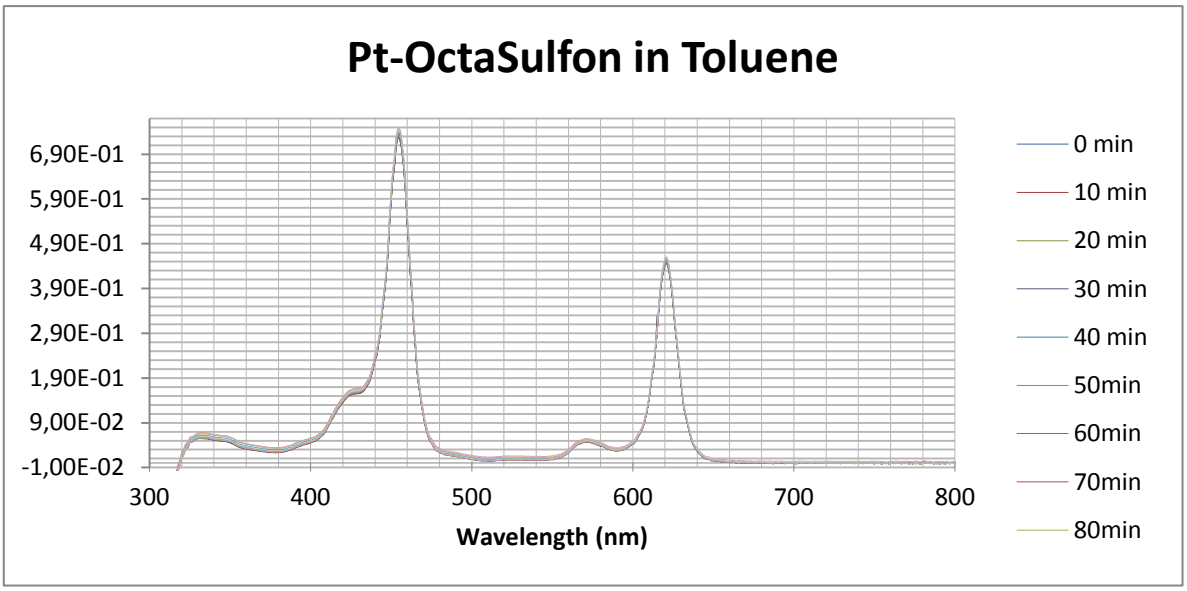

Absorption values		
Wavelength=454,9463196nm		
Time [min]	Abs	Norm Abs
0	0,73240905	1
10	0,72569497	0,99083288
20	0,72712152	0,99278063
30	0,72594101	0,99116881
40	0,72760505	0,99344083
50	0,7304604	0,9973394
60	0,73132105	0,99851448
70	0,7335762	1,00159357
80	0,73239027	0,99997436
90	0,73530809	1,00395822
100	0,73802421	1,0076667
110	0,74680104	1,01965021
120	0,74342531	1,01504112
130	0,74893552	1,02256453
140	0,74370606	1,01542445
150	0,74259569	1,0139084

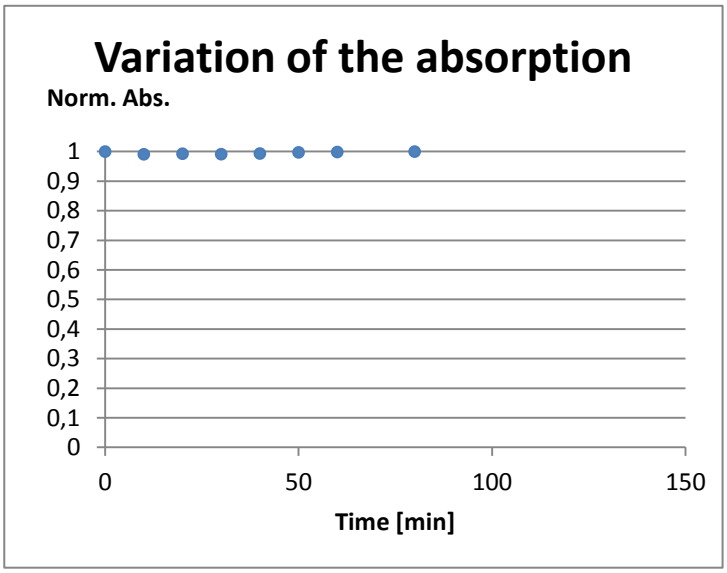

Pt-OctaSulfon in Toluene (long)

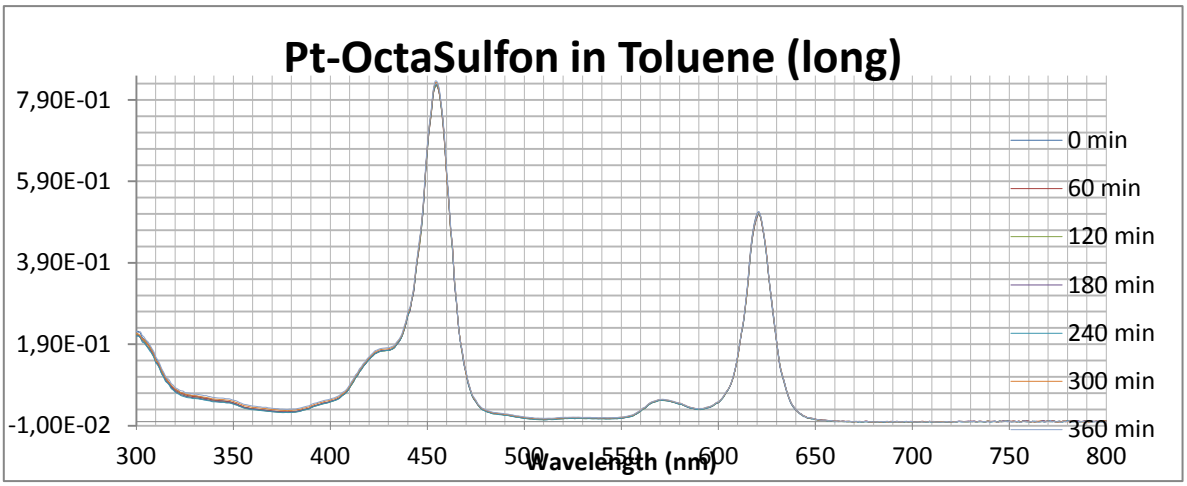

Pt-OctaSulfon in Toluene (long)		
Wavelength=454,9463196nm		
Time [min]	Abs	Norm Abs
0	0,83256483	1
60	0,82508541	0,99101641
120	0,82393936	0,98963989
180	0,82650328	0,99271942
240	0,82720455	0,99356172
300	0,83216254	0,99951681
360	0,83547723	1,0034981

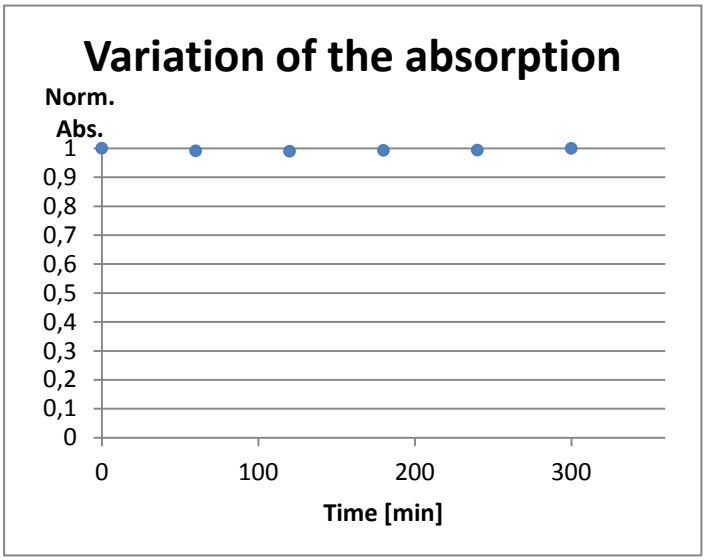

Appendix 2: Deoxygenated photostability measurements

Pt-TPTBP in PS deox

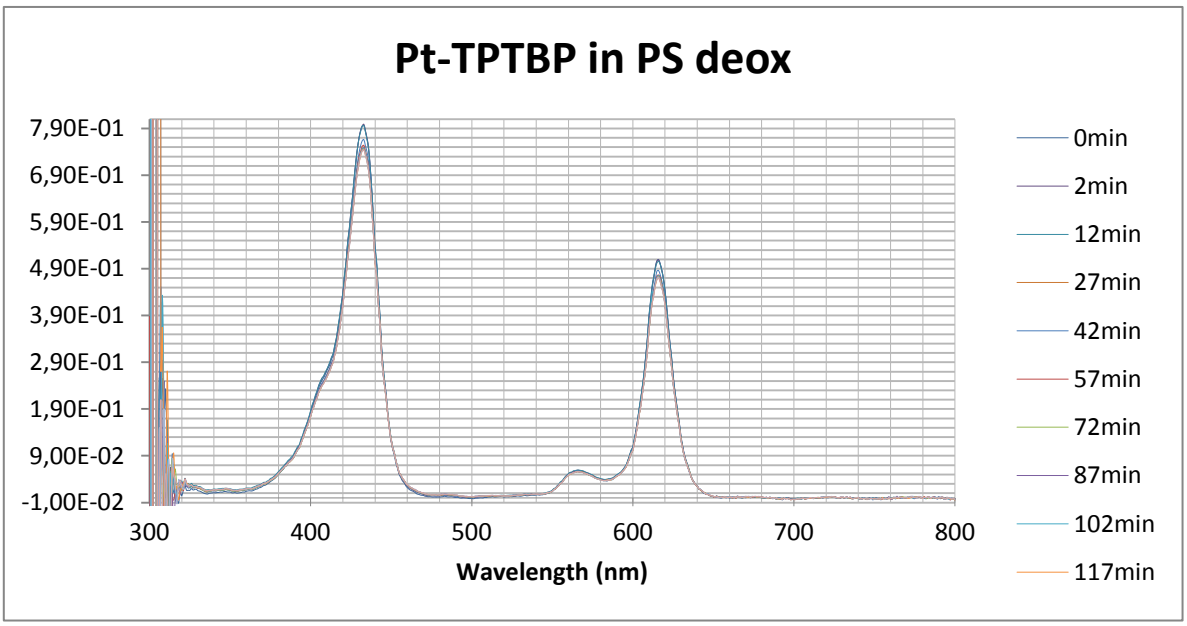

Absorption values		
Wavelength=433,072052nm		
Time [min]	Abs	Norm Abs
0	0,79654257	1
2	0,79875651	1,00277943
12	0,7959727	0,99928457
27	0,79994913	1,00427668
42	0,76617245	0,96187257
57	0,75392165	0,9464926
72	0,74833012	0,93947284
87	0,74844	0,93961079
102	0,74747958	0,93840506
117	0,74559309	0,93603671
132	0,74382795	0,9338207
147	0,74295114	0,93271994

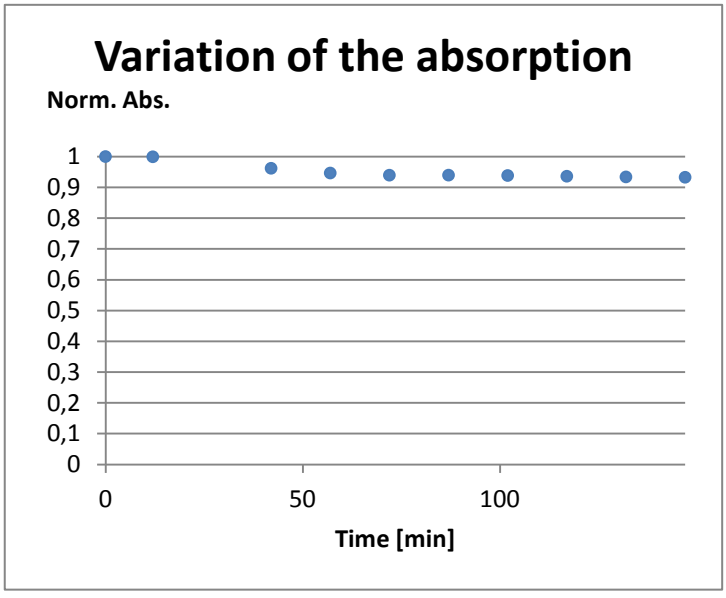

Pt-TPTBP in TMB deox

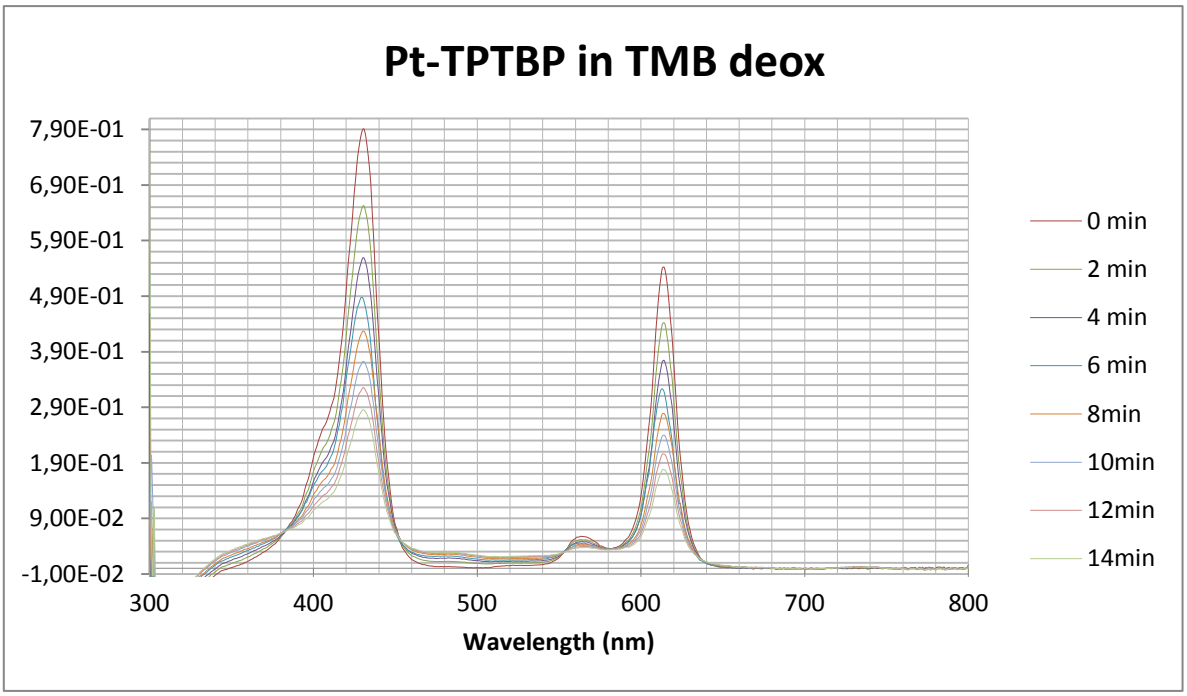

Absorption values		
Wavelength=430,9252625nm		
Time [min]	Abs	Norm Abs
0	0,7908044	1
2	0,65231685	0,82487761
4	0,55884181	0,70667514
6	0,48062935	0,60777272
8	0,42694882	0,53989181
10	0,37239644	0,4709084
12	0,32473766	0,41064221
14	0,28558225	0,36112881

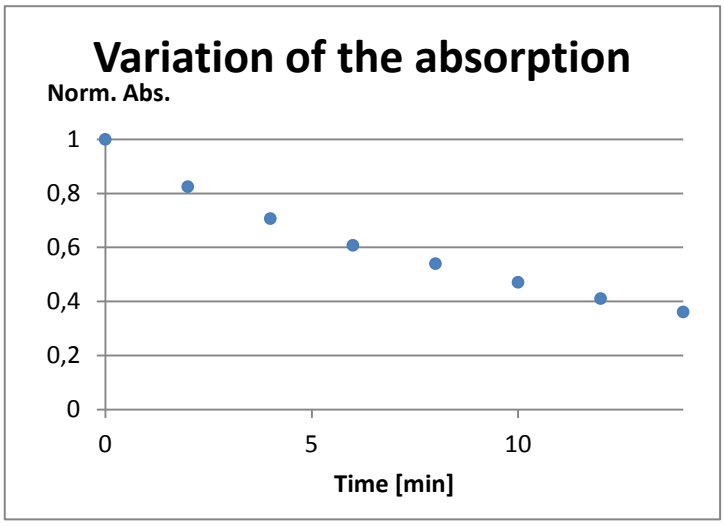

Pt-TertButyil in PS deox

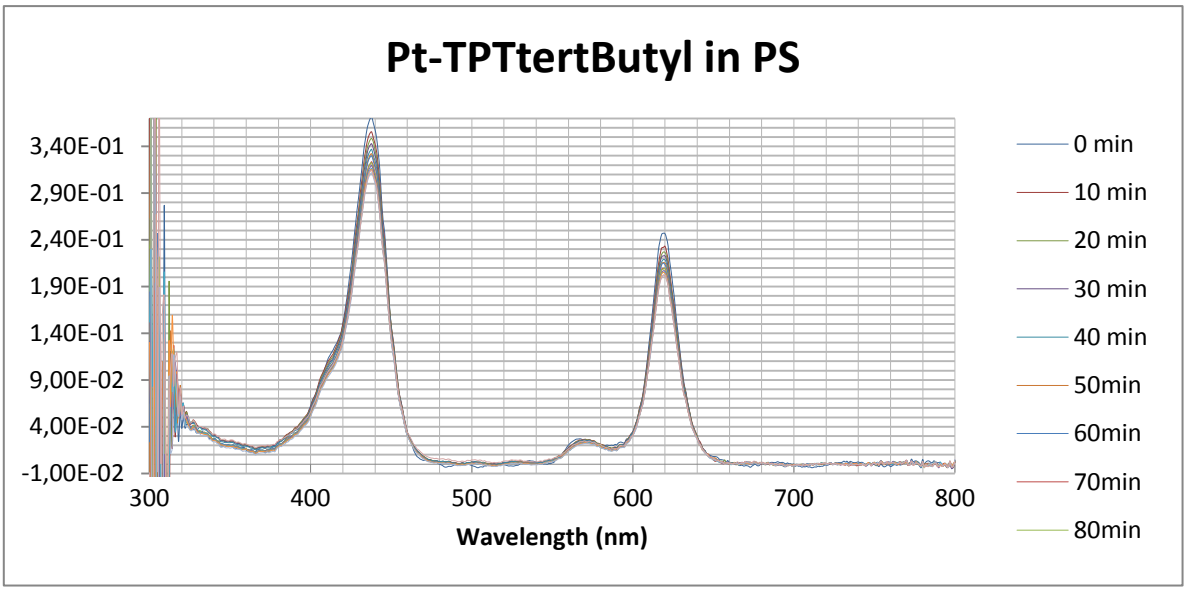

Absorption values		
Wavelength=437,9759216nm		
Time [min]	Abs	Norm Abs
0	0,35168979	1
2	0,34977583	0,99455782
12	0,35147273	0,99938282
27	0,34918258	0,99287098
42	0,34944607	0,99362017
57	0,34791917	0,98927858
72	0,34627585	0,98460593
87	0,3477501	0,98879783
102	0,34733044	0,98760457
117	0,34517273	0,98146931
132	0,34565815	0,98284956
147	0,34116868	0,97008412

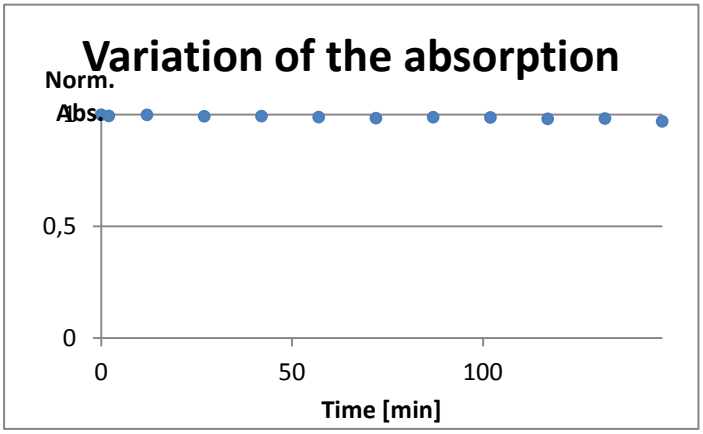

Pt-tBut in TMB deox

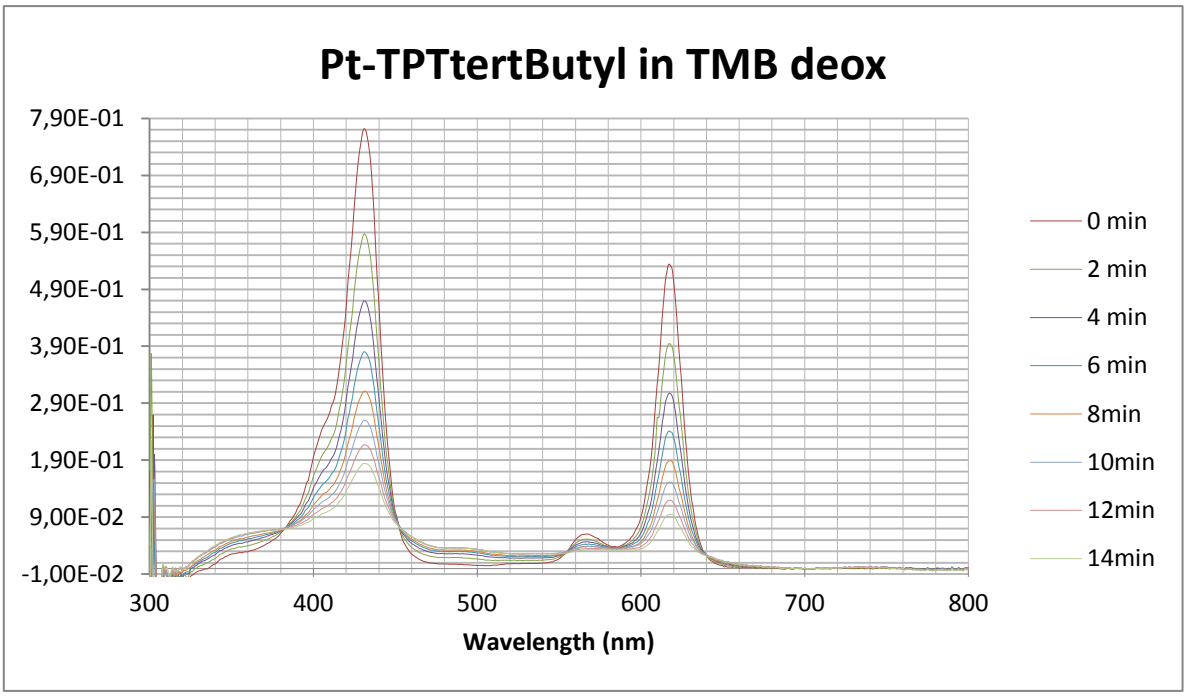

Absorption values		
Wavelength=430,9252625nm		
Time [min]	Abs	Norm Abs
0	0,7719017	1
2	0,58690439	0,76033565
4	0,46947721	0,60820854
6	0,38031324	0,49269647
8	0,31079105	0,40263035
10	0,25936343	0,33600577
12	0,21700739	0,28113346
14	0,18452198	0,23904855

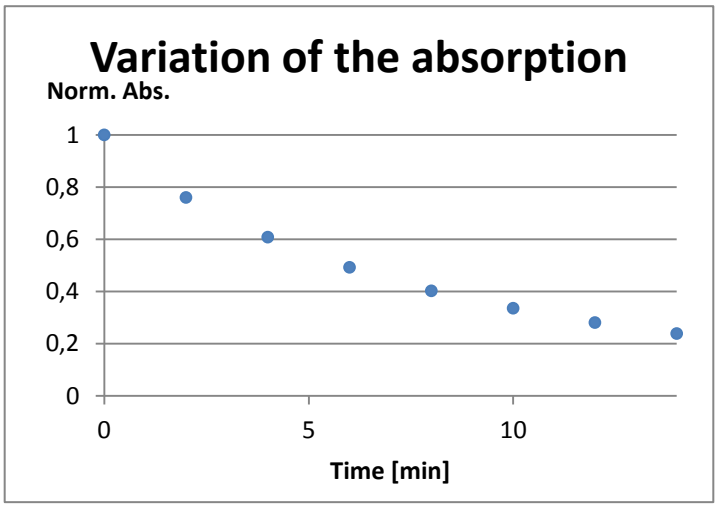

Pt-Cl-Benzo in PS deox

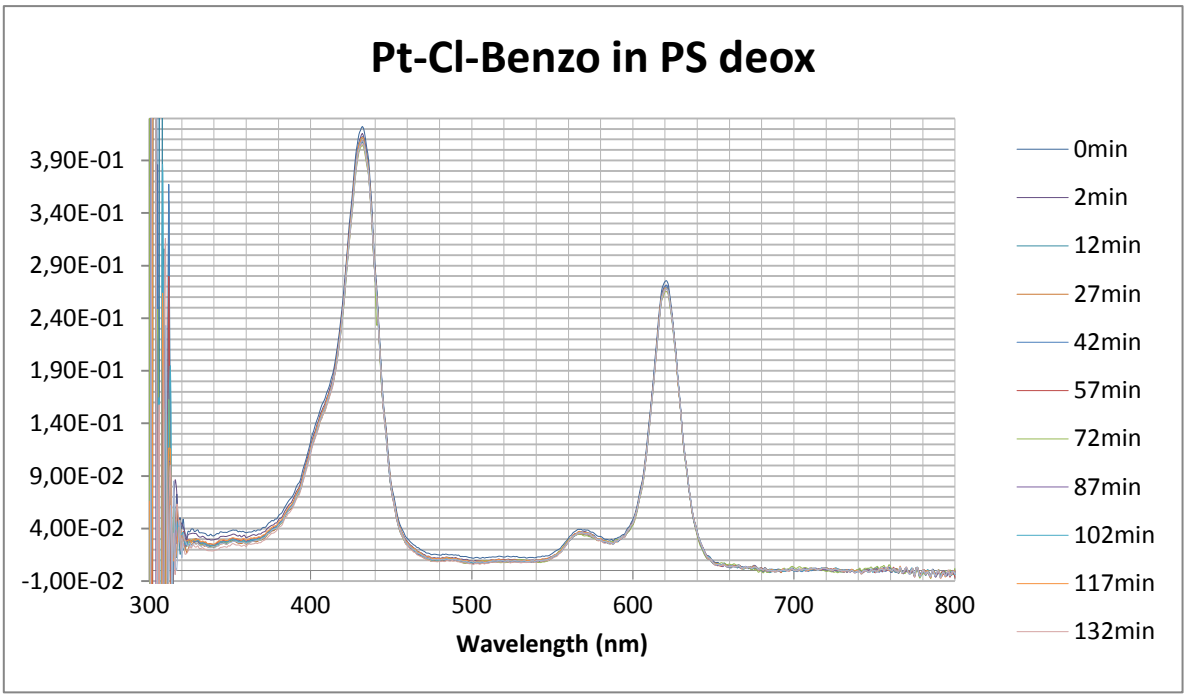

Absorption values		
Wavelength=432,0570068nm		
Time [min]	Abs	Norm Abs
0	0,42219261	1
2	0,41570862	0,98464209
12	0,40756208	0,96534631
27	0,40890635	0,96853031
42	0,41275148	0,97763785
57	0,4116676	0,97507058
72	0,40425966	0,95752423
87	0,40889381	0,96850061
102	0,41140922	0,9744586
117	0,4120377	0,9759472
132	0,40580094	0,9611749
147	0,40862919	0,96787385

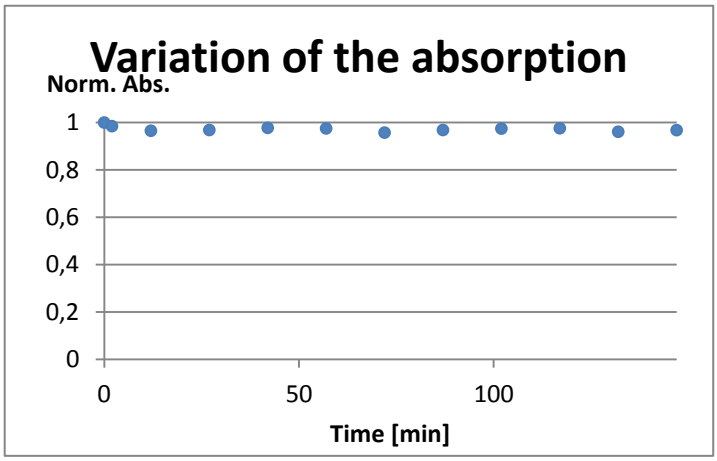

Pt-Cl-Benzo in TMB deox

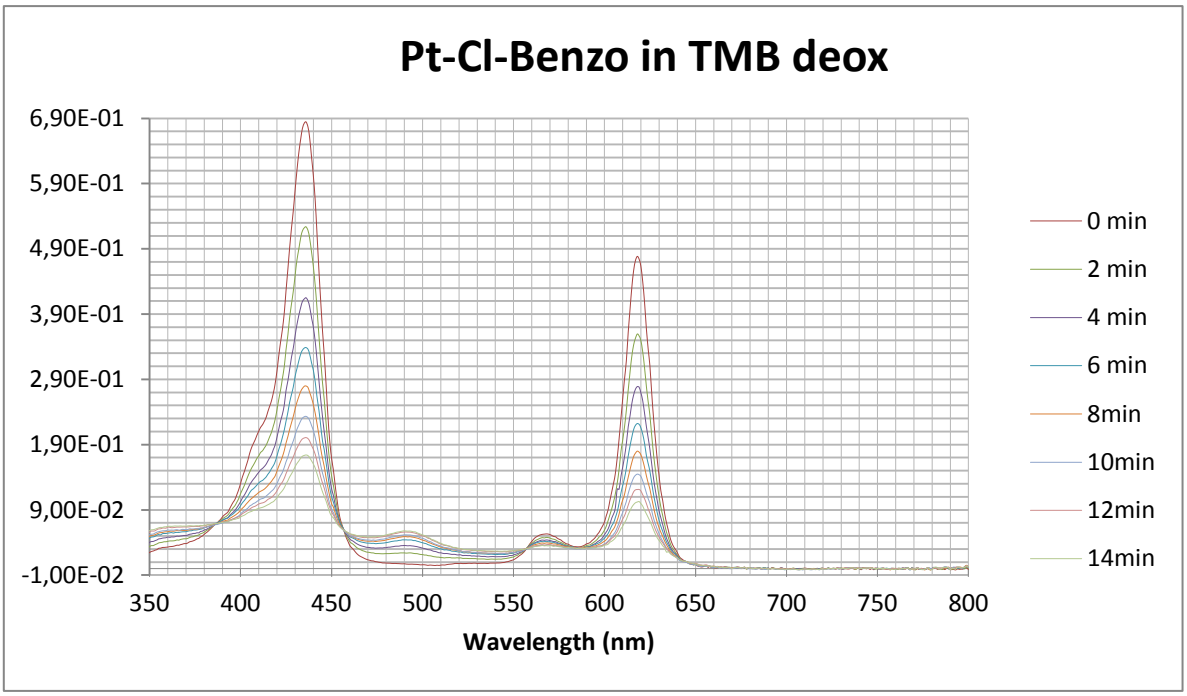

Absorption values		
Wavelength=435,9842529nm		
Time [min]	Abs	Norm Abs
0	0,68474729	1
2	0,52356231	0,76460662
4	0,41521361	0,60637496
6	0,33848258	0,49431751
8	0,27974457	0,40853695
10	0,23334152	0,34077027
12	0,20064271	0,29301716
14	0,17421827	0,25442711

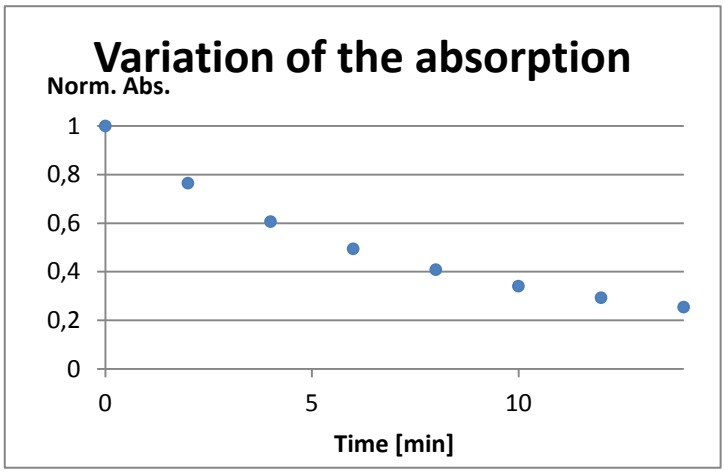

Pt-TetraSulfon in PS deox

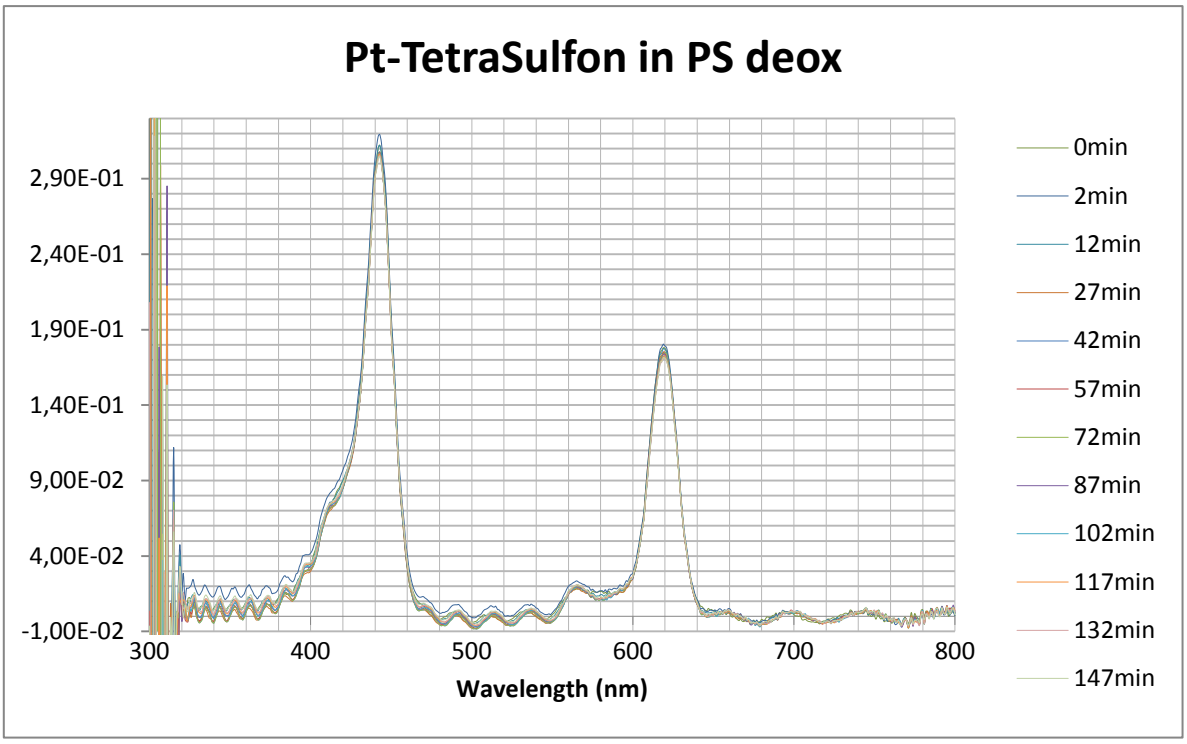

Absorption values		
Wavelength=442,0151062nm		
Time [min]	Abs	Norm Abs
0	0,31049244	1
2	0,31819098	1,02479464
12	0,31065684	1,00052951
27	0,30594407	0,98535113
42	0,30603827	0,9856545
57	0,30582872	0,98497961
72	0,30563341	0,98435059
87	0,30518561	0,98290837
102	0,3056674	0,98446005
117	0,30464425	0,9811648
132	0,30358551	0,97775493
147	0,30327453	0,97675335

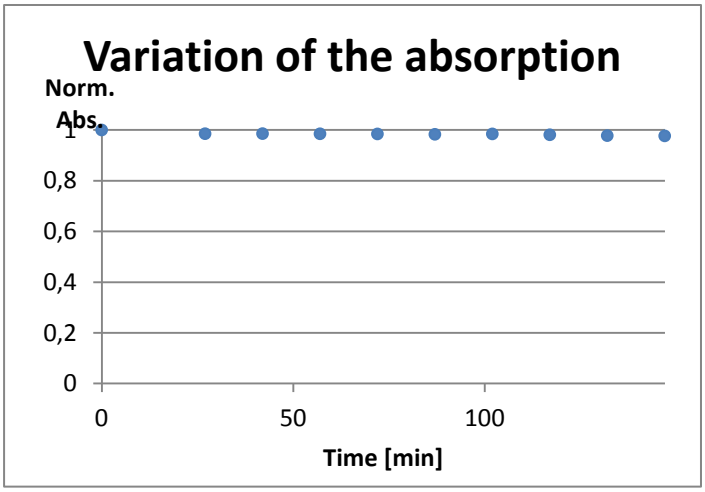

Pt-TetraSulfon in TMB deox

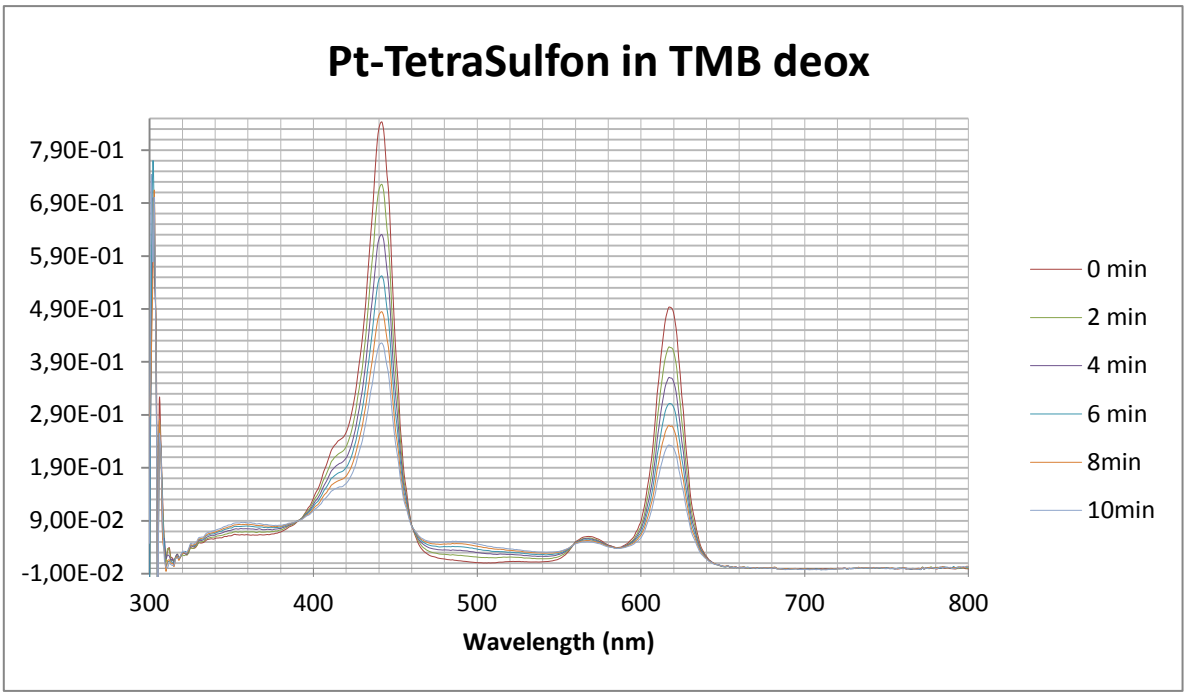

Absorption values		
Wavelength=441,9571228nm		
Time [min]	Abs	Norm Abs
0	0,84302067	1
2	0,72478435	0,85974683
4	0,63007192	0,74739795
6	0,55195839	0,65473886
8	0,4841209	0,57426931
10	0,42517343	0,5043452

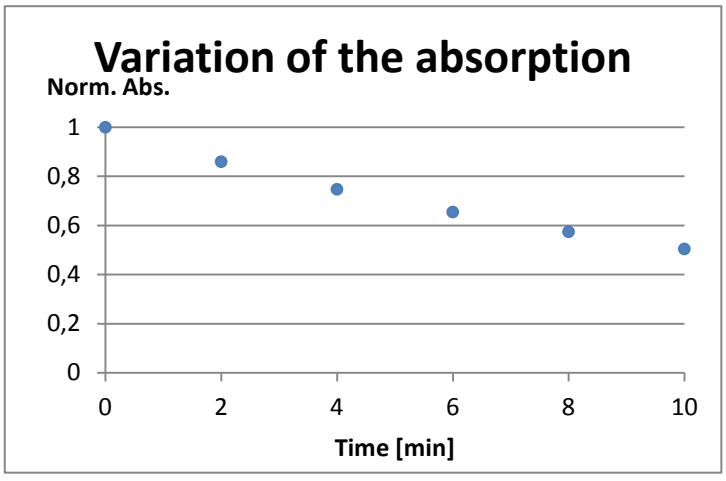

Pt-OctaSulfon in PS deox

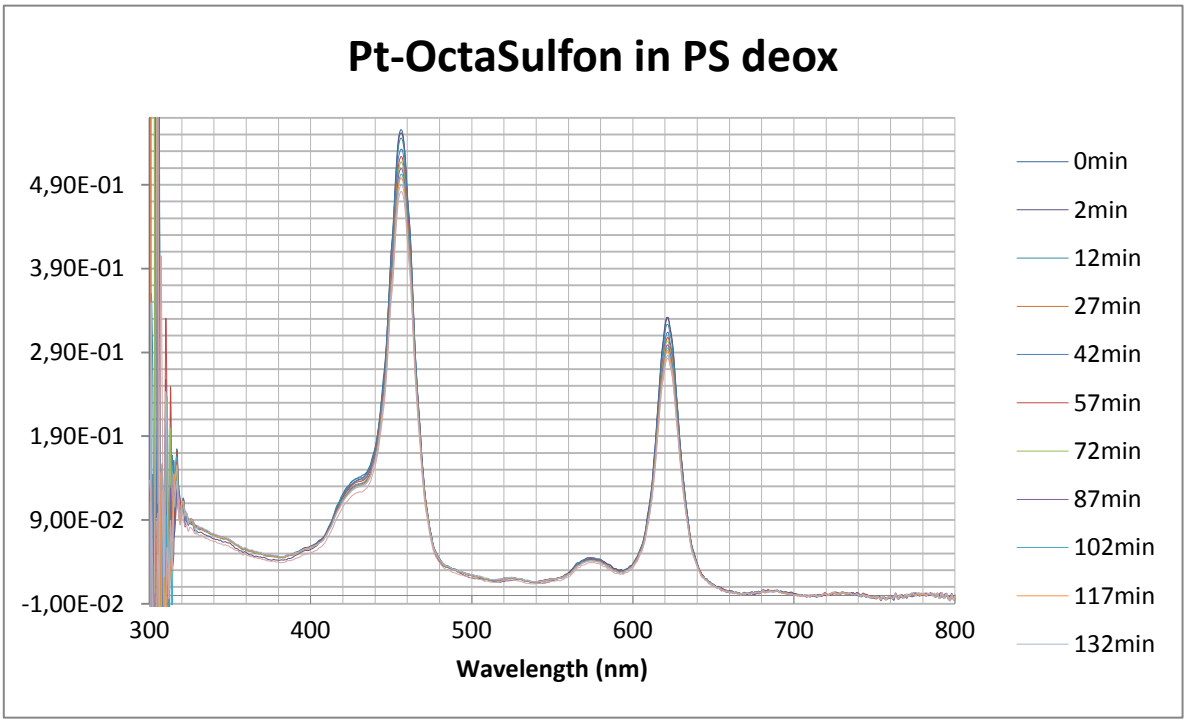

Pt-OctaSulfon in PS deox		
Wavelength=456,0212097nm		
Time [min]	Abs	Norm Abs
0	0,55589072	1
2	0,55206855	0,99312425
12	0,54578269	0,98181652
27	0,53915914	0,96990132
42	0,53254699	0,95800662
57	0,52373908	0,94216195
72	0,51696897	0,92998309
87	0,5094313	0,91642347
102	0,50258094	0,90410025
117	0,49822996	0,89627321
132	0,48967474	0,8808831
147	0,4819061	0,86690798

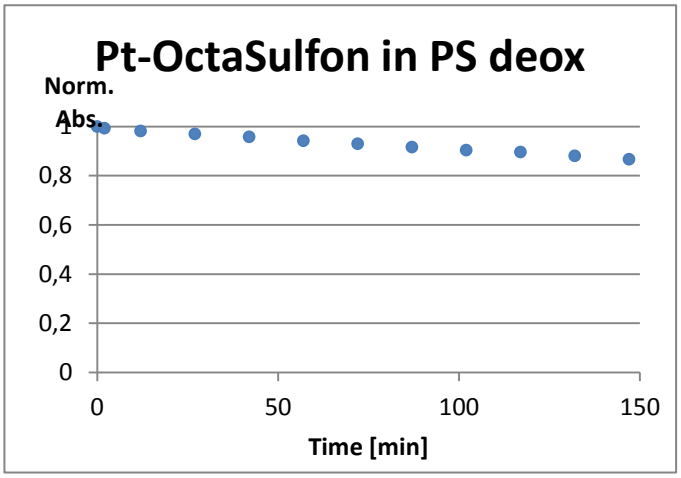

Pt-OctaSulfon in TMB deox

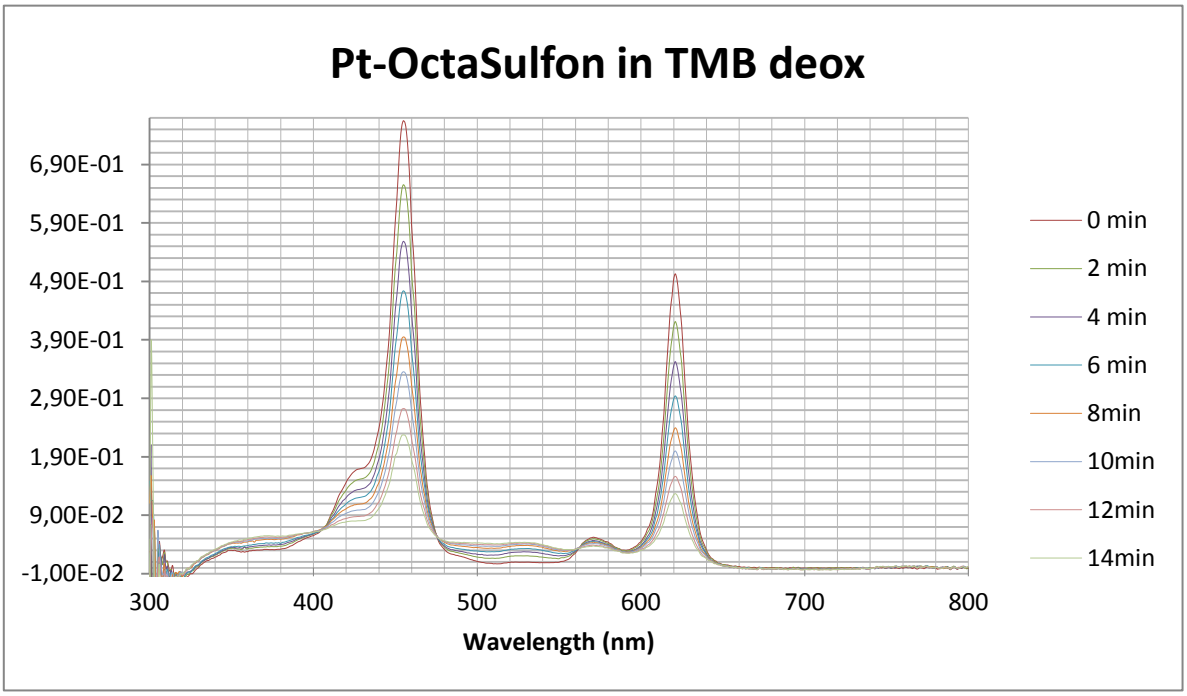

Pt-OctaSulfon in TMB deox		
Wavelength=454,9524231nm		
Time [min]	Abs	Norm Abs
0	0,76501545	1
2	0,65528397	0,85656305
4	0,5585177	0,73007375
6	0,47400225	0,61959827
8	0,39519202	0,51658045
10	0,33529707	0,43828797
12	0,27256147	0,35628231
14	0,22729386	0,29711016

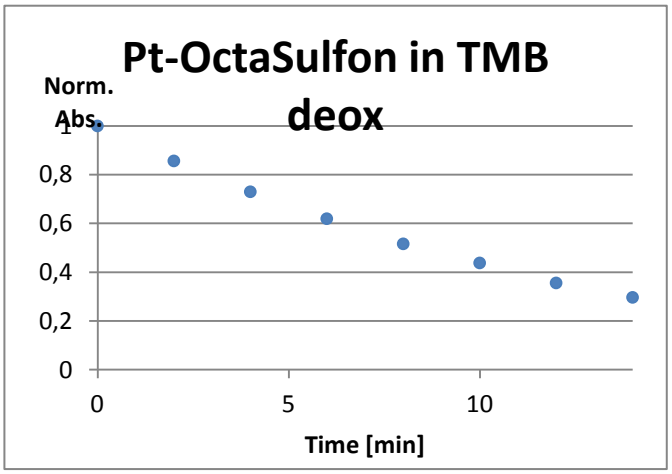

Pt-OctaSulfon in TMB deox 50% filter

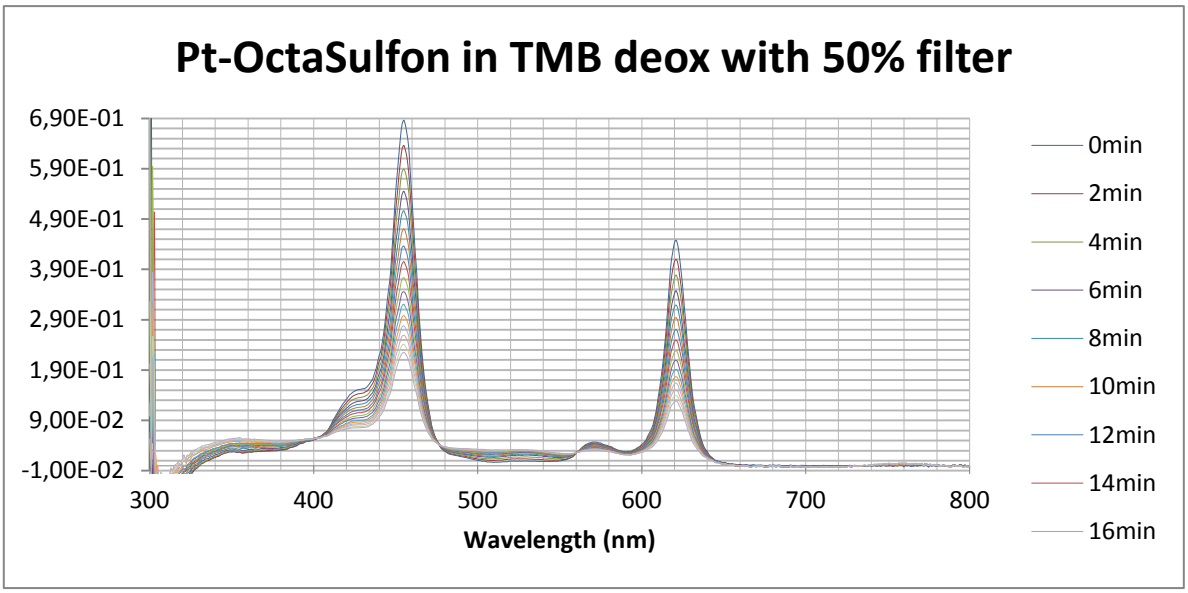

Absorption values		
Wavelength=455,0100098nm		
Time [min]	Abs	Norm. Abs.
0	0,68624296	1
2	0,6362968	0,92721796
4	0,58948941	0,85900978
6	0,54553276	0,79495572
8	0,50657987	0,73819317
10	0,47042474	0,68550756
12	0,43645387	0,63600489
14	0,40541963	0,59078148
16	0,37356867	0,54436795
18	0,34551171	0,50348307
20	0,3207395	0,46738475
22	0,2984522	0,43490748
24	0,27764721	0,40459025
26	0,25924709	0,37777741
28	0,24105568	0,35126871
30	0,2250219	0,32790413

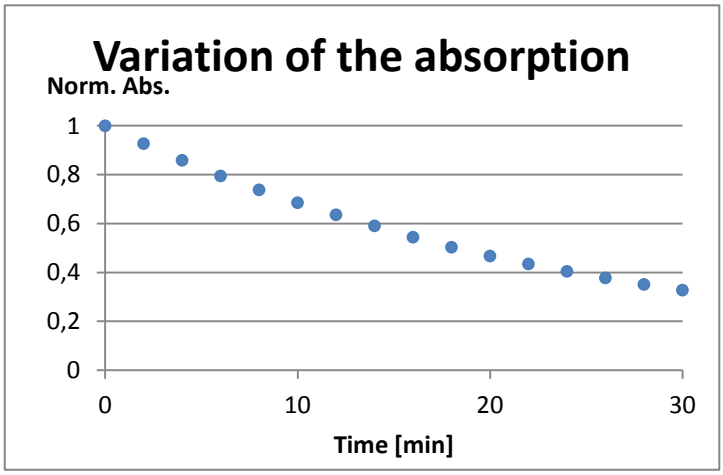

Pt-OctaSulfon TMB deox 25% filter

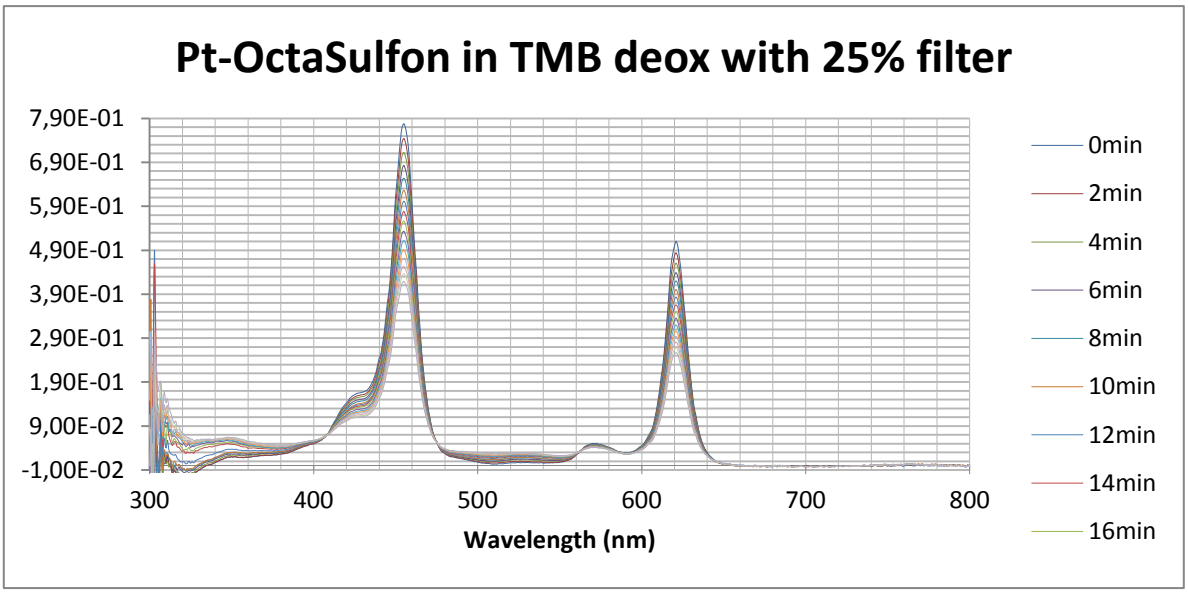

Absorption values		
Wavelength=455,0100098nm		
Time [min]	Abs	Norm. Abs.
0	0,77766026	1
2	0,74389887	0,95658594
4	0,71207048	0,91565754
6	0,68327833	0,87863347
8	0,65395915	0,84093168
10	0,62633141	0,80540493
12	0,60131579	0,77323713
14	0,57857398	0,74399325
16	0,55671106	0,71587953
18	0,533214	0,68566445
20	0,51153369	0,65778555
22	0,49114189	0,63156357
24	0,47173065	0,60660249
26	0,45336192	0,58298197
28	0,43611177	0,56079986
30	0,41913325	0,53896704

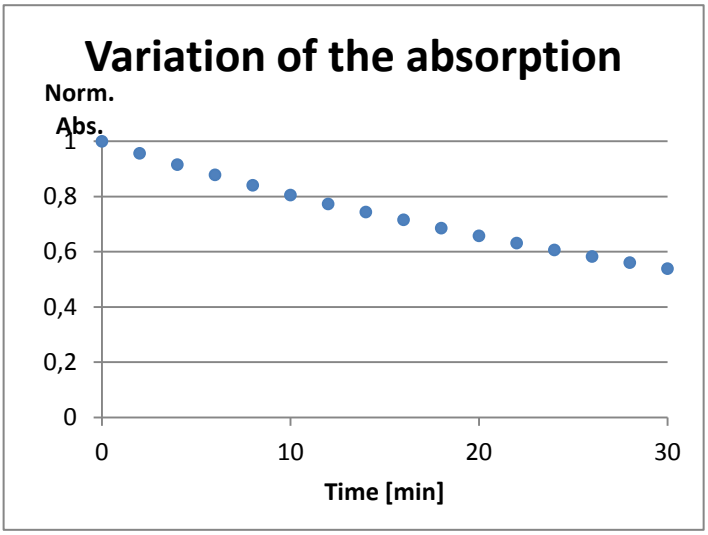

Pt-OctaSulfon in Toluene deox

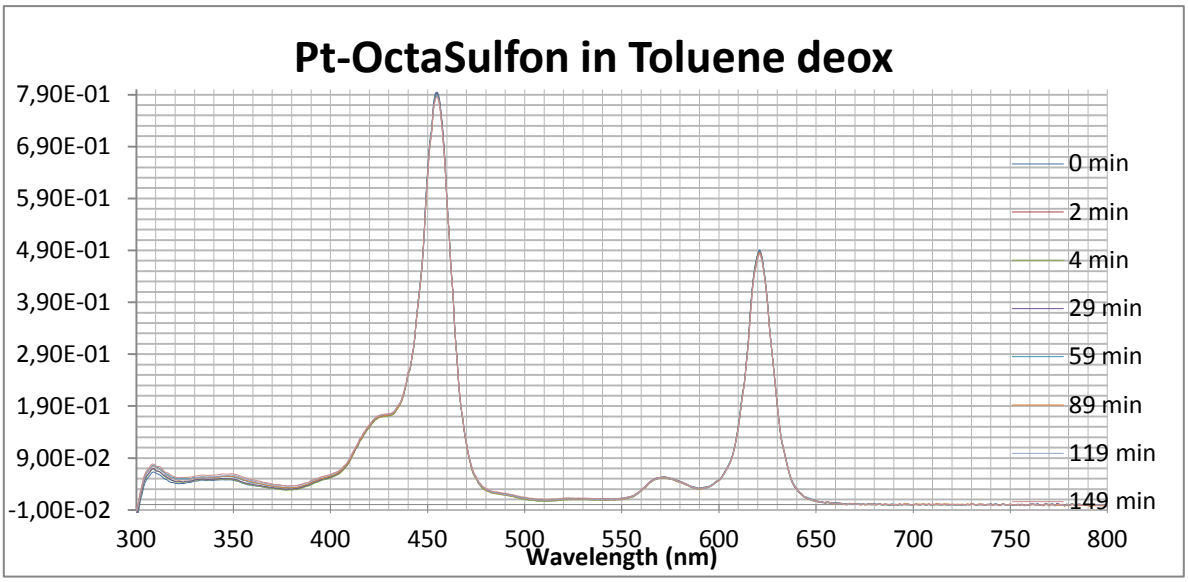

Absorption values		
Wavelength=454,9463196nm		
Time [min]	Abs	Norm. Abs.
0	0,7943231	1
2	0,79249179	0,9976945
4	0,79192837	0,99698519
14	0,7923912	0,99756786
29	0,78955672	0,99399943
59	0,78721727	0,99105423
89	0,78706891	0,99086745
119	0,78468147	0,98786183
149	0,78861609	0,99281525

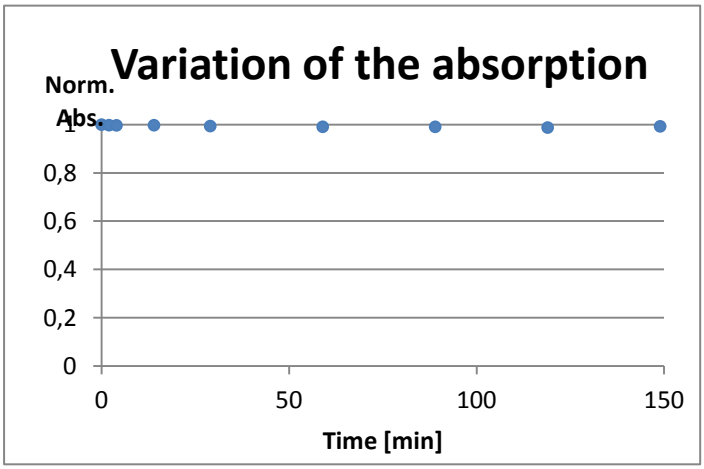

Appendix 3: Photobleaching of all the dyes

Pt-TPTBP			
Medium Time [min]	PS deox [147]	TMB deox [14]	Toluene [540]
Wavelength Soret [nm]	433,0721	430,9253	430,9235
Absorption Soret Start	0,7965	0,7908	0,7119
Absorption Soret End	0,7430	0,2856	0,7072
Decrease of Absorption [%]	6,7280	63,8871	0,6570
Wavelength Q-band [nm]	615,9774	614,0638	614,0281
Absorption Q-band Start	0,5098	0,2789	0,4706
Absorption Q-band End	0,4698	0,1780	0,4684
Decrease of Absorption [%]	7,8484	36,1919	0,4846

Pt-TertButyl I			
Medium Time [min]	TMB [120]	TMB deox [14]	Toluene [450]
Wavelength Soret [nm]	430,0033	430,9253	430,9235
Absorption Soret Start	0,6377	0,7719	0,6951
Absorption Soret End	0,1556	0,1845	0,6285
Decrease of Absorption [%]	75,5958	76,0951	9,5846
Wavelength Q-band [nm]	619,0298	617,0074	618,0006
Absorption Q-band Start	0,4513	0,5338	0,4690
Absorption Q-band End	0,0919	0,0950	0,4211
Decrease of Absorption [%]	79,6298	82,2007	10,2070

Pt-TertButyl II		
Medium Time [min]	PS [130]	PS deox [147]
Wavelength Soret [nm]	437,9729	437,9759
Absorption Soret Start	0,3713	0,3517
Absorption Soret End	0,3142	0,3412
Decrease of Absorption [%]	15,3776	2,9916
Wavelength Q-band [nm]	619,0298	619,0665
Absorption Q-band Start	0,2472	0,2266
Absorption Q-band End	0,2025	0,2220
Decrease of Absorption [%]	18,0686	2,0591

Pt-Cl-Benzo				
Medium Time [min]	PS 150]	PS deox [147]	TMB [120]	TMB deox [14]
Wavelength Soret [nm]	431,9968	432,0570	435,0622	435,9843
Absorption Soret Start	0,4437	0,4222	0,6845	0,6847
Absorption Soret End	0,2746	0,4086	0,3920	0,1742
Decrease of Absorption [%]	38,1103	3,2126	42,7230	74,5573
Wavelength Q-band [nm]	620,9404	621,0293	618,0006	618,0370
Absorption Q-band Start	0,2934	0,2755	0,4725	0,4787
Absorption Q-band End	0,1630	0,2675	0,2582	0,1021
Decrease of Absorption [%]	44,4569	2,8912	45,3549	78,6661

Pt-TetraSulfon					
Medium Time [min]	PS [150]	PS deox [147]	TMB [120]	TMB deox [10]	Toluene [420]
Wavelength Soret [nm]	443,0245	442,0151	441,9534	441,9571	441,0350
Absorption Soret Start	0,2822	0,3105	0,8191	0,8430	0,9066
Absorption Soret End	0,2360	0,3033	0,5473	0,4252	0,9049
Decrease of Absorption [%]	16,3732	2,3247	33,1823	49,5655	0,1843
Wavelength Q-band [nm]	619,0298	618,9714	618,0006	617,0074	618,0006
Absorption Q-band Start	0,1595	0,1780	0,4806	0,4931	0,5087
Absorption Q-band End	0,1291	0,1714	0,3129	0,2331	0,5059
Decrease of Absorption [%]	19,0365	3,7179	34,9018	52,7352	0,5470

Pt-OctaSulfon								
Medium	PS	PS deox	TMB	TMB deox	TMB deox 50%f	TMB deox 25%f	Toluene	Toluene deox
Time [min]	[150]	[147]	[100]	[14]	[30]	[30]	[360]	[149]
Wavelength Soret [nm]	456,0149	456,0212	454,9463	454,9524	455,0100	455,0100	454,9463	454,9463
Absorption Soret Start	0,5112	0,5559	0,6887	0,7650	0,6862	0,7777	0,7324	0,8326
Absorption Soret End	0,4303	0,4819	0,5445	0,2273	0,2250	0,4191	0,7426	0,8355
Decrease of Absorption [%]	15,8284	13,3092	20,9434	70,2890	67,2096	46,1033	0	0
Wavelength Q-band [nm]	621,9688	620,9774	620,9404	620,9774	621,0293	621,0293	620,9404	620,9404
Absorption Q-band Start	0,3111	0,3316	0,4512	0,5032	0,4477	0,5104	0,4504	0,5147
Absorption Q-band End	0,2577	0,2813	0,3517	0,1269	0,1282	0,2572	0,4583	0,5155
Decrease of Absorption [%]	17,1710	15,1575	22,0514	74,7827	71,3562	49,5962	0	0

Appendix 4: Phase angle measurements

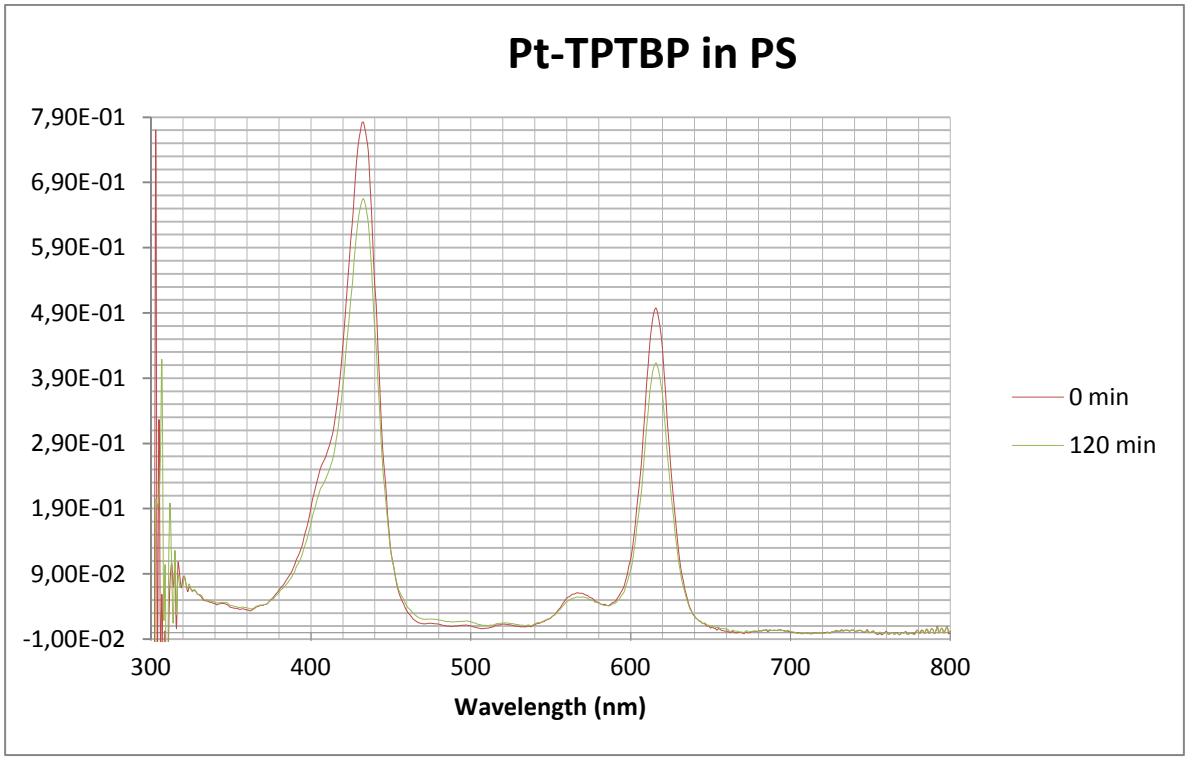

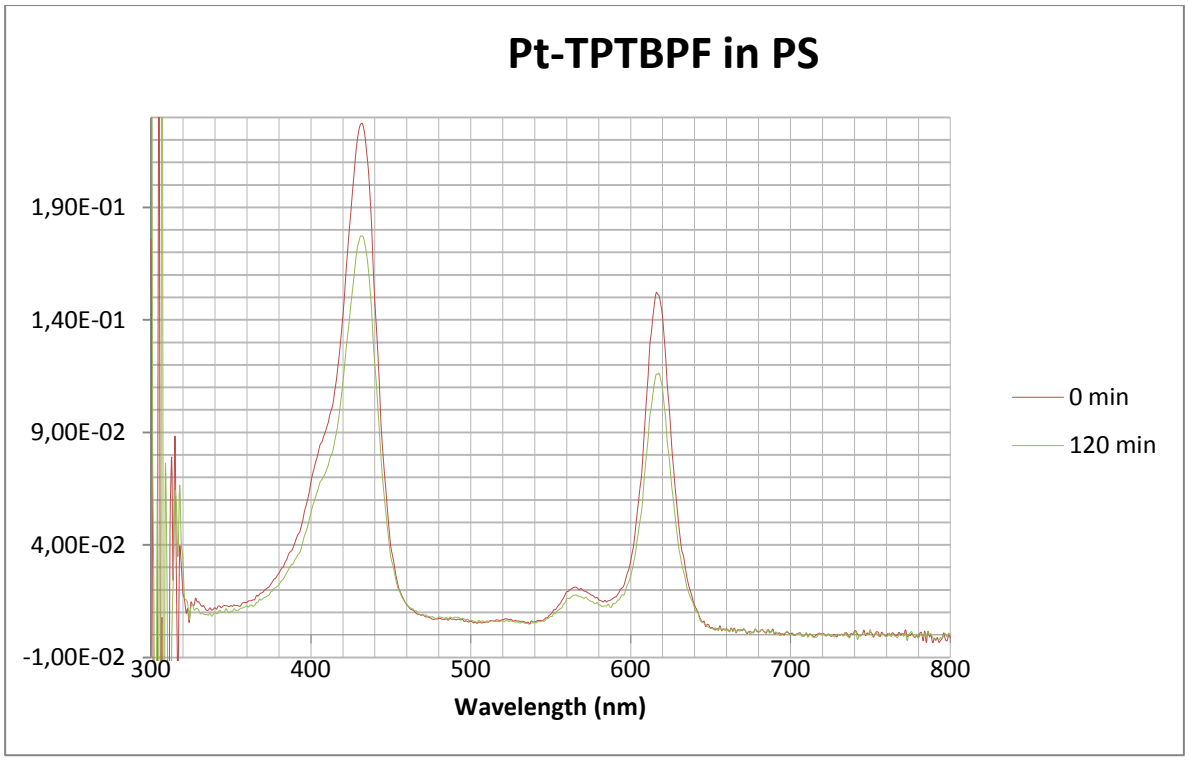

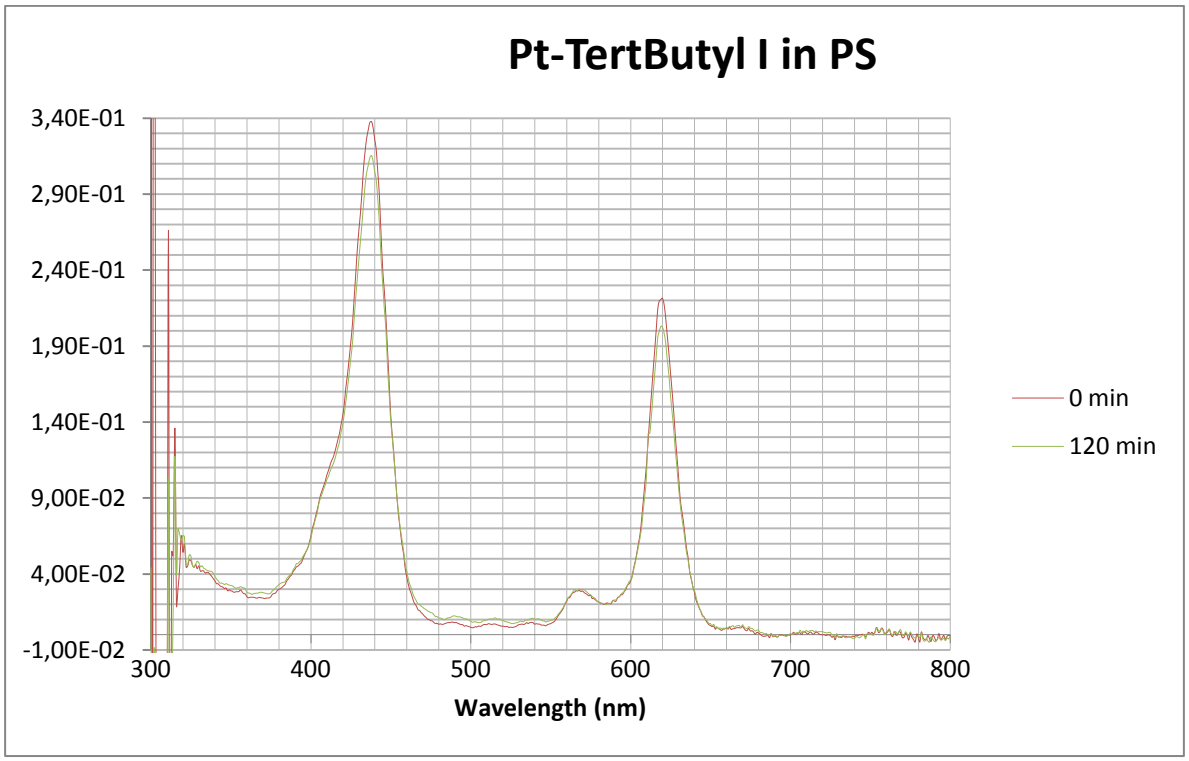
Pt-TertButyl I in PS
3,40E-01
2,90E-01
2,40E-01
1,90E-01
1,40E-01
9,00E-02
4,00E-02
-1,00E-02
300
400
500
600
700
800
Wavelength (nm)
0 min
120 min

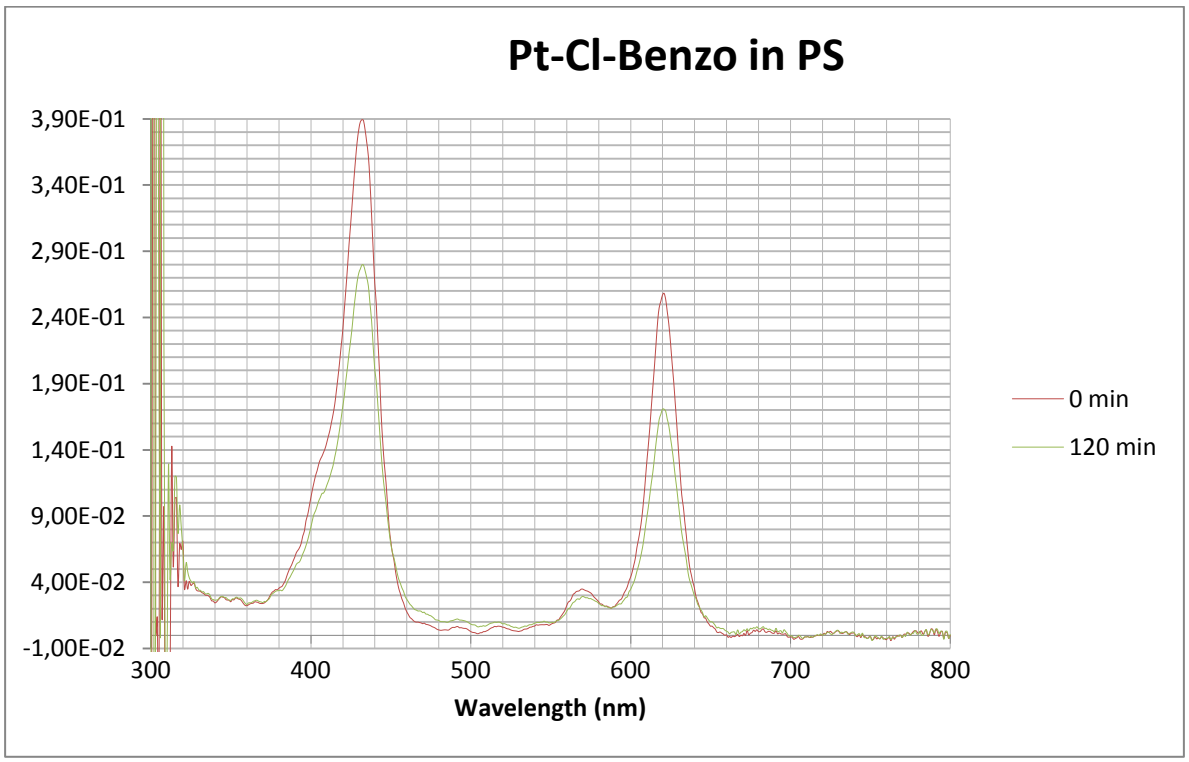
Pt-Cl-Benzo in PS
3,90E-01
3,40E-01
2,90E-01
2,40E-01
1,90E-01
1,40E-01
9,00E-02
4,00E-02
-1,00E-02
300
400
500
600
700
800
Wavelength (nm)
0 min
120 min

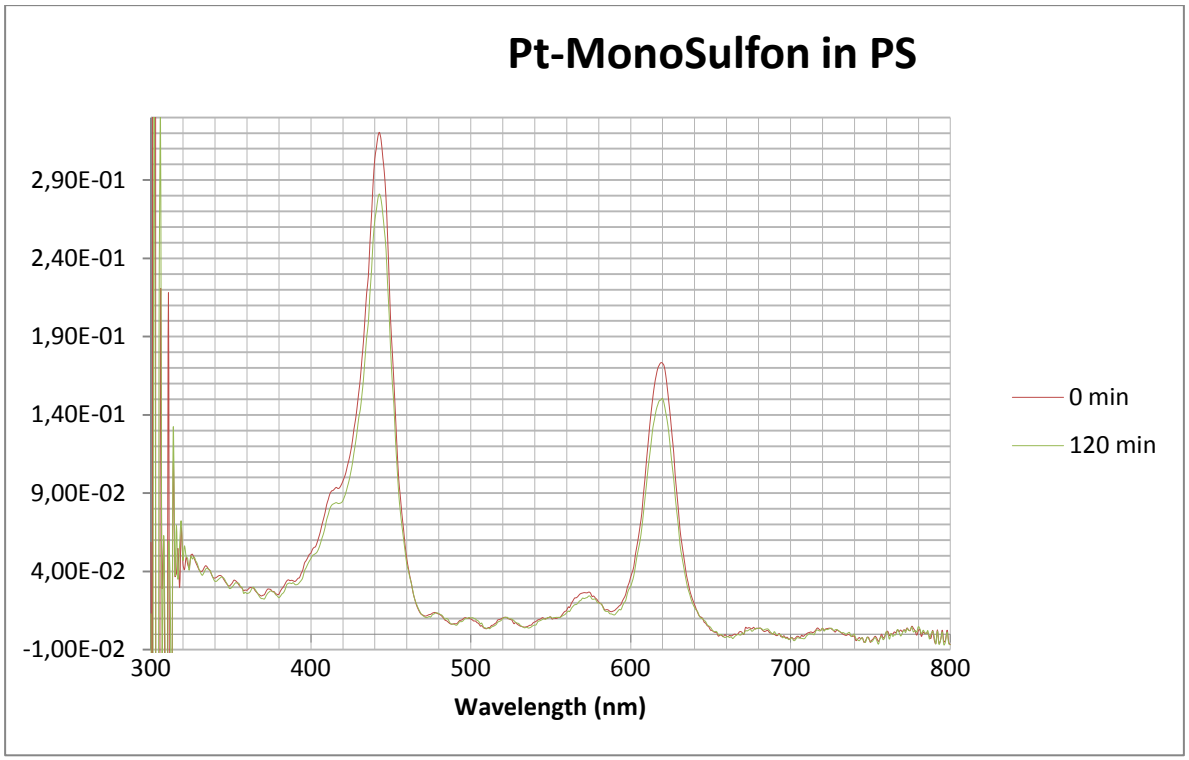
Pt-MonoSulfon in PS
2,90E-01
2,40E-01
1,90E-01
1,40E-01
9,00E-02
4,00E-02
-1,00E-02
300
400
500
600
700
800
Wavelength (nm)
0 min
120 min

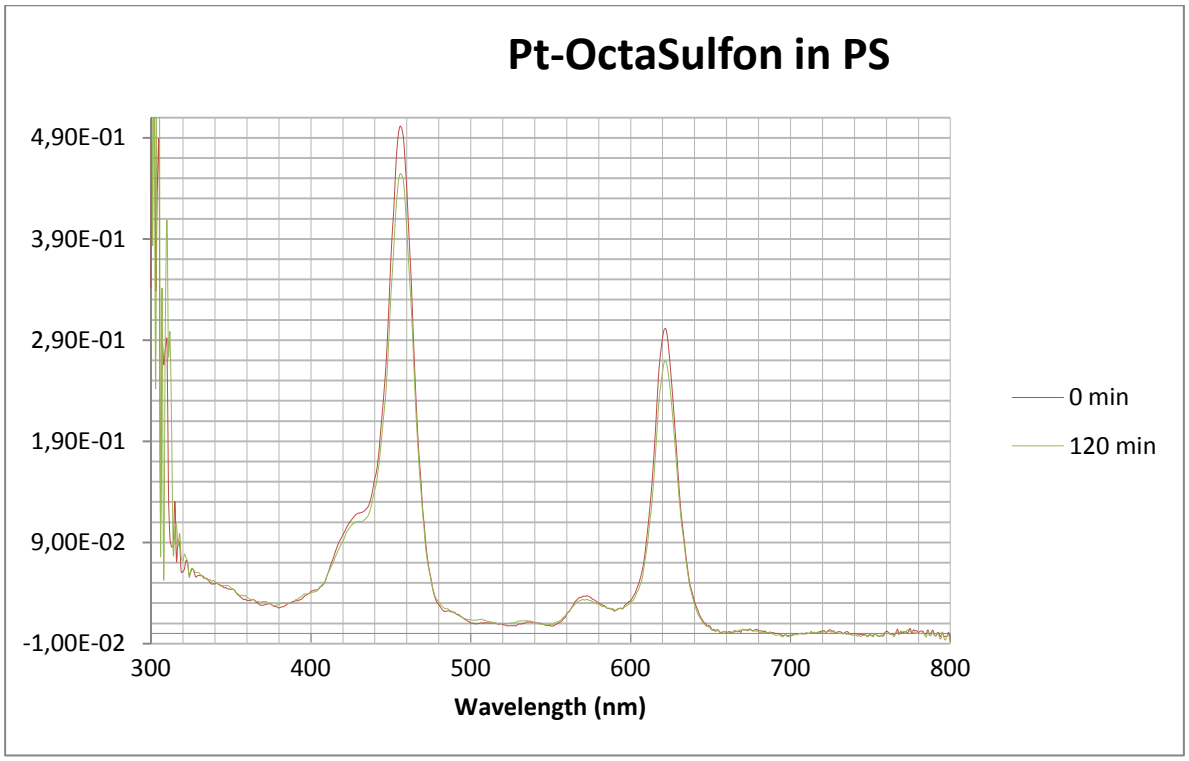
Pt-OctaSulfon in PS
4,90E-01
3,90E-01
2,90E-01
1,90E-01
9,00E-02
-1,00E-02
300
400
500
600
700
800
Wavelength (nm)
0 min
120 min

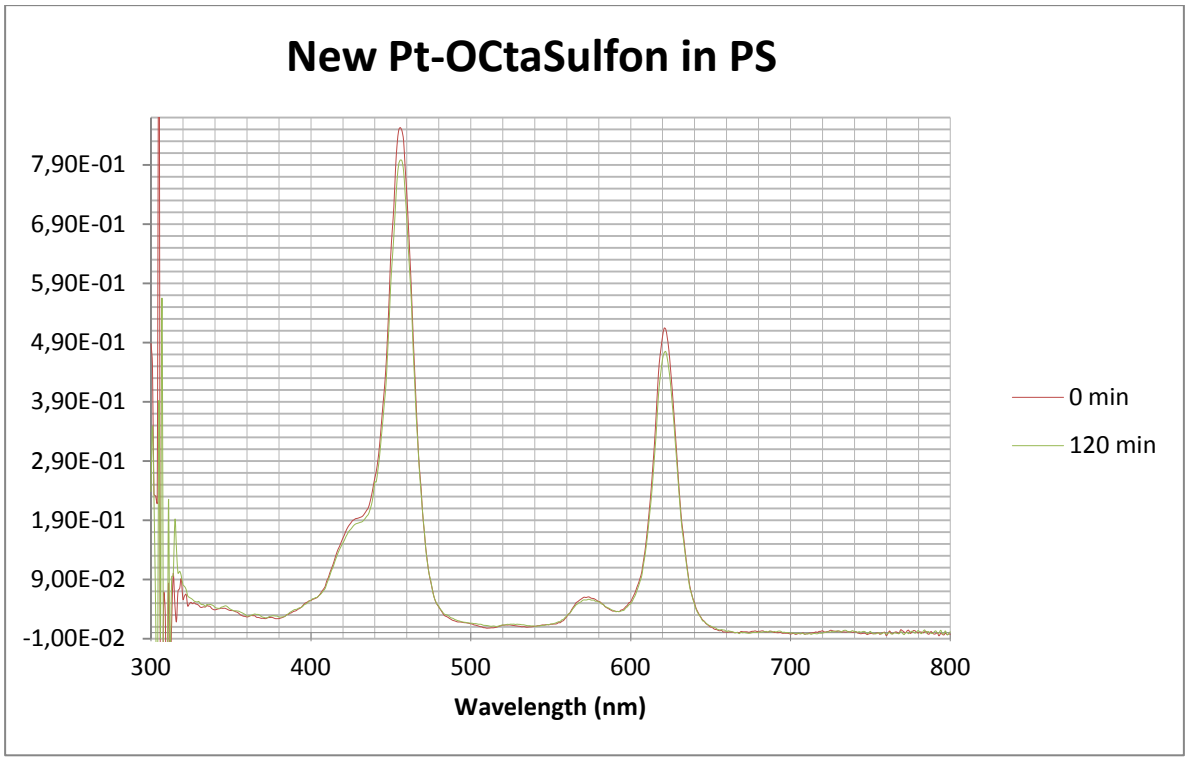
New Pt-OCtaSulfon in PS
7,90E-01
6,90E-01
5,90E-01
4,90E-01
3,90E-01
2,90E-01
1,90E-01
9,00E-02
-1,00E-02
300
400
500
600
700
800
Wavelength (nm)
0 min
120 min